DEVELOPMENT AND SCALE-UP OF ENHANCED POLYMERIC MEMBRANE REACTOR SYSTEMS FOR ORGANIC SYNTHESIS

by

FAN ZHANG

B.E., Tianjin University of Science and Technology, 2007

AN ABSTRACT OF A DISSERTATION

submitted in partial fulfillment of the requirements for the degree

DOCTOR OF PHILOSOPHY

Department of Chemical Engineering
College of Engineering

KANSAS STATE UNIVERSITY
Manhattan, Kansas

2012

Abstract

Reversible organic reactions, such as esterification, transesterification, and acetalisation, have enjoyed numerous laboratory uses and industrial applications since they are convenient means to synthesize esters and ketals. Reversible organic reactions are limited by thermodynamic equilibrium and often do not proceed to completion. High yields for these equilibrium driven reactions can be obtained either by adding a large excess of one of the reactants, which results a reactant(s)/product(s) mixture requiring a separation, or by the selective removal of by-products. Conventional removal techniques including distillation, adsorption, and absorption have drawbacks in terms of efficiency as well as reactor design. Pervaporation membrane reactors are promising systems for these reactions since they have simpler designs, and are more energy efficient compared to conventional downstream separation techniques.

This project created a general protocol that can guide one to carry out experiments and collect necessary data for transferring membrane reactor design concepts to the construction of industrial-scale membrane reactors for organic synthesis. Demonstration of this protocol was achieved by (1) experimental evaluation of membrane reactor performance, (2) modeling, and (3) scale-up. The capability of membranes for water/organic separations and organic/organic separations during reversible reactions was investigated. Our results indicated that enhanced membrane reactors selectively removed the by-product water and methanol from reaction mixtures and achieved high conversions for all investigated reactions. Second, modeling and simulation of pervaporation membrane reactor performance for reversible reactions were carried out. The simulated performance agrees well with experimental data. Using the developed model, the effects of permeate pressure and membrane selectivity on membrane reactor yield were examined. Finally, a scale-up on transesterification membrane reactors was carried out. The membrane modules investigated included a bench-scale flat sheet membrane, a bench-scale hollow fiber membrane module, and a pilot-scale hollow fiber membrane module. A 100% conversion was obtained by the selective methanol removal. It is found that with high methanol selectivity membranes, the reaction time to achieve a given conversion continuously decreases with increasing the methanol removal capacity of the reactor system. However, this is a highly nonlinear relationship.

DEVELOPMENT AND SCALE-UP OF ENHANCED POLYMERIC MEMBRANE REACTOR SYSTEMS FOR ORGANIC SYNTHESIS

by

FAN ZHANG

B.E., Tianjin University of Science and Technology, 2007

A DISSERTATION

submitted in partial fulfillment of the requirements for the degree

DOCTOR OF PHILOSOPHY

Department of Chemical Engineering
College of Engineering

KANSAS STATE UNIVERSITY
Manhattan, Kansas

2012

Approved by:

Major Professor
Dr. Mary E. Rezac

Copyright

Abstract

Reversible organic reactions, such as esterification, transesterification, and acetalisation, have enjoyed numerous laboratory uses and industrial applications since they are convenient means to synthesize esters and ketals. Reversible organic reactions are limited by thermodynamic equilibrium and often do not proceed to completion. High yields for these equilibrium driven reactions can be obtained either by adding a large excess of one of the reactants, which results a reactant(s)/product(s) mixture requiring a separation, or by the selective removal of by-products. Conventional removal techniques including distillation, adsorption, and absorption have drawbacks in terms of efficiency as well as reactor design. Pervaporation membrane reactors are promising systems for these reactions since they have simpler designs, and are more energy efficient compared to conventional downstream separation techniques.

This project created a general protocol that can guide one to carry out experiments and collect necessary data for transferring membrane reactor design concepts to the construction of industrial-scale membrane reactors for organic synthesis. Demonstration of this protocol was achieved by (1) experimental evaluation of membrane reactor performance, (2) modeling, and (3) scale-up. The capability of membranes for water/organic separations and organic/organic separations during reversible reactions was investigated. Our results indicated that enhanced membrane reactors selectively removed the by-product water and methanol from reaction mixtures and achieved high conversions for all investigated reactions. Second, modeling and simulation of pervaporation membrane reactor performance for reversible reactions were carried out. The simulated performance agrees well with experimental data. Using the developed model, the effects of permeate pressure and membrane selectivity on membrane reactor yield were examined. Finally, a scale-up on transesterification membrane reactors was carried out. The membrane modules investigated included a bench-scale flat sheet membrane, a bench-scale hollow fiber membrane module, and a pilot-scale hollow fiber membrane module. A 100% conversion was obtained by the selective methanol removal. It is found that with high methanol selectivity membranes, the reaction time to achieve a given conversion continuously decreases with increasing the methanol removal capacity of the reactor system. However, this is a highly nonlinear relationship.

Table of Contents

List of Figures

List of Tables

Nomenclature

Symbol	Definition	Units
A or S	membrane area	cm^2
FM	fractional removal	%
j	molar flux of the component	$mmol \cdot cm^{-2} \cdot h^{-1}$
K_{eq}	equilibrium constant	–
l	thickness of the membrane selective layer	cm
m	mass of a species passing through a flow area	g
n	stage or iteration number in the model	–
N	amount of the component	mmol
ΔN	changed amount of the component	mmol
p	pressure	Torr or bar
P^G	permeability coefficient	$mol \cdot cm \cdot cm^{-2} \cdot s^{-1} \cdot$unit pressure^{-1}
P^G/l	permeance of the component	$mmol \cdot cm^{-2} \cdot h^{-1} \cdot bar^{-1}$ or GPU, 1 GPU $=10^{-6}$ cm^3 (STP)/$cm^2 \cdot s \cdot cmHg$
Q	reaction quotient	–
R	gas constant	8314472 $cm^3 \cdot Pa/(mol \cdot K)$
T	Temperature	°C
t	time	h
V	volume	cm^3
X	conversion	%
x	mol fraction of the component in the feed side	–
y	mol fraction of the component in the permeate side	–
α	membrane selectivity	–
β	membrane separation factor	–
ν	stoichiometric coefficient of reaction	–
γ	activity coefficient	–

Subscripts

i, j	components
ℓ	permeate side
o	feed side

Supercripts

G	gas
L	liquid
feed	feed side
perm	permeate side
sat	saturated

Acknowledgements

Five years ago, I decided to pursue a PhD, and I was eager to learn knowledge and skills in process development. Now, I have achieved my goal. I feel so happy about the tremendous knowledge I have learned over the past five years. I also feel thankful for people who helped me.

First and foremost, I would like to express my deepest gratitude to my major advisor, Dr. Mary Rezac, for her invaluable guidance and continuous encouragement on various aspects of both research and life. I want to thank her for introducing me to the fascinating world of membranes and the benefits membrane separation technology can bring to society. I really appreciate all her contributions of time, patience, ideas and career advice to make my PhD experience productive. She has helped guide me to more fully realize who I am professionally and what I can accomplish. I would also like to give a very special thanks to Dr. Peter Pfromm, for providing insightful discussions about my research and suggestions on presentations.

I appreciate Dr. John Schlup, Dr. Jennifer Anthony, Dr. Christopher Culbertson, and Dr. Zhijian Pei, for taking time to serve on my PhD committee. I am grateful to all faculty members in the Department of Chemical Engineering for teaching high quality courses and staff members for their assistance. I would also like to thank Dr. Dan Boyle for performing SEM and James Hodgson for his great help on designing and making glass reactors.

I thank all the former and current members of the Rezac/Pfromm research group: Dr. Devinder Singh, Dr. Juan Cruz (thanks for teaching me how to operate the membrane reactor system at the beginning), Dr. Mohammed Hussain, Dr. Ronald Michalsky, Dr. Alexander Brix, Sebastian Wendel, Volker Bleim (with special thanks for his contribution on acetalisation reactions and modeling), Martin Kramer, John Stanford (thanks for his helping on setting up the pilot-scale system), Leslie Schulte, Elizabeth Boyer, Neha Dhiman, Mandeep Kular, Alexandru Avram, Mattew Young and Michael Wales for their support and the enjoyable time we shared.

A very special thanks goes out to Yi Zhang, Xin Sun, and Li Du for their friendship and support–you made my life in Manhattan as fun as in China.

Finally, I would like to thank my parents for supporting my decisions and providing lots of love, and my beloved husband, Michael Worley, for his increasing love, patience, and encouragement. His optimism always relieves my tension from research and influences my life in a positive way. I truly thank him for his faith in me all the time.

Dedication

To mom (Li Qiu), dad (Zhongdi Zhang), and my husband (Michael Worley)
for their endless love, support and encouragement.

Chapter 1 - Introduction

1.1 Research motivation

Reversible organic reactions are an important class of synthetic processes used to synthesize various esters, ethers, and ketals. These reactions have been broadly employed in both laboratory and industry. The diversity of the reactant acids, aldehydes, ketones, and alcohols result in a multitude of products such as polymers, pharmaceuticals, surfactants, fungicides, insecticides, and biologically active compounds. Reversible organic reactions are limited by thermodynamic equilibrium and often do not proceed to completion. High yields of these reactions can be obtained either by adding a large excess of one of the reactants, which results a reactant(s)/product(s) mixture requiring a separation, or by the selective removal of by-products.

Water or low molecular weight alcohols are the typical by-products from these reactions. Traditional removal technologies include distillation, adsorption, and absorption. These methods have drawbacks such as complex system design, large amounts of energy for direct heating, regeneration of any solvent or dehydrating agent, storage, heating and moving of the solvent, and treatment of the generated waste [1-10]. Pervaporation membrane reactors are promising systems for achieving this separation due to their relative simplicity, lower energy consumption, and lower operating costs [11-14].

In recent years, pervaporation membrane reactor systems have been intensively studied in assisting esterification reactions [15-28]. During a pervaporation assisted esterification reaction, the membrane is required to selectively remove water from esters and the reactant alcohol. While pervaporation-esterification reactor systems have already been industrially realized, membrane reactors for transesterification reactions are rarely studied [12, 29]. In transesterification reactions, the separation to be achieved is between the by-product and reactant alcohols, a difficult organic/organic separation. There is a lack of economical solvent-resistant pervaporation membrane modules that have sufficient selectivity for organic/organic separations. Having said that, research on membranes for pervaporation organic/organic separations and solvent-resistant modules are ranked 1 and 7 respectively out of 38 research needs in the membrane separation industry [30].

Several researchers have developed models describing reversible reaction kinetics and species permeation in membrane reactor systems [28, 31-38]. These studies have provided a

useful foundation from which models that can predict membrane reactor performance based on system design and operating conditions can be developed. Some studies have also been done on the scale-up of pervaporation membrane assisted esterification reactions [39-43]. The effect of membrane area to reaction volume ratio (S/V) on reaction time has been discussed in these papers. Unfortunately, experimental data obtained from these studies are limited to a relatively small range of S/V ($0 \sim 250\ m^{-1}$) since almost all of these studies employed flat sheet membranes with limited membrane area. From an industrial perspective, it will be useful to investigate a broader range of S/V ratio while employing different scales of membrane modules.

1.2 Research objectives

The ultimate goal of this research is to create a general protocol that can guide one to carry out experiments and collect necessary data for transferring membrane reactor design concepts to the construction of industrial-scale membrane reactors for organic synthesis. To achieve this goal, the specific technical objectives of this research include:

1) Evaluation of the ability of the membrane reactor system to enhance the performance of various types of reversible organic reactions with special interest in transesterification reactions,

2) Development of a mathematical model to predict the membrane reactor performance to system design and operating conditions, and

3) Investigation of the performance of different scales of membrane reactor systems for transesterification reactions.

1.3 Dissertation outline

This dissertation is organized in the order corresponding to the technical objectives. Most chapters are published papers or in the process for publications. These chapters are reproduced here as they were prepared for publications.

Following this introduction chapter, Chapter 2 provides general background information on reversible reactions, pervaporation membrane reactors, and polymeric membranes for pervaporation. Description of membrane characterization methods employed in this research is also provided.

Chapter 3 is a manuscript submitted to the Journal of Membrane Science [44]. This paper studies the esterification of oleic acid with ethanol and the transesterification of methyl benzoate with *n*-butanol in pervaporation membrane reactors. Reaction conversions and rates obtained in membrane reactors are compared to those achieved in batch reactors. The chemical resistance, long-term stability, and by-product selectivity of employed membranes are evaluated under reaction conditions.

Chapter 4 is an accepted paper, which will be published in the Journal of Membrane Science [45]. This paper focuses on the development of a model to predict transesterification and acetalisation reaction conversions exceeding thermodynamic equilibrium in a membrane rector based on membrane permeation data and operating conditions. The effect of membrane selectivity and permeate pressure on membrane reactor performance are investigated by the developed model.

Chapter 5 is a manuscript submitted to the Industrial & Engineering Chemistry Research [46]. It compares the performance of different scale membrane reactors for the transesterification production of β-keto esters. The influence of methanol removal on reaction conversion is explored by analyzing permeate composition. The effect of methanol removal capacity of a membrane reactor system on reaction time to reach high conversions is also examined.

Finally, in Chapter 6, results and important findings in this research are summarized along with the recommendations for future work.

1.4 References

[1] A. Carton, G. Gonzalez, A.I. Delatorre, J.L. Cabezas, Separation of ethanol water mixtures using 3a molecular-Sieve, Journal of Chemical Technology and Biotechnology, 39 (1987) 125-132.

[2] W.K. Teo, D.M. Ruthven, Adsorption of water from aqueous ethanol using 3-a molecular-sieves, Industrial & Engineering Chemistry Process Design and Development, 25 (1986) 17-21.

[3] V. Van Hoof, L. Van den Abeele, A. Buekenhoudt, C. Dotremont, R. Leysen, Economic comparison between azeotropic distillation and different hybrid systems combining distillation with pervaporation for the dehydration of isopropanol, Sep Purif Technol, 37 (2004) 33-49.

[4] V. Gomis, R. Pedraza, O. Frances, A. Font, J.C. Asensi, Dehydration of ethanol using azeotropic distillation with isooctane, Ind Eng Chem Res, 46 (2007) 4572-4576.

[5] R.S. Morse, High vacuum dehydration and distillation, Chem Ind-London, (1948) S13-S19.

[6] A.I. Yeh, L. Berg, The dehydration of ethanol by extractive distillation, Chem Eng Commun, 113 (1992) 147-153.

[7] J.P. Lange, V. Otten, Dehydration of phenyl ethanol to styrene under reactive distillation conditions: Understanding the catalyst deactivation, Ind Eng Chem Res, 46 (2007) 6899-6903.

[8] J.B. Cho, J.K. Jeon, Optimization study on the azeotropic distillation process for isopropyl alcohol dehydration, Korean J Chem Eng, 23 (2006) 1-7.

[9] A. Chianese, F. Zinnamosca, Ethanol dehydration by azeotropic distillation with a mixed-solvent entrainer, Chem Eng J Bioch Eng, 43 (1990) 59-65.

[10] M.R.W. Maciel, R.P. Brito, Evaluation of the dynamic behavior of an extractive distillation column for dehydration of aqueous-ethanol mixtures, Comput Chem Eng, 19 (1995) S405-S408.

[11] B.V.d. Bruggen, Pervaporation membrane reactors, in: Comprehensive Membrane Science and Engineering, Elsevier Science, 2010, pp. 135-163.

[12] F. Lipnizki, R.W. Field, P.K. Ten, Pervaporation-based hybrid process: a review of process design, applications and economics, Journal of Membrane Science, 153 (1999) 183-210.

[13] R.M. Waldburger, F. Widmer, Membrane reactors in chemical production processes and the application to the pervaporation-assisted esterification, Chem Eng Technol, 19 (1996) 117-126.

[14] M.T. Ravanchi, T. Kaghazchi, A. Kargari, Application of membrane separation processes in petrochemical industry: a review, Desalination, 235 (2009) 199-244.

[15] Q.L. Liu, Z.B. Zhang, H.F. Chen, Study on the coupling of esterification with pervaporation, Journal of Membrane Science, 182 (2001) 173-181.

[16] D. Barahona, P.H. Pfromm, M.E. Rezac, Effect of water activity on the lipase catalyzed esterification of geraniol in ionic liquid [bmim]PF6, Biotechnol Bioeng, 93 (2006) 318-324.

[17] A. Hasanoglu, Y. Salt, S. Keleser, S. Dincer, The esterification of acetic acid with ethanol in a pervaporation membrane reactor, Desalination, 245 (2009) 662-669.

[18] S. Korkmaz, Y. Salt, A. Hasanoglu, S. Ozkan, I. Salt, S. Dincer, Pervaporation membrane reactor study for the esterification of acetic acid and isobutanol using polydimethylsiloxane membrane, Applied Catalysis a-General, 366 (2009) 102-107.

[19] J. Ma, M.H. Zhang, L.Y. Lu, X. Yin, J. Chen, Z.Y. Jiang, Intensifying esterification reaction between lactic acid and ethanol by pervaporation dehydration using chitosan-TEOS hybrid membranes, Chemical Engineering Journal, 155 (2009) 800-809.

[20] S.G. Adoor, L.S. Manjeshwar, S.D. Bhat, T.M. Aminabhavi, Aluminum-rich zeolite beta incorporated sodium alginate mixed matrix membranes for pervaporation dehydration and esterification of ethanol and acetic acid, Journal of Membrane Science, 318 (2008) 233-246.

[21] K.C.D. Figueiredo, V.M.M. Salim, C.P. Borges, Synthesis and characterization of a catalytic membrane for pervaporation-assisted esterification reactors, Catal Today, 133 (2008) 809-814.

[22] K. Bartling, J.U.S. Thompson, P.H. Pfromm, P. Czermak, M.E. Rezac, Lipase-catalyzed synthesis of geranyl acetate in n-hexane with membrane-mediated water removal, Biotechnol Bioeng, 75 (2001) 676-681.

[23] P. Delgado, M.T. Sanz, S. Beltran, L.A. Nunez, Ethyl lactate production via esterification of lactic acid with ethanol combined with pervaporation, Chemical Engineering Journal, 165 (2010) 693-700.

[24] S. Lauterbach, P. Kreis, Experimental and theoretical investigation of a pervaporation membrane reactor for a heterogeneously catalysed esterification, Desalination, 199 (2006) 418-420.

[25] X.S. Feng, R.Y.M. Huang, Studies of a membrane reactor: Esterification facilitated by pervaporation, Chem Eng Sci, 51 (1996) 4673-4679.

[26] M.T. Sanz, J. Gmehling, Esterification of acetic acid with isopropanol coupled with pervaporation. Part II. Study of a pervaporation reactor, Chem Eng J, 123 (2006) 9-14.

[27] S.J. Parulekar, Analysis of pervaporation-aided esterification of organic acids, Ind Eng Chem Res, 46 (2007) 8490-8504.

[28] S.Y. Lim, B. Park, F. Hung, M. Sahimi, T.T. Tsotsis, Design issues of pervaporation membrane reactors for esterification, Chem Eng Sci, 57 (2002) 4933-4946.

[29] A.P. de los Rios, F.J. Hernandez-Fernandez, H. Presa, D. Gomez, G. Villora, Tailoring supported ionic liquid membranes for the selective separation of transesterification reaction compounds, Journal of Membrane Science, 328 (2009) 81-85.

[30] R.W. Baker, Research needs in the membrane separation industry: Looking back, looking forward, Journal of Membrane Science, 362 (2010) 134-136.

[31] K. Tanaka, R. Yoshikawa, C. Ying, H. Kita, K. Okamoto, Application of zeolite membranes to esterification reactions, Catalysis Today, 67 (2001) 121-125.

[32] X.H. Li, L.F. Wang, Kinetic model for an esterification process coupled by pervaporation, Journal of Membrane Science, 186 (2001) 19-24.

[33] M.O. David, R. Gref, T.Q. Nguyen, J. Neel, Pervaporation-esterification coupling .1. basic kinetic-model, Chemical Engineering Research & Design, 69 (1991) 335-340.

[34] P.G. Cao, A.Y. Tremblay, M.A. Dube, Kinetics of canola oil transesterification in a membrane reactor, Ind. Eng. Chem. Res., 48 (2009) 2533-2541.

[35] A. Hasanoglu, S. Dincer, Modelling of a pervaporation membrane reactor during esterification reaction coupled with separation to produce ethyl acetate, Desalin Water Treat, 35 (2011) 286-294.

[36] M.T. Sanz, J. Gmehling, Esterification of acetic acid with isopropanol coupled with pervaporation. Part I: kinetics and pervaporation studies, Chem Eng J, 123 (2006) 1-8.

[37] K. Wasewar, S. Patidar, V.K. Agarwal, Esterification of lactic acid with ethanol in a pervaporation reactor: modeling and performance study, Desalination, 243 (2009) 305-313.

[38] K.L. Wasewar, S. Patidar, V.K. Agarwal, Pervaporation reactor for esterification of acetic acid with n-butanol: modeling and simulation, Int J Chem React Eng, 6 (2008).

[39] J.T.F. Keurentjes, G.H.R. Janssen, J.J. Gorissen, The esterification of tartaric acid with ethanol - kinetics and shifting the equilibrium by means of pervaporation, Chemical Engineering Science, 49 (1994) 4681-4689.

[40] S. Korkmaz, Y. Salt, S. Dincer, Esterification of acetic acid and isobutanol in a pervaporation membrane reactor using different membranes, Ind. Eng. Chem. Res., 50 (2011) 11657-11666.

[41] K. Okamoto, M. Yamamoto, Y. Otoshi, T. Semoto, M. Yano, K. Tanaka, H. Kita, Pervaporation-aided esterification of oleic-acid, Journal of Chemical Engineering of Japan, 26 (1993) 475-481.

[42] T. Roth, S. Lauterbach, A. Hoffmann, P. Kreis, Scale-up and detailed process analysis of a membrane assisted esterification reaction, Chem-Ing-Tech, 83 (2011) 456-464.

[43] M.O. David, T.Q. Nguyen, J. Neel, Pervaporation-Esterification Coupling .2. Modeling of the influence of different operating parameters, Chemical Engineering Research & Design, 69 (1991) 341-346.

[44] F. Zhang, M.E. Rezac, S. Majumdar, P. Kosaraju, S. Nemser, Improving chemical production processes by selective by-product removal in a pervaporation membrane reactor, manuscript submitted to the Journal of Membrane Science, 2012.

[45] F. Zhang, V. Bliem, M.E. Rezac, P. Kosaraju, S. Nemser, Pervaporation membrane reactors for reversible organic reactions: modeling of the membrane-reactor performance to system design and operating conditions, accepted by the Journal of Membrane Science, 2011.

[46] F. Zhang, M.E. Rezac, P. Kosaraju, S. Nemser, Scale-up of a pervaporation membrane assisted transesterification reactor for butyl acetoacetate production, manuscript submitted to the Industrial & Engineering Chemistry Research, 2012.

Chapter 2 - Background

2.1 Reversible organic reaction

A reversible reaction is a chemical reaction in which the conversion of reactants to products (the forward reaction) and the conversion of products to reactants (the reverse reaction) occur simultaneously [1]. There are many reversible organic reactions that have water or low molecular weight alcohols as by–products (Reaction 1). These reactions have been broadly employed in laboratory and industry.

In Table 2-1, several types of frequently used reversible organic reactions with water or low molecular weight alcohols as by-products are listed as examples. The diversity of the acids, aldehydes, ketones, esters and alcohols, that is, straight chain, ring and other attached R groups, result in a multitude of products such as polymers, pharmaceuticals, surfactants, fungicides, insecticides, and biologically active compounds [2].

$$\text{A (see Table 2-1)} + \text{B (see Table 2-1)} \overset{\text{Catalyst}}{\rightleftharpoons} \text{C (Product)} + \text{Water or Low Mw alcohol} \quad \text{Reaction 1}$$

Table 2-1 Reversible organic reactions with water or low molecular weight alcohols as by-products

Reactant A	Reactant B	Product	By-Product
Acid	Alcohol	Ester	Water
Acid	2 Alcohols	Orthoester	Water
Ketone	Alcohol	Ketal	Water
Ester	Alcohol	Ester	Alcohol
Aldehyde	Alcohol	Ether	Water
Aldehyde or Ketone	Amine	Imine	Water

Esterification reactions are an industrially important class of reactions where an organic acid and an alcohol combine, usually in the presence of an acid catalyst, to produce an ester and water (Reaction 2). Within all the reversible organic reactions with water as the by-product, esterification reactions are the most often investigated since its product, organic esters, are important fine

chemicals that have applications in a variety of areas such as cosmetics, flavors, pharmaceuticals, plasticizers, solvents, and monomers.

$$R_1COOH + R_2OH \overset{\text{Catalyst}}{\rightleftharpoons} R_1COOR_2 + H_2O \qquad \text{Reaction 2}$$

While ester synthesis can be achieved from esterification, often transesterification (Reaction 3) is used to synthesize a specific ester. Transesterification can be used as an alternative method to synthesize various carboxylic esters. On some occasions, transesterification is more advantageous than esterification. For instance, some carboxylic acids are sparingly soluble in organic solvents and accordingly difficult to subject to homogeneous esterification. Transesterification is particularly useful when the parent carboxylic acids that can be used for esterification are labile or difficult to isolate [3].

$$R_1COOR_2 + R_3OH \overset{\text{Catalyst}}{\rightleftharpoons} R_1COOR_3 + R_2OH \qquad \text{Reaction 3}$$

Acetalisation (Reaction 4) is an important synthetic process to produce ketals. Ketals are key intermediates in the manufacture of clarithromycin, polymers and various organic compounds [4, 5]. They also can be used as chemical dehydration agents and flavoring compound in distilled beverages [6, 7].

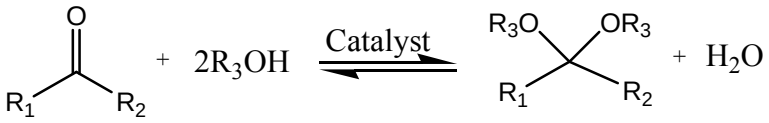

Reaction 4

Reversible organic reactions are limited to less than 100% conversion due to thermodynamic equilibrium limitations [8]. Frequently, for these equilibrium limited reactions, a large excess of one of the reactants is employed to obtain high yields. If the by-product from these reactions can be selectively removed, high yields can be obtained. For a reversible reaction, the separation of a product affects the rate and extent of reaction in this way: a reversible reaction, e.g. $A + B \underset{k_2}{\overset{k_1}{\rightleftharpoons}} R + S$, has the rate equation $-r_A = k_1 C_A C_B - k_2 C_R C_S$. As either R or S is

removed from the reaction mixture, the reverse reaction term in the rate equation becomes smaller and the forward reaction rate r_A increases. Meanwhile, the reaction quotient $Q = \frac{C_R \cdot C_S}{C_A \cdot C_B}$ is going to decrease and become smaller than the equilibrium constant. To restore equilibrium, the reaction is forced towards the products momentarily until the reaction quotient is equal to the equilibrium constant [8].

While selective removal of by-products can help increase reaction rates and product yields of reversible reactions, the technology employed for by-product removal largely determines energy consumption and capital investment for these production processes.

Removing water or low molecular weight alcohols from reversible reactions by conventional methods is usually energetically demanding. Removal technologies range from distillation to adsorption and absorption [9-14]. In every case, the removal of water or low molecular weight alcohols requires large amounts of energy for direct heating, regeneration of any solvent or dehydrating agent, storage, heating and moving of the solvent, and treatment of the generated waste.

2.2 Pervaporation membrane reactor

Selective removal of water or low molecule weight alcohols by-products from revisable reactions through pervaporation membranes is a promising alternative to traditional separation methods.

Membrane reactors have been investigated since the 1970s and are receiving increased attentions. A membrane reactor system combines reaction and membrane separation in a single unit [15]. Membranes in these systems perform a variety of functions, including: (1) the membrane as a contactor performing no separation function – a catalyst or the liquid reaction medium being immobilized in (or on) a membrane; (2) the membrane as a separating barrier – separation of products from the reaction mixture, separation of a reactant from a mixed stream for introduction into the reactor, and controlled addition of one reactant or two reactants; (3) the membrane combines the functions of contactor and separator.

Pervaporation is a well-known membrane technique for separating compounds of a liquid mixture. In pervaporation, a multicomponent feed liquid passes across a membrane that

preferentially permeates one or more of the components. A vacuum is applied to the permeate side to create a driving force. One (or several) of the feed components sorbs into the membrane, diffuses through the membrane, and desorbs into the vapor phase at the permeate side [16]. Transport through the membrane is induced by the partial pressure difference between the feed solution and the permeate [17].

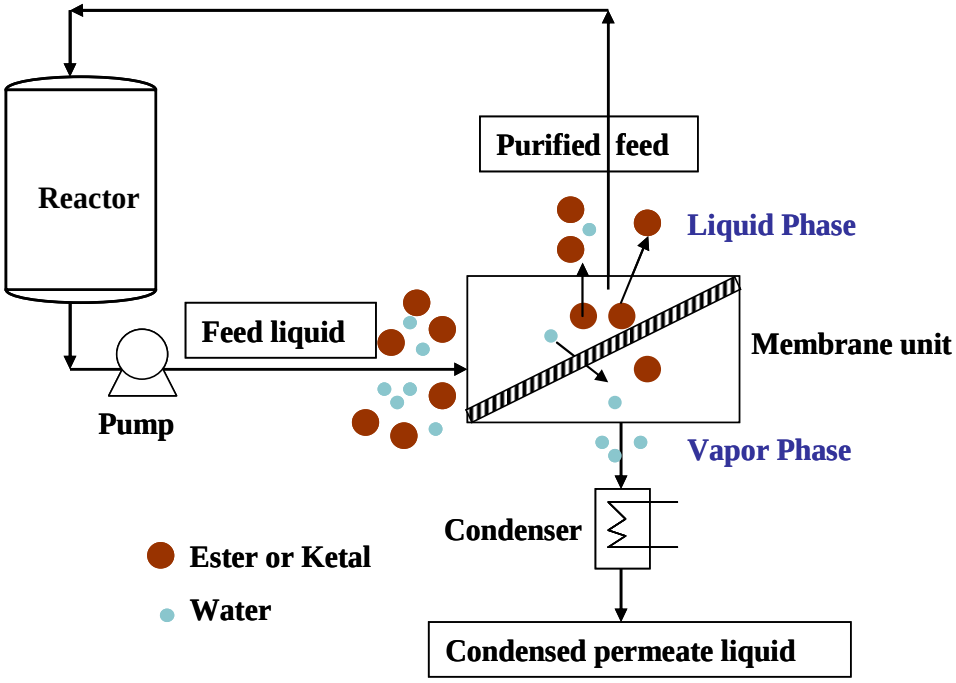

Figure 2-1 Schematic of a continuous pervaporation membrane reactor.

Membrane reactors operating in pervaporation conditions simultaneously combine reaction and purification. Figure 2-1 schematically shows a continuous pervaporation membrane reactor to separate the by-product from liquid mixtures. The reversible reaction takes place inside the reactor and the reaction mixture is sent to the feed side of a membrane by a circulation pump, the by-product water or low molecular weight alcohol is selectively removed from the reaction mixture by pervaporation and condensed in a cold trap. The retentate with lower by-product concentration circulates back to the reactor.

Pervaporation membrane reactor may reduce production costs in four ways: higher yield, faster reaction, purer products and less energy [18-21]. By using a proper pervaporation membrane, the by-product can be removed from the reaction mixture while reactants are still maintained inside the reactor. As a result, pervaporation membrane reactors can reduce the

reaction time and the amount of reactants used in reversible reactions. A conventional reactor system requires a separation device to separate the products from any unreacted feeds and to separate the products from each other. With a membrane reactor and its by-product removal, the separation of unreacted reactants from the product will be a smaller device, and the separation of the two reaction products may no longer be necessary—eliminating downstream processing and reducing energy consumption.

2.3 Transport through membranes during pervaporation

The capability of a pervaporation membrane reactor is largely determined by the pervaporation membrane employed. Flux and selectivity are important parameters to evaluate the performance or efficiency of a pervaporation membrane.

Molecular transport through a membrane during the pervaporation process can be described by the solution-diffusion mechanism, i.e. Permeability=Solubility×Diffusivity [22]. The model involves sorption of molecules in the feed side of the membrane and diffusion of molecules through the membrane. In a more detailed way, the first step is evaporation from the feed liquid to form a saturated vapor phase in equilibrium with the liquid. This evaporation step produces a separation because of the different volatilities of the components of the feed liquid. This separation can be defined as β_{evap}, the ratio of the component concentrations in the feed vapor to their concentrations in the feed liquid.

$$\beta_{evap} = \frac{p_{i0} / p_{j0}}{n_{i0} / n_{j0}} \qquad \text{Equation 2-1}$$

where p_{io} and p_{j0} are partial pressure of component *i* and *j* on feed side, n_{i0}, n_{j0} are the mole fractions in the feed liquid of the two components.

The second step is permeation of components through the membrane. The driving force for permeation is the partial pressure difference between the feed liquid and permeate vapors. The separation achieved in this step is described by Equation 2-2:

$$\beta_{mem} = \frac{p_{il} / p_{jl}}{p_{i0} / p_{j0}} \qquad \text{Equation 2-2}$$

where p_{il} and p_{jl} are partial pressure of component *i* and *j* on permeate side.

The total separation achieved in pervaporation β_{pervap} is called a separation factor. It is equal to the product of the separation achieved by evaporation and the selective permeation.

$$\beta_{pervap} = \beta_{evap} \times \beta_{mem} \qquad \text{Equation 2-3}$$

The flux of a component will not only depend on its solubility and diffusion in the membrane material, but also on the driving force and thickness of the membrane. Increasing driving force or decreasing the membrane thickness can lead to a higher flux.

$$j_i = \frac{P_i^G}{l}\left(p_{io} - p_{il}\right) \qquad \text{Equation 2-4}$$

where j_i is the molar flux of component *i* permeating through the membrane (mol/cm^2·s), P_i^G is the molar permeability coefficient of component *i* through the membrane material (mol·cm·cm^{-2}·s^{-1}·unit pressure^{-1}), *l* is the thickness of the membrane layer and p_{io} , p_{il} are partial pressure of component *i* on feed side and permeate side.

The ratio of the molar membrane permeability coefficients of component *i* and *j* is the membrane selectivity, $\alpha_{i/j}$ [23].

$$\alpha_{i/j} = P_i^G \big/ P_j^G \qquad \text{Equation 2-5}$$

2.4 Membranes for pervaporation

2.4.1 Membrane types

Membranes can be classified according to different view points. The first is by material. A variety of membrane materials have been reported in literature as having potential for pervaporative removal of water, such as polymeric [24-30], inorganic [31-36] or mixed matrix [37-42]. Each membrane material has limitations in terms of synthesis and/or application, and there is potential for improvement. The advantages versus disadvantages for these membrane materials are compared in Table 2-2. Polymeric membranes have already been employed for commercial membrane reactor applications. Their separation performances are moderate. Some polymeric membranes may lack chemical resistance and thermal stability under harsh reaction conditions, but these properties can be improved by polymer modification. Inorganic membranes, such as NaA zeolite membranes, may show better separation performance than organic membranes under certain conditions, but major disadvantages limiting their application

are that they are not acid stable and that the ceramic membranes in general are more expensive and difficult to make than the polymeric membranes [43]. Mixed matrix membranes (MMMs) consist of a bulk organic polymer phase and dispersed inorganic particles, which may be zeolite, carbon molecular sieves, or nano-size particles [44]. Increasing inorganic particles loading can help increase the total permeate flux and the partial water flux of a mixed matrix membrane, but in practice, it is difficult to produce defect-free MMMs [45]. Defects will reduce the apparent selectivity of a mixed matrix membrane [46]. To date, few inorganic membranes and no mixed matrix membranes have overcome the stated limitations and become economically viable.

Table 2-2 Comparison of different types of membrane materials for pervaporation dehydration of ethanol

Membrane Materials	Selectivity ($\alpha_{H_2O/EtOH}$)	Advantage	Disadvantage
Polymeric Membranes	5~2000	Easy and cheap	Limited solvent and temperature stability; Swelling
Inorganic Membranes	50~16000	High temperature stability; Free of swelling	High cost; Poor reproducibility
Mixed Matrix Membranes	200~7000	Swelling resistant	Tough to eliminate organic/inorganic interfacial defects; Inorganic particles aggregation

* Selectivity is expressed in terms of separation factor. Data are collected for ethanol-water azeotrope at 20~65°C and laboratory data may not represent commercial results.

Suitable membranes for the removal of by–product water or low molecular weight alcohols during reversible organic reactions in membrane reactors should be able to withstand reaction conditions and have optimum flux and selectivity. By weighing the pros and cons of these membranes, polymeric membranes are the most feasible membrane type to be employed in commercial scale pervaporation membrane reactors for reversible reactions with the water or methanol by-product in the long run.

The second way to classify membranes is by morphology or structure. Two major types of geometries can be distinguished: symmetric films and asymmetric membranes. A composite membrane is an asymmetric membrane which has a structure showing in Figure 2-2. In a composite membrane, a selective membrane material is deposited as a thin layer upon a porous sublayer. The toplayer and sublayer originate from different membrane materials. Each layer of can be optimized independently. A composite membrane can combine the high selectivity of a dense membrane with the high flux of a very thin membrane [47].

In a well-designed polymeric composite membrane, the actual selectivity is usually determined by the nonporous toplayer, whereas the sublayer merely serves as a support. If the flux of the uncoated support layer is at least 10 times that of the selective layer, more than 90% of the resistance to mass transfer lies within the selective toplayer, which is to say, molecular transport through the porous support layer is mainly by convective flow, and no separation occurs in this layer [48].

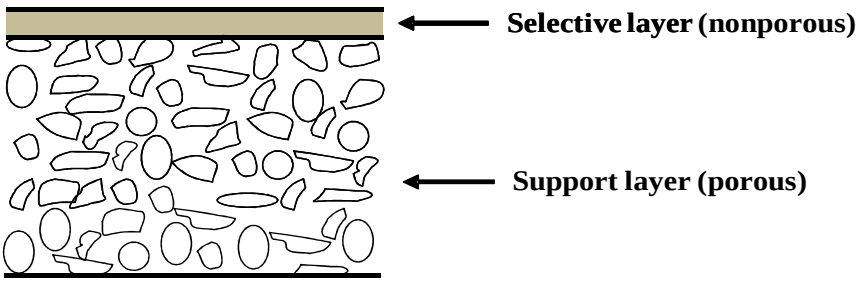

Figure 2-2 Schematic structure of a composite membrane

In this research, polymeric composite membranes (CMS-7 or CMS-3) are used. These membranes are supplied by Compact Membrane Systems, Inc. (CMS). The thin selective layer of CMS membranes is made of perfluoro-2,2-dimethyl-1,1,3-dioxole copolymerized with tetrafluoroethylene with varying copolymer ratios (such as AF2400 and AF1600) and are commercially available from Dupont [49-53]. The porous support is usually made from polytetrafluoroethylene (PTFE).

2.4.2 Membrane modules

A general mass transport equation has the form of $m_i = J_i \cdot A \cdot \Delta t$, where A is the flow area (cm^2), m_i is the mass of a species *i* that passes through that area (g), and Δt is the time interval of mass flow. A large membrane area is beneficial to process a large amount of feed.

In pilot-scale or industrial-scale processes, membranes are packed into compact, high-surface-area, and economical membrane modules. Membrane module types include hollow fiber membrane modules, plate-and-frame modules, tubular modules, spiral-wound modules and vibrating-rotating modules. Each type of these modules has its own advantages and restrictions and thus one type is more often used in certain applications than others. The details of these modules can be found easily in any membrane technology books [17, 20, 47]. In this research, hollow fiber membrane modules supplied by Compact Membrane Systems, Inc. (CMS) are employed. Figure 2-3 is a schematic of a shell-side feed hollow fiber membrane module. The selective layer is on the outside of the fibers. In such a module, a closed bundle of thousands of fibers is contained in a vessel. The feed solution comes from the shell side. Permeate passes through the fiber wall and exists through the open fiber ends potted with an epoxy resin.

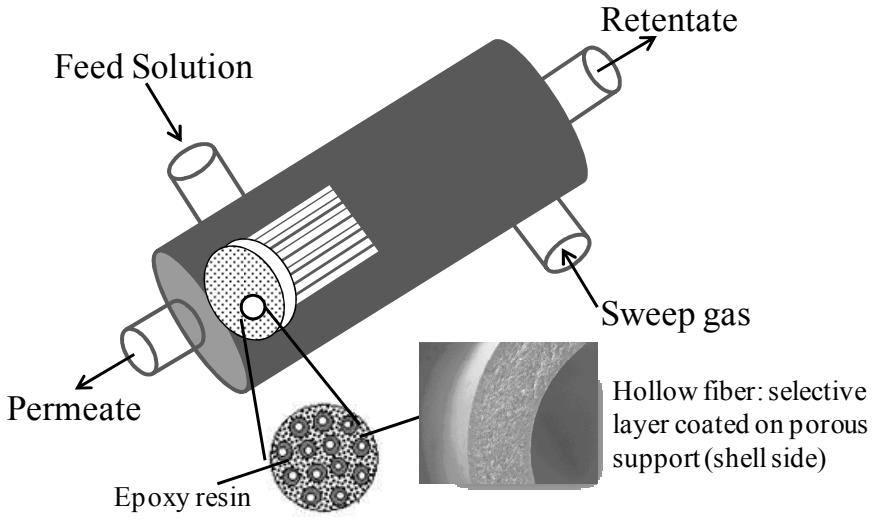

Figure 2-3 Schematic of the construction of a shell-side feed hollow fiber module

2.4.3 Membrane characterization

The structure of membranes used in this research is characterized by scanning electron microscopy (SEM). The overall structure including the top surface, the cross-section and the bottom surface can be observed clearly. The thickness of each layer can be obtained. Significant changes in the membranes after use in pervaporation experiments, if any, can be observed by SEM also.

A common characterization that has been done on almost all membranes after they are fabricated is the pure gas permeance measurement. Two types of test apparatuses based on the same theoretical mechanism are used here: constant pressure/variable volume system and constant volume/variable pressure system [54].

Figure 2-4 displays the schematic of a constant pressure/variable volume system.

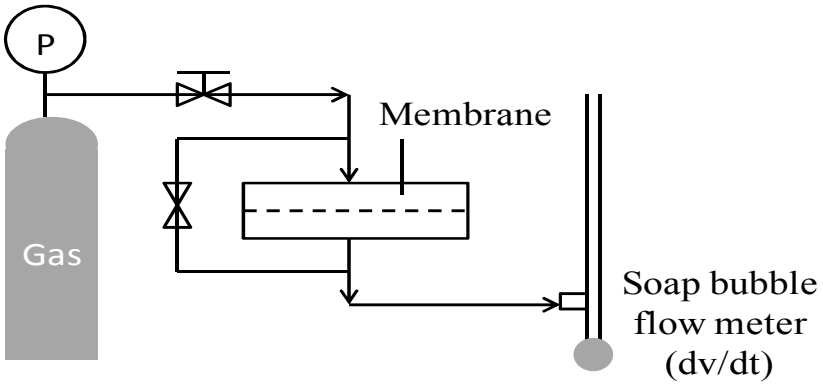

Figure 2-4 Constant pressure/variable volume system set-up

The apparatus consists of a Millipore filter holder with an effective membrane area of 13.8 cm^2. Prior to each test, the upstream and downstream sides of the permeation cell are purged with the test gas. Gas is fed to the upstream side of the membrane cell at fixed pressure. The downstream pressure is maintained at one atmosphere. The system temperature is not controlled, and is only recorded from a digital temperature indicator. The flow rate of the gas permeating through the membrane is measured by a bubble flow meter and stop watch. Therefore, during the experiment, dV/dt is recorded. The permeance is calculated from Equation 2-6.

$$\frac{P^G}{l} = 22414 \frac{p_1}{RT} \frac{dV}{dt} \frac{1}{(p_2 - p_1) \cdot A} \qquad \text{Equation 2-6}$$

where $\frac{P^G}{l}$ is the permeance with a unit GPU (1 GPU =10^{-6} cm^3 (STP)/cm^2·s·cmHg), 22414 is the volume occupied by one mole of ideal gas at standard pressure and temperature (cm^3(STP)), p_1 is the downstream pressure (atmospheric pressure in this case), p_2 is the upstream pressure (cmHg), R is the gas constant (82.05746 cm^3·atm/(mol·K)), T is the temperature (K), A is the membrane/film area (cm^2), l is the membrane/film thickness (cm), and dV/dt is the volumetric displacement rate of the soap film in the bubble flow meter (cm^3/s). The permeability coefficient P^G is the product of permeance and membrane thickness. It is usually reported with a unit called Barrer (1 Barrer = 10^{-10} cm^3 (STP)·cm/cm^2·s·cmHg).

For conditions of a low flow rate of permeating gas, permeability coefficients were measured in a constant volume/variable pressure apparatus. This apparatus measures the amount of gas permeating through the membrane into a known volume chamber. Figure 2-5 displays the set-up of a constant volume/variable pressure system.

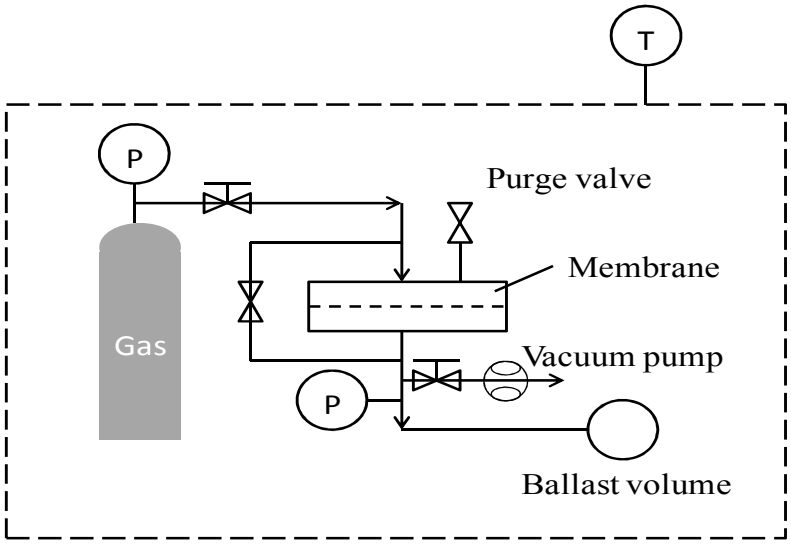

Figure 2-5 Constant volume/variable pressure system set-up

This apparatus is maintained at 35°C using a temperature controller. The leak rate of the system is measured and determined to be less than 0.001 Torr/hour. Prior to each experiment, the permeate side of the membrane cell is evacuated to below 0.5 Torr and. During the test, gas is fed from the upstream side of the membrane/film at fixed pressure, permeates through and is accumulated inside the chamber of known volume. The pressure in the downstream chamber is measured by a pressure transducer (MKS instruments, type 122AA-00010-10), and the time is

recorded using a stop watch. The pressure is allowed to increase up to a maximum of 10 Torr to maintain the condition of negligible downstream pressure as compared to the upstream pressure. The following expression is used to calculate the permeance:

$$\frac{P^G}{l} = 22414 \frac{V}{RT} \frac{dp}{dt} \frac{1}{p_{abs} \cdot A} \qquad \text{Equation 2-7}$$

where 22414 is the volume occupied by one mole of ideal gas at standard pressure and temperature (cm^3(STP)), V is the downstream chamber volume (cm^3), R is the gas constant (8314472 cm^3·Pa/(mol·K)), T is the temperature (306.85 K in this case), d*p*/dt is the pressure increase rate in the chamber (Pa/s), *l* is the membrane/film thickness (cm), A is the membrane/film area (cm^2), and p_{abs} is the absolute upstream pressure (cmHg).

The ideal gas selectivity of a membrane can be calculated as the ratio of the permeance of two gases (e.g. $\alpha_{O_2/N_2} = \frac{P_{O_2}^G / l}{P_{N_2}^G / l}$) [55, 56]. The ideal gas selectivity is an excellent indicator of membrane integrity. With an absolutely perfect membrane selective layer, the membrane will show a characteristic gas selectivity. By comparing the performance of the membrane before and after use in membrane reactor systems, any difficulties that develop with use can be monitored.

2.5 References

[1] H.S. Stoker, General, Organic, and Biological Chemistry, 6th ed., Brooks/Cole, Cengage Learning, 2012.

[2] J. Koskikallio, Alcoholysis, acidolysis and redistribution of esters, in: S. Patai (Ed.) The Chemistry of Carboxylic Acids and Esters, John Wiley & Sons, Ltd., Chichester, 1969.

[3] J. Otera, Transesterification, Chemical Reviews, 93 (1993) 1449-1470.

[4] J.H. Teles, N. Rieber, K. Breuer, D. Demuth, H. Hibst, H. Etzrodt, U. Rheude, Method for producing enol ethers, US Patent US006211416 B1, (2001).

[5] X. Rao, Z. Ding, H. Lou, J. Wu, Y. Fang, B. Deng, Method of preparing clarithromycin, US Patent US2010/0280230 A1, (2010).

[6] C.H. Lin, R.H. Falk, C.R. Stocking, Rapid chemical dehydration of plant material for light and electron-microscopy with 2,2-dimethoxypropane and 2,2-diethoxypropane, Am J Bot, 64 (1977) 602-605.

[7] H. Maarse, Volatile Compounds in Foods and Beverages (Food Science and Technology), 1st ed., CRC Press, 1991.

[8] D.D. Ebbing, S.D. Gammon, General Chemistry, 9th ed., Brooks/Cole, Cengage Learning, 2010.

[9] A. Carton, G. Gonzalez, A.I. Delatorre, J.L. Cabezas, Separation of ethanol water mixtures using 3a molecular-sieve, Journal of Chemical Technology and Biotechnology, 39 (1987) 125-132.

[10] W.K. Teo, D.M. Ruthven, Adsorption of water from aqueous ethanol using 3-a molecular-sieves, Industrial & Engineering Chemistry Process Design and Development, 25 (1986) 17-21.

[11] V. Van Hoof, L. Van den Abeele, A. Buekenhoudt, C. Dotremont, R. Leysen, Economic comparison between azeotropic distillation and different hybrid systems combining distillation with pervaporation for the dehydration of isopropanol, Sep Purif Technol, 37 (2004) 33-49.

[12] V. Gomis, R. Pedraza, O. Frances, A. Font, J.C. Asensi, Dehydration of ethanol using azeotropic distillation with isooctane, Ind Eng Chem Res, 46 (2007) 4572-4576.

[13] R.S. Morse, High vacuum dehydration and distillation, Chem Ind-London, (1948) S13-S19.

[14] A.I. Yeh, L. Berg, The dehydration of ethanol by extractive distillation, Chem Eng Commun, 113 (1992) 147-153.

[15] K.K. Sirkar, P.V. Shanbhag, A.S. Kovvali, Membrane in a reactor: A functional perspective, Ind. Eng. Chem. Res., 38 (1999) 3715-3737.

[16] B.V.d. Bruggen, Pervaporation membrane reactors, in: Comprehensive Membrane Science and Engineering, Elsevier Science, 2010, pp. 135-163.

[17] R.W. Baker, Membrane Technology and Applications, 2nd ed., John Wiley & Sons, Ltd., England, 2004.

[18] F. Lipnizki, R.W. Field, P.K. Ten, Pervaporation-based hybrid process: a review of process design, applications and economics, Journal of Membrane Science, 153 (1999) 183-210.

[19] B. Smitha, D. Suhanya, S. Sridhar, M. Ramakrishna, Separation of organic-organic mixtures by pervaporation - a review, Journal of Membrane Science, 241 (2004) 1-21.

[20] W. Ho, K. Sirkar, Membrane Handbook, 1 ed., Springer, 1992.

[21] A. Jonquieres, R. Clement, P. Lochon, J. Neel, M. Dresch, B. Chretien, Industrial state-of-the-art of pervaporation and vapour permeation in the western countries, Journal of Membrane Science, 206 (2002) 87-117.

[22] J.G. Wijmans, R.W. Baker, The solution-diffusion model - a review, Journal of Membrane Science, 107 (1995) 1-21.

[23] R.W. Baker, J.G. Wijmans, Y. Huang, Permeability, permeance and selectivity: A preferred way of reporting pervaporation performance data, Journal of Membrane Science, 348 (2010) 346-352.

[24] Y.C. Wang, S.C. Fan, K.R. Lee, C.L. Li, S.H. Huang, H.A. Tsai, J.Y. Lai, Polyamide/SDS-clay hybrid nanocomposite membrane application to water-ethanol mixture pervaporation separation, Journal of Membrane Science, 239 (2004) 219-226.

[25] Y.S. Zhu, H.F. Chen, Pervaporation separation and pervaporation-esterification coupling using crosslinked PVA composite catalytic membranes on porous ceramic plate, Journal of Membrane Science, 138 (1998) 123-134.

[26] B.B. Li, Z.L. Xu, F.A. Qusay, R. Li, Chitosan-poly (vinyl alcohol)/poly (acrylonitrile) (CS-PVA/PAN) composite pervaporation membranes for the separation of ethanol-water solutions, Desalination, 193 (2006) 171-181.

[27] Q.G. Zhang, Q.L. Liu, A.M. Zhu, Y. Xiong, L. Ren, Pervaporation performance of quaternized poly(vinyl alcohol) and its crosslinked membranes for the dehydration of ethanol, Journal of Membrane Science, 335 (2009) 68-75.

[28] P. Shao, R.Y.M. Huang, Polymeric membrane pervaporation, J Membrane Sci, 287 (2007) 162-179.

[29] Y. Wang, M. Gruender, T.S. Chung, Pervaporation dehydration of ethylene glycol through polybenzimidazole (PBI)-based membranes. 1. Membrane fabrication, J Membrane Sci, 363 (2010) 149-159.

[30] W.L. Qiu, M. Kosuri, F.B. Zhou, W.J. Koros, Dehydration of ethanol-water mixtures using asymmetric hollow fiber membranes from commercial polyimides, J Membrane Sci, 327 (2009) 96-103.

[31] Y. Ma, J.H. Wang, T. Tsuru, Pervaporation of water/ethanol mixtures through microporous silica membranes, Separation and Purification Technology, 66 (2009) 479-485.

[32] O. de la Iglesia, R. Mallada, M. Menendez, J. Coronas, Continuous zeolite membrane reactor for esterification of ethanol and acetic acid, Chemical Engineering Journal, 131 (2007) 35-39.

[33] S.L. Wee, C.T. Tye, S. Bhatia, Membrane separation process-Pervaporation through zeolite membrane, Separation and Purification Technology, 63 (2008) 500-516.

[34] H. Zhou, D. Korelskiy, T. Leppajarvi, M. Grahn, J. Tanskanen, J. Hedlund, Ultrathin zeolite X membranes for pervaporation dehydration of ethanol, Journal of Membrane Science, 399 (2012) 106-111.

[35] D.A. Fedosov, A.V. Smirnov, E.E. Knyazeva, I.I. Ivanova, Zeolite membranes: synthesis, properties, and application, Petrol Chem, 51 (2011) 657-667.

[36] L.J. Shan, J. Shao, Z.B. Wang, Y.S. Yan, Preparation of zeolite MFI membranes on alumina hollow fibers with high flux for pervaporation, Journal of Membrane Science, 378 (2011) 319-329.

[37] Z. Huang, Y. Shi, R. Wen, Y.H. Guo, J.F. Su, T. Matsuura, Multilayer poly(vinyl alcohol)-zeolite 4A composite membranes for ethanol dehydration by means of pervaporation, Separation and Purification Technology, 51 (2006) 126-136.

[38] H.M. Guan, T.S. Chung, Z. Huang, M.L. Chng, S. Kulprathipanja, Poly(vinyl alcohol) multilayer mixed matrix membranes for the dehydration of ethanol-water mixture, Journal of Membrane Science, 268 (2006) 113-122.

[39] H.L. Sun, L.Y. Lu, X. Chen, Z.Y. Jiang, Pervaporation dehydration of aqueous ethanol solution using H-ZSM-5 filled chitosan membranes, Separation and Purification Technology, 58 (2008) 429-436.

[40] D. Yang, J. Li, Z.Y. Jiang, L.Y. Lu, X. Chen, Chitosan/TiO2 nanocomposite pervaporation membranes for ethanol dehydration, Chemical Engineering Science, 64 (2009) 3130-3137.

[41] S. Amnuaypanich, T. Naowanon, W. Wongthep, P. Phinyocheep, Highly water-selective mixed matrix membranes from natural rubber-blend-poly(acrylic acid) (NR-blend-PAA) incorporated with zeolite 4A for the dehydration of water-ethanol mixtures through pervaporation, Journal of Applied Polymer Science, 124 (2012) E319-E329.

[42] H.S. Samanta, S.K. Ray, P. Das, N.R. Singha, Separation of acid-water mixtures by pervaporation using nanoparticle filled mixed matrix copolymer membranes, Journal of Chemical Technology and Biotechnology, 87 (2012) 608-622.

[43] V. Van Hoof, C. Dotremont, A. Buekenhoudt, Performance of Mitsui NaA type zeolite membranes for the dehydration of organic solvents in comparison with commercial polymeric pervaporation membranes, Separation and Purification Technology, 48 (2006) 304-309.

[44] T.S. Chung, L.Y. Jiang, Y. Li, S. Kulprathipanja, Mixed matrix membranes (MMMs) comprising organic polymers with dispersed inorganic fillers for gas separation, Prog Polym Sci, 32 (2007) 483-507.

[45] S. Amnuaypanich, J. Patthana, P. Phinyocheep, Mixed matrix membranes prepared from natural rubber/poly(vinyl alcohol) semi-interpenetrating polymer network (NR/PVA semi-IPN) incorporating with zeolite 4A for the pervaporation dehydration of water-ethanol mixtures, Chemical Engineering Science, 64 (2009) 4908-4918.

[46] A.M.W. Hillock, S.J. Miller, W.J. Koros, Crosslinked mixed matrix membranes for the purification of natural gas: Effects of sieve surface modification, Journal of Membrane Science, 314 (2008) 193-199.

[47] M. Mulder, Basic Principles of Membrane Technology, Springer, 1996.

[48] I. Pinnau, J.G. Wijmans, I. Blume, T. Kuroda, K.V. Peinemann, Gas permeation through composite membranes, Journal of Membrane Science, 37 (1988) 81-88.

[49] A.M. Polyakov, L.E. Starannikova, Y.P. Yampolskii, Amorphous Teflons AF as organophilic pervaporation materials transport of individual components, J Membrane Sci, 216 (2003) 241-256.

[50] A.Y. Alentiev, Y.P. Yampolskii, V.P. Shantarovich, S.M. Nemser, N.A. Plate, High transport parameters and free volume of perfluorodioxole copolymers, Journal of Membrane Science, 126 (1997) 123-132.

[51] S.M. Nemser, I.C. Roman, Perfluorodioxole Membranes, US Patent 5051114, (1991).

[52] A.M. Polyakov, L.E. Starannikova, Y.P. Yampolskii, Amorphous Teflons AF as organophilic pervaporation materials Separation of mixtures of chloromethanes, J Membrane Sci, 238 (2004) 21-32.

[53] V. Smuleac, J. Wu, S. Nemser, S. Majumdar, D. Bhattacharyya, Novel perfluorinated polymer-based pervaporation membranes for the separation of solvent/water mixtures, Journal of Membrane Science, 352 (2010) 41-49.

[54] S.A. Stern, P.J. Gareis, T.F. Sinclair, P.H. Mohr, Performance of a versatile variable-volume permeability cell. Comparison of gas permeability measurements by the variable-volume and variable-pressure methods, Journal of Applied Polymer Science, 7 (1963) 2035-2051.

[55] D.R. Paul, Y. P.Yampolskii, Polymeric Gas Separation Membranes, 1st ed., CRC Press, 1993.

[56] B. Freeman, Y. Yampolskii, Membrane Gas Separation, 1st ed., John Wiley & Sons, 2011.

Chapter 3 - Improving Chemical Production Processes by Selective Byproduct Removal in a Pervaporation Membrane Reactor

3.1 Abstract

Esters have wide applications in industry and laboratory since they can be used as flavoring agents, pharmaceuticals, cosmetics or conveniently serve as starting materials in multiple reactions. Esterification and transesterification are convenient means to synthesize esters. Frequently, a large excess of one of the reactants is mandatory to obtain good yields for these equilibrium driven reactions. If water or methanol, the typical by-product from these reactions, can be selectively removed, the thermodynamic limitations of these reactions can be overcome thus higher yields can be obtained. Pervaporation membrane reactors are promising systems for these reactions since they can selectively remove the byproduct, increase reaction rate and are more energy efficient compared to conventional downstream separation techniques, such as distillation. In this paper, the esterification of oleic acid with ethanol and the more challenging case, transesterification of methyl benzoate with *n*-butanol were studied in pervaporation membrane reactors equipped with perfluorinated composite membranes. A 95% yield of ethyl oleate in the esterification reaction was reached within 60 hours and the conversion of methyl benzoate in the transesterification reaction was increased from 52% to 77%.

3.2 Introduction

Membrane reactors have been investigated since the 1970s and are receiving increased attention as an alternative to distillation [1]. In a pervaporation-aided membrane reactor, a feed liquid mixture contacts one side of a membrane; one or more components of the liquid permeate through the membrane and is removed as a vapor from the other side. The partial pressure difference between the vapor pressure of the feed solution and the permeate promotes transport through the membrane [2].

Membrane reactors operating in pervaporation conditions have the potential to significantly increase product yields and reaction rates achieved in conventionally equilibrium-limited reactions. In a pervaporation-aided membrane reactor, since the membrane inside the reactor allows selective permeation of one product component (usually the by-product, such as

water or low molecular weight alcohol) from the reaction mixture, it is possible to enhance the conversion of a thermodynamically or kinetically limited reaction by shifting the reaction towards higher yield direction [1, 3, 4]. As well as reaching higher yields, membrane reactors may also save energy and reduce cost [2, 5]. A conventional reactor system requires a downstream separator to purify the products from any unreacted feeds and allow for recycle of unreacted feed. Conventional separation methods are often energetically demanding. Traditional removal technologies include distillation, extraction, adsorption, and crystallization. For compounds which are heat or solvent sensitive, chemical entrainers are necessary. In every case, the removal of by-products requires large amounts of energy for direct heating, regeneration of any solvent or dehydrating agent, and treatment of the generated waste. Membrane reactors have the potential to simplify separations and reduce energy demand [6]. With a membrane reactor and its rapid selective removal of by-products, the separation of byproducts from the reaction mixture will be a smaller device, and the separation of the reaction products may no longer be necessary, thus saving energy and reducing cost.

Esters are very important fine chemicals. They have applications in a variety of areas such as cosmetics, flavors, pharmaceuticals, plasticizers, solvents, and monomers, and they can also serve conveniently as starting materials in multiple reactions. Esterification and transesterification reactions have been broadly employed in laboratory and industry for ester synthesis. Frequently, these reactions have low product yields due to the thermodynamic equilibrium limitation and a large excess of one of the reactants is mandatory to obtain good conversions. These reactions are well-suited for the use of a membrane reactor system in that if the by-product water or low molecular weight alcohol could be selectively removed from the reaction mixture, higher conversion than thermodynamic equilibrium conversion can be achieved and a large excess of one of the reactants may not be necessary.

Consequently, numerous studies have been conducted on ester synthesis via esterification reactions in membrane reactor systems [5, 7-14]. Recently, the esterification of oleic acid with ethanol has attracted research interest since this reaction is a typical model reaction widely studied as the pre-treatment step of lipids for the biodiesel (fatty acid esters) production [15-19]. Lipids used for biodiesel production usually contain more than 1% w/w free fatty acid (FFA) and water. FFA and water in the lipid feedstock can rapidly react with the base catalyst, consuming it and giving way to long chain soaps, which will reduce the yield and formation rate of the fatty

acid esters, also bring difficulty for the separation of glycerol in the final step of the biodiesel production process [20, 21]. Thus a pre-treatment esterification step to reduce the FFA content in lipid feedstock to levels below 1% w/w must be considered as mandatory [22]. Lucena et al. used a reactor coupled with a zeolite 3A filled adsorption column to study oleic acid esterification with ethanol. An ethyl ester yield of 99.9±0.1% was obtained at 110°C with an initial ethanol to oleic acid molar ratio of 3 and 1% w/w sulfuric acid catalyst concentration [15]. This high conversion was achieved by using water removing zeolites which require ex-situ regeneration following use. While possible in the laboratory, such a technique is inappropriate for commercial-scale production. Rather, this work investigates the heterogeneously catalyzed esterification of oleic acid with ethanol to produce ethyl oleate in a membrane reactor system (Scheme 3-1).

Transesterification is an important synthetic process used as an alternative method to synthesize esters. On some occasions, transesterification is more advantageous than esterification. For instance, some carboxylic acids are sparingly soluble in organic solvents and according difficult to subject to homogeneous esterification. Transesterification is particularly useful when the parent carboxylic acids that can be used for esterification are labile or difficult to isolate [23]. While esterification reactions are the main class of reactions that have been studied in pervaporation membrane reactors, transesterification reactions have rarely been investigated in pervaporation membrane reactor systems because of the limited availability of pervaporation membranes that have long-term stability and sufficient selectivity of the by-product to reactant alcohols [24-27]. This study is concerned with the homogenously catalyzed transesterification of methyl benzoate with butanol (Scheme 3-2) in an enhanced continuous pervaporation membrane reactor system.

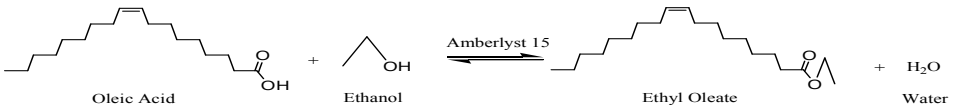

Scheme 3-1 Esterification of oleic acid and ethanol to ethyl oleate and water.

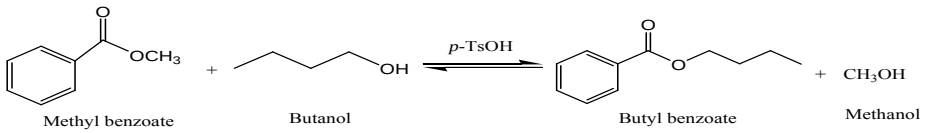

Scheme 3-2 Transesterification of methyl benzoate and butanol to butyl benzoate and methanol.

3.3 Materials and methods

3.3.1 Membranes and membrane reactor system

The membranes, CMS-7-ePTFE®, used in this work were supplied by Compact Membrane Systems, Inc. (CMS). The composite membranes are made of perfluoro-2,2-dimethyl-1,1,3-dioxole copolymerized with tetrafluoroethylene with varying copolymer ratios (such as AF2400 and AF1600) [28, 29] on e-PTFE support. Gas permeation tests (constant pressure/variable volume apparatus) with nitrogen, oxygen, and helium were performed on disc membranes before and after they were used for pervaporation experiments. Membranes were examined (cross-section and membrane surface) by Scanning Electron Microscopy (SEM) right after they were cut from a flat sheet and after they were used for pervaporation experiments. The membrane samples for SEM were prepared by sectioning with two tweezers in liquid nitrogen.

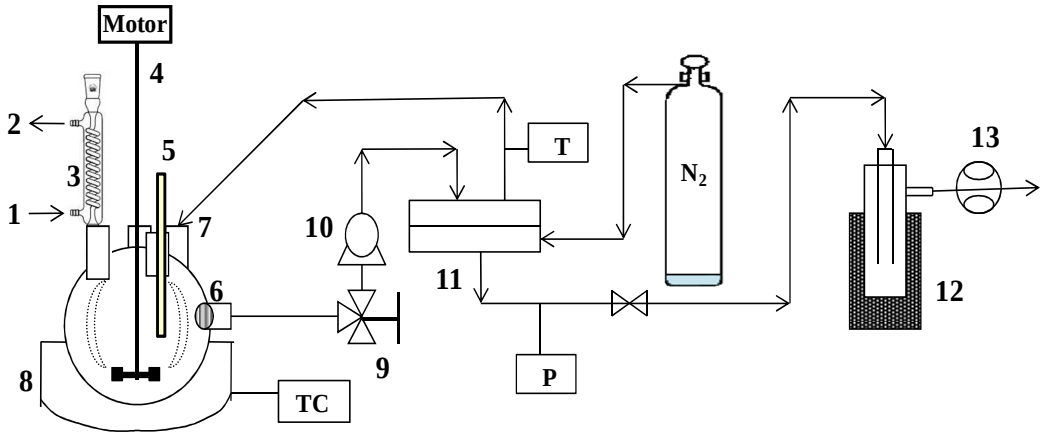

Figure 3-1: Schematic of the pervaporation membrane reactor system. 1,2–Cold water inlet-outlet to reflux condenser; 3–reflux condenser; 4–agitator; 5–thermocouple; 6–reaction mixture outlet with an inline filter; 7–retentate line; 8–heating mantle; 9–sample port; 10–circulation pump; 11–membrane; 12–liquid nitrogen cold trap; 13–vacuum pump.

The pervaporation membrane reactor system is shown in Figure 3-1. The feed solution was kept in a 500 mL five-neck round-bottom glass reactor with a reflux condenser. The reactor temperature was controlled by a hemispherical mantle (Thermo Scientific). An inline filter in the reactor maintains the catalyst inside the reactor. A circulation pump (FMI lab pump Model QV,

fluid metric Inc.) was used to circulate the reactant mixture through the membrane module. The selected membrane was installed into a modified 47 mm stainless steel filter holder (EMD Millipore), which provided a filtration area of 13.8 cm^2. All components of the feed side circulation system were built using 1/8' stainless steel tubing and fittings (Swagelok, Inc.). On the permeate side, a liquid nitrogen cold trap was connected to condense the permeate, and a vacuum pump (RV5, BOC Edwards) created low pressure at the permeate side of the membrane cell (typically 0.002-0.004 bar). The permeate pressure was measured using an absolute pressure transducer (MKS instruments, type 122AA-00010-10). The permeate side of the membrane was purged with nitrogen (UHP/zero grade) to assist the byproduct removal.

3.3.2 Esterification and transesterification experiments

For esterification reactions, oleic acid (NF/FCC grade), hexane (GC resolv grade) and ethyl oleate (>=98%) were obtained from Fischer Scientific. Ethanol (EtOH, 99.5%, anhydrous, 200 proof) was purchased from Acros Organics. The catalyst Amberlyst® 15 (hydrogen form, strongly acidic, cation exchanger, dry, moisture ~5%) was purchased from Sigma-Aldrich. The reactor was heated to 65°C and was charged sequentially with oleic acid (0.5 mol), ethanol (1.0 mol) and catalyst (5% w/w). Once all components were charged into the reactor, aliquots (200 μL) were sampled periodically from the sample port. Then, 2 mL of hexane (an internal standard for gas chromatography analysis) were added to the sample and mixed by a vortex mixer. 1 μL analyte was injected into a HP 6890 series gas chromatograph (FID detector, capillary column CP-Sil 88, 100 m length, 0.25 mm i.d., oven temperature 250°C, column temperature 181°C; J&W Scientific) for analysis. During pervaporation experiments, permeate was collected in a cold trap over the entire duration of an individual experiment and was analyzed at the end of each experiment. The control experiments were carried out in the apparatus without the membrane and under the same conditions as pervaporation experiments to determine the contribution of pervaporation to the completion of the reaction.

For transesterification reactions, n-butanol (BuOH, 99%), methanol (MeOH, 99.9%, HPLC grade), methyl benzoate (MeBe, reagent grade), p-xylene (>=99%, certified), homogeneous catalyst *p*-toluenesulfonic acid (monohydrate, crystalline/certified) and sodium bicarbonate (99.7+%, reagent ACS, powder) were purchased from Fischer Scientific. Butyl

benzoate (BuBe, 98+%) and molecular sieves (4Å, 4-8 mesh) were purchased from Sigma-Aldrich. To determine the thermodynamic equilibrium, both forward and reverse reactions were carried out in the batch reactor system without membranes. In forward reactions, methyl benzoate (0.04 mol), catalyst *p*-toluenesulfonic acid (0.02 g/mmol total reactants) and organic solvent p-xylene (the molar ratio of p-xylene/methyl benzoate=1) were charged into the reactor with a stirring speed of 200 rpm. After the mixture was heated to 75°C, n-butanol (0.04 mol) was added. In reverse reactions, butyl benzoate (0.04 mol) and methanol (0.04 mol) were used as reactants and remains were the same as forward reactions. For pervaporation experiments in the membrane reactor system, an equimolar ratio of reactants methyl benzoate and butanol, plus p-xylene (molar ratio of p-xylene/methyl benzoate=4) or toluene (molar ratio of toluene/methyl benzoate=3) and catalyst *p*-toluenesulfonic acid (0.05 g/mmol total reactants) were used. The reason that organic solvents were included in reaction mixtures was to evaluate CMS-7 membranes performance after exposure to aggressive solvents, as well as the membrane byproduct removal ability at low byproduct concentrations. For analysis, aliquots (200 μL) were withdrawn periodically from the sample port. Then, 1 mL of hexane and 1 mL of oversaturated sodium bicarbonate solution were added to quench the reaction and neutralize the catalyst. Two phases were observed immediately. The supernatant was removed and injected into a Varian 3800 gas chromatograph equipped with a capillary column DB-WAX (30 m length, 0.25 mm i.d., J&W Scientific) and a flame ionization detector (FID).

3.4 Results and discussion

3.4.1 Esterification reaction results

Since the oleic acid is NF/FCC grade, it is a mixture of oleic acid and trace amount of other fatty acids. Therefore, the ester products are a mixture of ethyl esters. Figure 3-2 shows the yield of ethyl esters against the time for esterification reactions in the membrane reactor system and in the conventional system. In the conventional system, the product yield increases to 71% after 75 hours and is still slowly increasing. According to Okamoto [30], the equilibrium constant of this esterification reaction is predicted to be 3.0 at 65°C. Thus, the equilibrium conversion should be 81% for a 2/1 molar ratio of ethanol to oleic acid reacted at 65°C. In the membrane reactor system operating at these conditions, a relatively faster reaction rate

(exceeding equilibrium after 35 hours) is observed and the product yield reached 96% with selective water removal. The GC analysis of the permeate collected at the end of the pervaporation experiment shows that no ethyl esters permeate the membrane. This result indicates that the membrane reactor is capable of selectively removing by-product water and increasing the product yield. Lucena, et al. reported equivalently high ethyl ester yields of 95.5 ± 0.7% but required higher temperatures (110°C), an initial molar ratio of ethanol to oleic acid of 9, and the use of a reactor system with an adsorption column for water removal [15]. By employing a membrane reactor system in this work, the product yield is increased by more than 15% beyond the conventional thermodynamic limit via a reactor operating at relatively mild conditions with limited excess reactants.

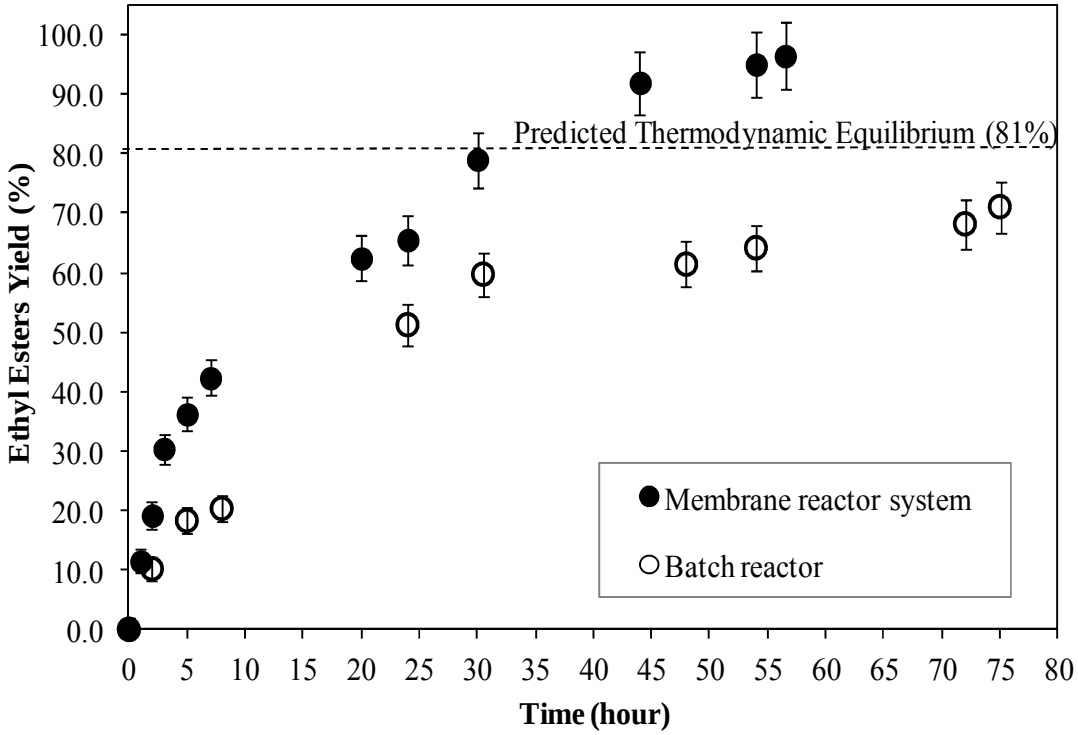

Figure 3-2 Esterification reaction ethyl esters yield versus time. A membrane reactor system equipped with a CMS7-ePTFE® membrane was employed. This run was made at 65°C and with a molar ratio of ethanol/oleic acid =2.

3.4.2 Transesterification reaction results

Kinetic curves of methyl benzoate conversion for both forward reaction and reverse reaction carried out in a batch reactor are shown in Figure 3-3. The forward reaction kinetic curve and the reverse reaction kinetic curve are almost symmetric, which means that the forward reaction rate constant should be almost equal to the reverse reaction rate constant. After 25 hours, the reaction conversion reached 52% and remained constant for the rest of the test period, which indicated that the thermodynamic equilibrium is 52% conversion when operated with an equimolar reactant ratio at 75°C. This result also indicates that there is no side reaction happened in the reaction system.

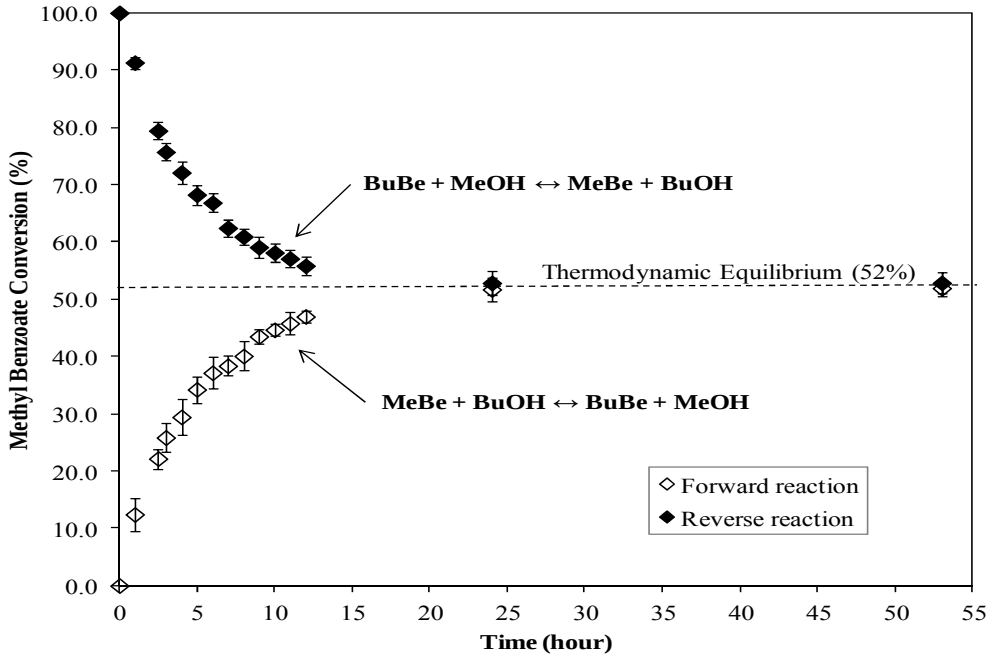

Figure 3-3 Transesterification forward and reverse reaction conversion versus time in a batch reactor without pervaporation. This run was made at 75°C and with a molar ratio of MeBe/BuOH/p-xylene =1.

In Figure 3-4, a typical transesterification conversion profile in a pervaporation-assisted membrane reactor is presented, along with the corresponding profile in a conventional reactor. With the assistance of pervaporation, the system rapidly reached 77% conversion, which exceeds the thermodynamic equilibrium by 25%. Compared to the batch reaction without pervaporation, a relatively fast reaction rate (nearly 20% conversion within the first hour) and a short reaction

time (5 hours) prior to exceeding equilibrium were also achieved in the membrane reactor system. Analysis of the permeate collected during the membrane-assisted reaction indicates that the permeate consists of 96 mol % methanol, 1 mol% butanol and 3 mol% p-xylene. Therefore, the membrane reactor is capable of selectively removing methanol and shifting the equilibrium towards higher conversion.

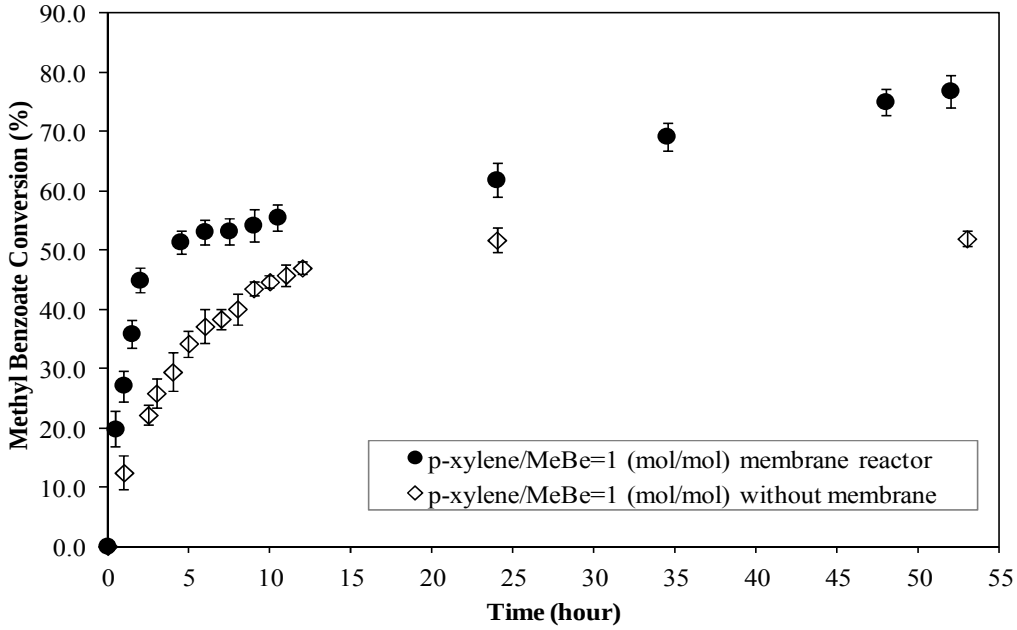

Figure 3-4 Transesterification reaction conversion versus time. A membrane-assisted reactor equipped with a CMS7-ePTFE® membrane was employed. This run was made at 75°C and with a molar ratio of MeBe/BuOH/p-xylene =1.

Figure 3-5 compares the conversions of transesterification reaction in different solvent medium in a membrane reactor system. The reaction rates and conversion achieved in the membrane reactor system were in all cases distinctly higher than those achieved in a conventional reactor. Bazi et al carried out the same transesterification reaction in a batch reactor at 110°C and obtained 100% conversion after 48 hours of reaction time using a molar ratio of butanol/MeBe of 11/2 and in toluene medium [31]. Clearly, by incorporating CMS-7 membranes, which are capable of selectively removing methanol, the transesterification reaction can be operated at a lower temperature and no excess alcohol is required. It has also been seen from the plot that the ability of methanol removal by the CMS-7 membrane is almost unaffected by the methanol concentration. As the concentration of solvent inside the reactor increases, the

concentration of byproduct methanol decreases. Since the methanol permeability of the membrane almost remain the same as the methanol concentration decreases, the difference of promoted conversion among all membrane reactor runs are insignificant.

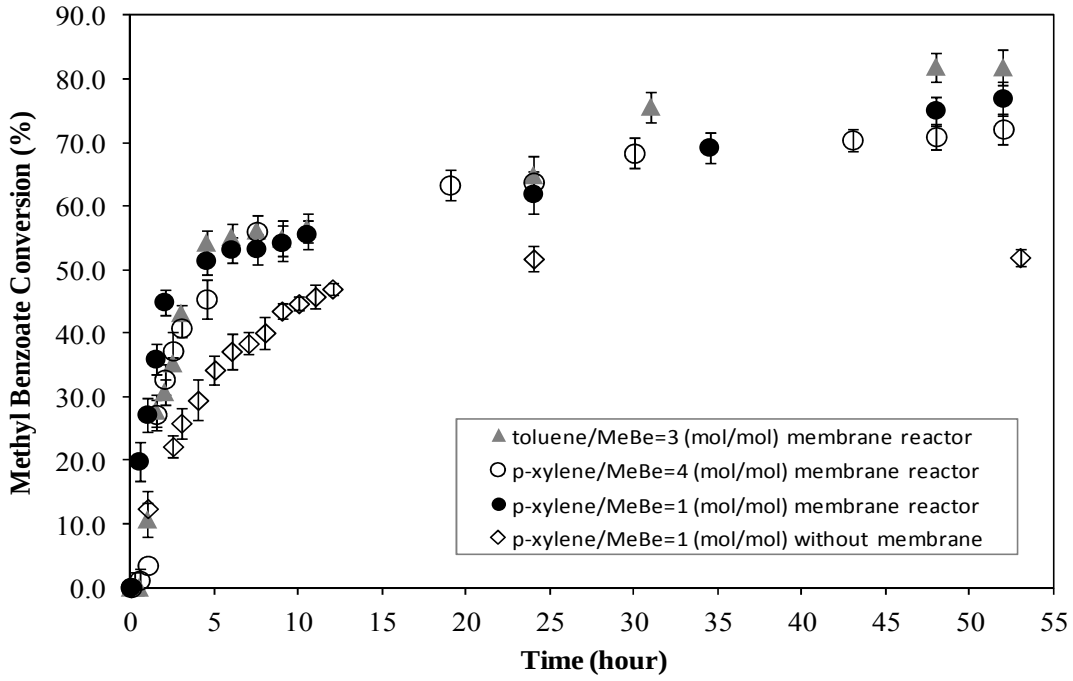

Figure 3-5 Process dynamics for transesterification reaction with differnet solvent. All runs were carried out at 75°C and with a catalyst concentration of 0.05 g catalyst /mmol total reactants.

Table 3-1 compares the percentage of methanol captured in cold traps with the calculated percentage of methanol removal to achieve the measured conversion. The solvent type and the amount of solvent were varied in each run for this comparison. The evaluated permeate molar compositions were a cumulative average over the entire reaction period. The MeOH capture is the percentage of the methanol produced in the reaction that was recovered in the trap. The methanol capture for these three runs is in the range of 75%-91%. By analyzing the permeate of all pervaporation assisted transesterification reaction runs, we have found that the permeate was primarily methanol with lesser amounts of butanol and p-xylene or toluene and no esters. If we assume there is no butanol permeating through the membrane and the equilibrium is achieved inside the reactor at the end of the reaction, the mole of methanol inside the reactor can be calculated out of the equilibrium constant of this transesterification reaction (K_{eq}=1.17) and the

esters and butanol concentrations calculated based on the conversion. Therefore, the MeOH removal can be defined as the percentage of the methanol that was produced that would have to be removed from the reactor to achieve the measured conversion. From Table 3-1, the methanol removal is in the range of 82%-94%. This range matches reasonably well with that of the methanol capture. As the concentration of p-xylene increased from run 1 to run 2, more p-xylene might dissolve in the selective layer and swell the membrane, which could cause the decrease of membrane selectivity of methanol over butanol. Compared to p-xylene, toluene has higher potential swelling capability, as evidenced by their Hansen solubility parameter (δ of toluene=18.2 $MPa^{0.5}$ and δ of p-xylene=17.9 $MPa^{0.5}$ [32]). Therefore, toluene is more likely to dissolve in the selective layer and to swell the membrane more than p-xylene, which would cause the membrane selectivity of MeOH/BuOH in run 3 to be lower than that in run 2 and run 1. This can also be proved by the fact that the permeate contained higher molar ratio of toluene than p-xylene even if less amount of p-xylene was feed into the reactor at the beginning. In all cases, the results indicate that CMS-7 membranes have high selectivity of methanol over butanol.

Table 3-1 The impact of amount of solvent and solvent type on the permeate composition of the pervaporation assisted transesterification of methyl benzoate with butanol at 75°C and equimolar reactant addition. The permeate was analyzed at the end of each run (after around 52 hours).

	Solvent Concentration (mol/mol)	MeOH Capture[a] (%)	MeOH Removal[b] (%)	Reaction Conversion (%)	Max Conversion[c] (%)	MeOH/BuOH (mol/mol) in permeate
1	p-xylene/MeBe=1	76	89	77	99	72
2	p-xylene/MeBe=4	75	82	72	97	18
3	Toluene/MeBe=3	91	94	82	91	9

a. MeOH Capture (%)=measured mmol of MeOH in trap/(mmol MeBe fed ×reaction conversion) ×100%

b. MeOH Removal (%)=calculated mmol of MeOH needed to be removed to achieve reaction conversion/(mmol MeBe fed ×reaction conversion) ×100%

c. Max Conversion (%)=(mmol MeBe fed−mmol of BuOH in trap)/ mmol MeBe fed ×100%

3.4.3 Pervaporation membranes

Figure 3-6A-E shows the SEM images of the entire CMS-7 ePTFE® membrane, which includes selective layer (before and after used for pervaporation) and porous support. From these images, the thickness of a new CMS-7 ePTFE® membrane can be estimated to be about 42 μm while the dense layer has an approximate thickness of 3.2 μm and the porous layer is about 38.8 μm. Figure 3-6D is an image of the back side of a used membrane. Since the membrane was sitting on top of the support screen inside the membrane holder during the pervaporation experiments, there are protrusions formed on the back side of the used membrane. It can be seen from Figure 3-6E that the whole thickness of used membranes is thinner than that of unused membranes. The selective layer of a used membrane has a thickness of about 1.8 μm and the porous support layer is about 10 μm. The decrease in thickness is due to the compression caused by the pressure difference on both sides of the membrane during the pervaporation process. It is also noticed that at some locations of membranes there is a separation between the dense layer and the porous layer after membranes are used in pervaporation experiments.

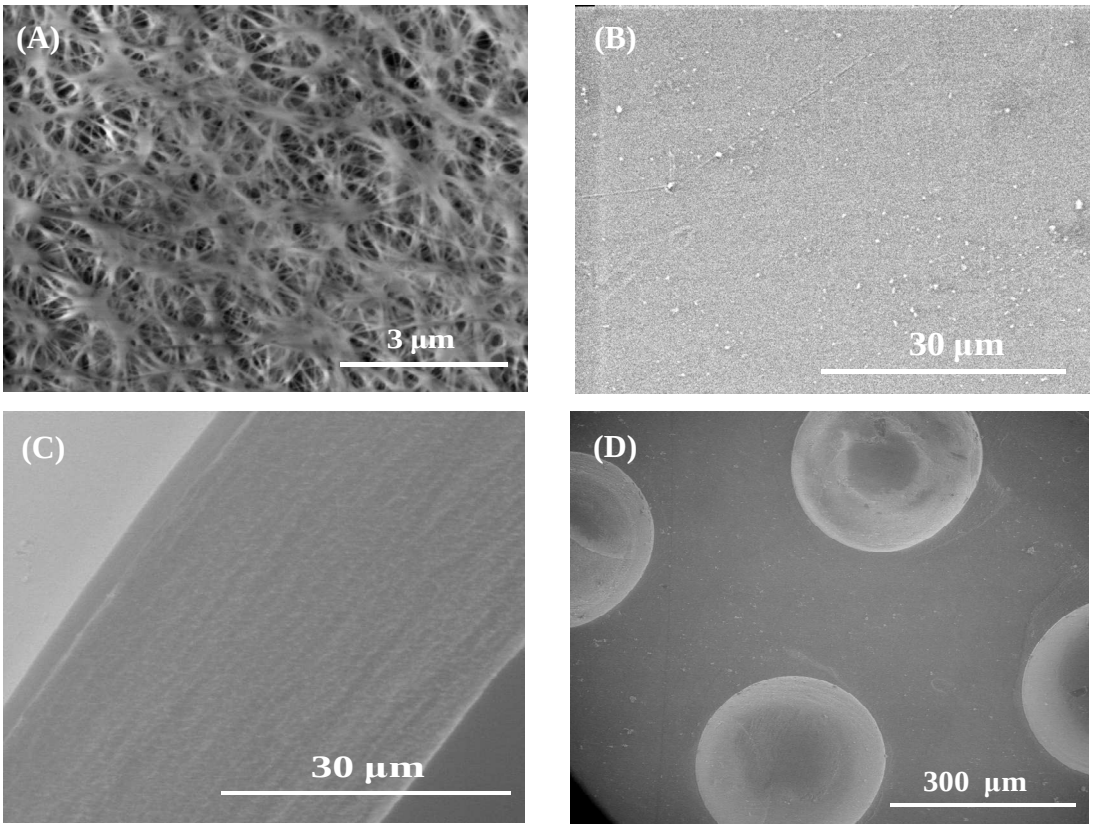

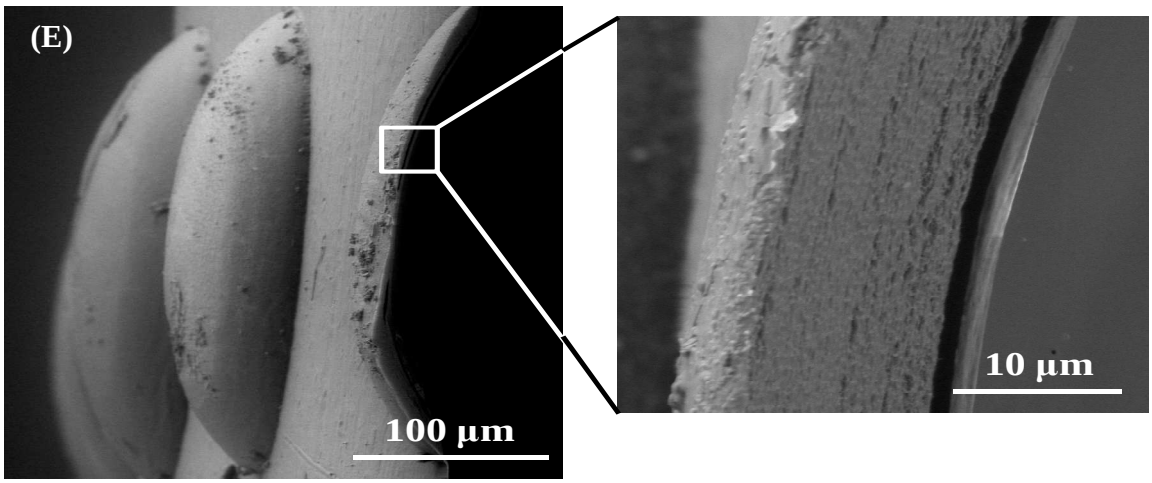

Figure 3-6 SEM images: (A) back side of an unused membrane (e-PTFE porous support) (B) denser layer of an unused membrane (C) cross-section of an unused membrane (D) back side of a used membrane (E) cross-section of a used membrane.

A series of 10 pervaporation experiments was carried out in a membrane reactor system equipped with a CMS-7 ePTFE® membrane. During a discrete 400 hours of reaction time, a single membrane stamp was kept in a temperature range of 20-75°C. The chemicals and solvents that contacted with membrane include methanol, butanol, ethanol, water, p-xylene, toluene, oleic acid, strong homogeneous acid catalyst *p*-toluenesulfonic acid, methyl benzoate and butyl benzoate. The measured gas selectivities for this CMS-7 ePTFE® membrane employed in all pervaporation experiments are listed in Table 3-2. From the data, we can observe that there are only small decreases in membrane selectivities and permeance after it was used for pervaporation-assisted esterification reactions and transesterification reactions. Therefore, we can conclude that CMS-7 ePTFE® membranes have excellent long-term stability as well as thermal and chemical resistance when they are used in the temperature range of room temperature to 75°C in the presence of organic solvents and strong homogeneous acid catalysts.

Table 3-2 CMS-7 ePTFE® membrane gas permeance and selectivity measured in a constant pressure/variable volume apparatus.

Gas	Permeance (GPU*)		Selectivity (over N_2)	
	Before	After	Before	After
N_2	117	117	—	—
O_2	241	204	2.1	1.8
H_2	525	444	4.5	3.8
He	579	501	5.0	4.3

* 1 GPU = 1×10^{-6} cm^3 (STP)/cm^2 ·s · cmHg

3.5 Conclusions

A continuous pervaporation-assisted membrane reactor system was developed with CMS7-ePTFE® membranes. Esterification reaction of oleic acid with ethanol and transesterification reaction of methyl benzoate with butanol were studied as two model reactions for organic synthesis in this membrane reactor system. In both cases, a relatively fast reaction rate and a markedly high conversion were achieved in the membrane reactor system than those achieved in batch reactor. CMS7-ePTFE® membranes have high selectivity of byproduct (water or methanol) over reactants and ester products. The loss of esters and reactant alcohols into permeate during reactions carried out in the membrane reactor system can be neglected under experiment conditions in this work. By selective removal of a by-product (water or methanol), the reaction conversion was promoted by 15% for esterification reaction and 25 % for transesterification reaction. To achieve the same or even higher degree of conversion than that reached in a conventional reactor, the pervaporation-assisted membrane reactor system equipped with CMS7-ePTFE® membranes can be operated at lower temperature and consume much less amount of alcohol reactants. Good stability and chemical resistance of these membranes have been proved by no significant loss of gas permeance and selectivity after all pervaporation experiments. This membrane reactor system can be employed to improve chemical synthesis process in terms of operation conditions and reactant consumption, and it is especially suitable for reactions involving temperature and pH sensitive substances.

3.6 Reference

[1] M. Mulder, Basic Principles of Membrane Technology, Springer, 1996.

[2] R.W. Baker, Membrane Technology and Applications, 2nd ed., John Wiley & Sons, Ltd., England, 2004.

[3] W. Ho, K. Sirkar, Membrane Handbook, 1 ed., Springer, 1992.

[4] D. Barahona, P.H. Pfromm, M.E. Rezac, Effect of water activity on the lipase catalyzed esterification of geraniol in ionic liquid [bmim]PF6, Biotechnol Bioeng, 93 (2006) 318-324.

[5] R.M. Waldburger, F. Widmer, Membrane reactors in chemical production processes and the application to the pervaporation-assisted esterification, Chem Eng Technol, 19 (1996) 117-126.

[6] K.K. Sirkar, P.V. Shanbhag, A.S. Kovvali, Membrane in a reactor: A functional perspective, Ind. Eng. Chem. Res., 38 (1999) 3715-3737.

[7] A. Hasanoglu, Y. Salt, S. Keleser, S. Dincer, The esterification of acetic acid with ethanol in a pervaporation membrane reactor, Desalination, 245 (2009) 662-669.

[8] K. Tanaka, R. Yoshikawa, C. Ying, H. Kita, K. Okamoto, Application of zeolite T membrane to vapor-permeation-aided esterification of lactic acid with ethanol, Chem Eng Sci, 57 (2002) 1577-1584.

[9] P.G. Cao, M.A. Dube, A.Y. Tremblay, High-purity fatty acid methyl ester production from canola, soybean, palm, and yellow grease lipids by means of a membrane reactor, Biomass Bioenerg, 32 (2008) 1028-1036.

[10] K. Bartling, J.U.S. Thompson, P.H. Pfromm, P. Czermak, M.E. Rezac, Lipase-catalyzed synthesis of geranyl acetate in n-hexane with membrane-mediated water removal, Biotechnol Bioeng, 75 (2001) 676-681.

[11] O. de la Iglesia, R. Mallada, M. Menendez, J. Coronas, Continuous zeolite membrane reactor for esterification of ethanol and acetic acid, Chemical Engineering Journal, 131 (2007) 35-39.

[12] S. Korkmaz, Y. Salt, S. Dincer, Esterification of acetic acid and isobutanol in a pervaporation membrane reactor using different membranes, Ind. Eng. Chem. Res., 50 (2011) 11657-11666.

[13] J.J. Jafar, P.M. Budd, R. Hughes, Enhancement of esterification reaction yield using zeolite - A vapour permeation membrane, Journal of Membrane Science, 199 (2002) 117-123.

[14] J.E. Castanheiro, A.M. Ramos, I.M. Fonseca, J. Vital, Esterification of acetic acid by isoamylic alcohol over catalytic membranes of poly(vinyl alcohol) containing sulfonic acid groups, Applied Catalysis a-General, 311 (2006) 17-23.

[15] I.L. Lucena, R.M.A. Saboya, J.F.G. Oliveira, M.L. Rodrigues, A.E.B. Torres, C.L. Cavalcante, E.J.S. Parente, G.F. Silva, F.A.N. Fernandes, Oleic acid esterification with ethanol under continuous water removal conditions, Fuel, 90 (2011) 902-904.

[16] H.D. Hanh, T.D. Nguyen, K. Okitsu, R. Nishimura, Y. Maeda, Biodiesel production by esterification of oleic acid with short-chain alcohols under ultrasonic irradiation condition, Renew Energ, 34 (2009) 780-783.

[17] I.L. Lucena, G.F. Silva, F.A.N. Fernandes, Biodiesel production by esterification of oleic acid with methanol using a water adsorption apparatus, Ind. Eng. Chem. Res., 47 (2008) 6885-6889.

[18] A.C. Oliveira, M.F. Rosa, M.R. Aires-Barros, J.M.S. Cabral, Enzymatic esterification of ethanol and oleic acid - a kinetic study, J Mol Catal B-Enzym, 11 (2001) 999-1005.

[19] A.L. Cardoso, S.C.G. Neves, M.J. da Silva, Esterification of Oleic Acid for Biodiesel Production Catalyzed by SnCl(2): A Kinetic Investigation, Energies, 1 (2008) 79-92.

[20] J. Van Gerpen, Biodiesel processing and production, Fuel Processing Technology, 86 (2005) 1097-1107.

[21] F. Ma, L.D. Clements, M.A. Hanna, The effects of catalyst, free fatty acids, and water on transesterification of beef tallow, T Asae, 41 (1998) 1261-1264.

[22] R. Tesser, M. Di Serio, M. Guida, M. Nastasi, E. Santacesaria, Kinetics of oleic acid esterification with methanol in the presence of triglycerides, Ind. Eng. Chem. Res., 44 (2005) 7978-7982.

[23] J. Otera, Transesterification, Chemical Reviews, 93 (1993) 1449-1470.

[24] A.P. de los Rios, F.J. Hernandez-Fernandez, H. Presa, D. Gomez, G. Villora, Tailoring supported ionic liquid membranes for the selective separation of transesterification reaction compounds, Journal of Membrane Science, 328 (2009) 81-85.

[25] F. Zhang, V. Bliem, M.E. Rezac, P. Kosaraju, S. Nemser, Pervaporation membrane reactors for reversible organic reactions: modeling of the membrane-reactor performance to system design and operating conditions, accepted by the Journal of Membrane Science, 2011.

[26] A.Y. Tremblay, P.G. Cao, M.A. Dube, Biodiesel production using ultralow catalyst concentrations, Energy & Fuels, 22 (2008) 2748-2755.

[27] J.M. Fraile, R. Mallada, J.A. Mayoral, M. Menendez, L. Roldan, Shift of multiple incompatible equilibriums by a combination of heterogeneous catalysis and membranes, Chem-Eur J, 16 (2010) 3296-3299.

[28] A.Y. Alentiev, Y.P. Yampolskii, V.P. Shantarovich, S.M. Nemser, N.A. Plate, High transport parameters and free volume of perfluorodioxole copolymers, Journal of Membrane Science, 126 (1997) 123-132.

[29] V. Smuleac, J. Wu, S. Nemser, S. Majumdar, D. Bhattacharyya, Novel perfluorinated polymer-based pervaporation membranes for the separation of solvent/water mixtures, Journal of Membrane Science, 352 (2010) 41-49.

[30] K. Okamoto, M. Yamamoto, Y. Otoshi, T. Semoto, M. Yano, K. Tanaka, H. Kita, Pervaporation-aided esterification of oleic-acid, Journal of Chemical Engineering of Japan, 26 (1993) 475-481.

[31] F. Bazi, H. El Badaoui, S. Sokori, S. Tamani, M. Hamza, S. Boulaajaj, S. Sebti, Transesterification of methylbenzoate with alcohols catalyzed by natural phosphate, Synthetic Commun, 36 (2006) 1585-1592.

[32] C.M. Hansen, Hansen Solubility Parameters: A User's Handbook, 2 ed., CRC Press, Boca Raton, FL, 2007.

Chapter 4 - Pervaporation Membrane Reactors for Reversible Organic Reactions: Modeling of the Membrane-Reactor Performance to System Design and Operating Conditions

4.1 Abstract

Pervaporation membrane reactors are promising systems for reversible organic reactions since they can increase reaction rate and are more energy efficient compared to conventional separation techniques, such as distillation. As representative examples, the acetalisation of acetone with ethanol and transesterification of methyl benzoate with *n*-butanol in pervaporation membrane reactors equipped with CMS membranes were studied in the present paper. Membrane reactor experiments show that the yield of acetalisation reaction can be increased from 2% to 4% and the yield of transesterification reaction can be increased from 52% to 72%. Modeling and simulation of pervaporation membrane reactor performance for these two reactions were carried out. The simulated performance agrees well with experimental data. Using the model developed, the effect of various parameters, such as permeate pressure and membrane selectivity, on membrane reactor yield, was also examined.

4.2 Introduction

Reversible organic reactions are an important class of synthetic process used to synthesize various esters, orthoesters, ethers and ketals. These reactions have been broadly employed in laboratory and industry. The diversity of the reactant acids, aldehydes, ketones and alcohols, result in a multitude of products such as polymers, pharmaceuticals, surfactants, fungicides, insecticides, and biologically active compounds. Reversible organic reactions often do not proceed to completion, but reach equilibrium. Water or methanol is the typical by-product from these reactions. Selective removal of the by-product can overcome the thermodynamic limitation, thus reaching higher yield. Conventional removal technologies range from molecular sieves to more complex separations such as azeotropic distillation with solvents. For those compounds that are heat or solvent sensitive, chemical entrainers are necessary. In every case, the removal of water or methanol requires large amounts of energy for direct heating, regeneration of any solvent or dehydrating agent, and treatment of the generated waste. As an

alternative process to traditional methods, pervaporation membrane reactor systems are attractive due to their relative simplicity, less energy consumption and lower costs [1]. Membrane reactors operating in pervaporation conditions equipped with suitable membranes can selectively remove by-product water or methanol. Thus, they have the potential to significantly increase product yields and reaction rates achieved in conventionally equilibrium-limited reactions [2].

In recent years, a number of investigations have concentrated on pervaporation membranes applied to reversible organic reactions [3-5]. Okamoto et al. [6] used a hybrid system consisting of a batch reactor and an asymmetric polyimide hollow fiber module to study the esterification of oleic acid with ethanol. The membrane provided almost complete conversion in a short reaction time. Tanaka et al. [7] investigated the pervaporation-aided esterification of acetic acid with ethanol using zeolite T membranes. The results showed that the conversion exceeded the equilibrium limit and reached almost 100% within 8 hours. Vital et al. [8] studied the transesterification of triglycerides with methanol in a membrane reactor with sulfosuccinic acid modified poly(vinyl alcohol) membranes and Nafion membranes, respectively. The results suggested that glycerol was continuously removed from the reactor and the maximum reaction rates in a membrane reactor were higher than those in the batch reactor. A membrane reactor using a water selective organic/inorganic HybSi® membrane was used by Agirre et al. [9] to study the acetalisation reaction of ethanol with butyraldehyde. The experiments showed that the conversion of the acetalisation reaction was increased from the thermodynamic value of 40% to 70% at 70°C with a stoichiometric initial composition. Some investigations have also been done on developing kinetic models describing reaction kinetics and membrane permeation in terms of the concentration of the reacting species in membrane reactor systems. Li and Wang [10] developed a coupled kinetic model for esterification of acetic acid with n-butanol by combining the reaction kinetic equation and the permeation kinetic of water removal. Rezac et al. [11, 12] developed a simple model for the impact of reactant removal extent on the potential conversion achievable for equilibrium limited reactions. More details on kinetic models of pervaporation membrane reactors can be found in Lim et al. [13]. In this paper, we developed a preliminary model to predict membrane reactor performance with respect to membrane parameters and operating conditions.

In the present study, two types of reversible organic reactions were studied in membrane reactor systems: transesterification reactions and acetalisation reactions. The membranes

employed for membrane reactors were novel perfluorinated membranes. Transesterification is an important synthetic process to synthesize various carboxylic esters in the chemical and pharmaceutical industries [14]. The transesterification of dimethylterephthalate (DMT) with ethylene glycol is an essential part of the manufacturing process of polyester. The model reaction studied in this work for transesterification is the homogenously catalyzed transesterification of methyl benzoate with butanol (Scheme 4-1).

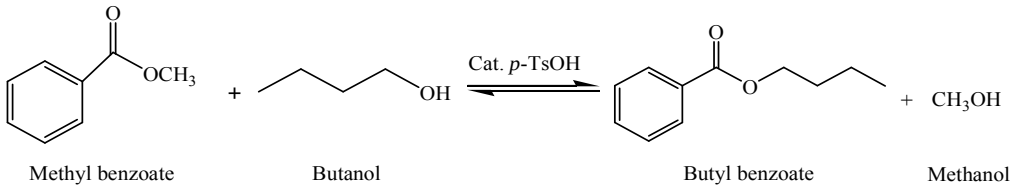

Scheme 4-1 Transesterification of methyl benzoate and butanol to butyl benzoate and methanol.

2,2-Diethoxypropane (DEP) is one of the most important members of the ketal family and is a key intermediate in the manufacture of clarithromycin, polymers and various organic compounds [15, 16]. It also can be used as a chemical dehydration agent [17]. DEP can be synthesized via the acetalisation reaction of acetone with ethanol (Scheme 4-2). Due to the exothermic nature of this reaction, the reaction favors being conducted at low temperature. The equilibrium conversion is 17% at -28°C and is only 2% at 24°C with an ethanol-acetone mole ratio of 4 [18]. To shift the equilibrium in favor of the DEP formation, it is necessary to remove the byproduct water by distillation or adding removal agents. This reaction is well suited for the use of a membrane reactor system since in that if water could be selectively removed from the reaction mixture, higher conversion can be expected.

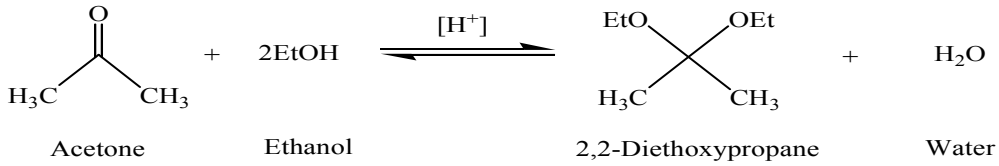

Scheme 4-2 Acetalisation of acetone and ethanol to 2,2-diethoxypropane (DEP).

4.3 Model development

The goal of this work is the development of a model which will predict steady-state conversions of reversible reactions in membrane reactor systems. Knowledge of the conversion achievable through the use of a membrane with specific properties will allow system designers to determine the selectivity and flux needed to achieve a given reaction result. This information allows one to focus on the selection of membranes with properties best suited for a given system. The desired result from the model is the product composition achievable from a membrane with given flux and selectivity properties. Thus, the value of the model is the prediction of the membrane reactor conversion exceeding the thermodynamics equilibrium conversion, not the precise identification of transient behavior. The model has been developed with the following assumptions:

- No side reactions;
- Thermodynamic equilibrium of the reaction mixture is reached instantaneously;
- Ideal mixtures, no concentration or temperature gradients in the system;
- Process is isothermal;
- Permeation properties are independent of concentration.

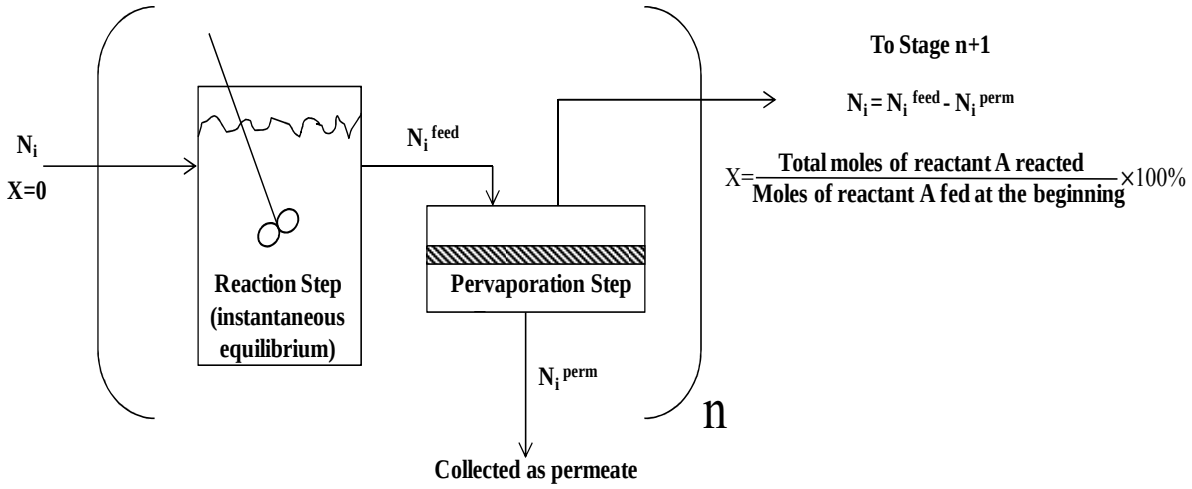

Figure 4-1 Schematic of the simulation model approach.

Figure 4-1 shows a schematic approach of the simulation model. N_i is the moles of component *i* in the reaction mixture before reaction; X is the conversion; Reactant A is the limiting reactant; n is the stage or iteration number in the model; $N_{i,}^{feed}$ is the moles of component

i in the feed to the membrane unit; $N_{i,}^{perm}$ is the moles of chosen component permeated through the membrane. The behavior of the membrane reactor system can be described by repeated units in the simulation model. Each unit is composed of one reaction step and one pervaporation step. The reaction mixture reacts at the reaction step and reaches the thermodynamic equilibrium instantaneously. Then the mixture with an equilibrium composition is fed to the pervaporation step. The retentate after the pervaporation step goes to a new reaction step in the next unit. The iterations continue until a prespecified criterion (99% of the water or alcohol by-product produced overall has been removed) is met. Hence, the model relies on two basic equations: the equilibrium equation calculating the new feed composition after a reaction step and the equation describing the flux of each component permeating through the membrane.

The reactor composition after a reaction step can be obtained by forcing the reaction quotient equal to the thermodynamic equilibrium constant K_{eq}. The equilibrium constant has to be known in order to estimate the progression of the reaction. It can be calculated either theoretically, out of the Gibbs energy change of the reaction, or experientially out of a batch reaction without pervaporation. The reaction quotient (Q) is calculated from Equation 4-1:

$$Q = \prod_i \left[\frac{(N_i + \Delta N_i)}{\sum_i (N_i + \Delta N_i)} \right]^{\nu_i} \qquad \text{Equation 4-1}$$

where N_i is the moles of component i in the reaction mixture before reaction, ΔN_i is the changed moles of component i during reaction and they are inherently related by stoichiometric coefficient. ν_i is the stoichiometric coefficient. ΔN_i and ν_i are positive for reaction products and are negative for reactants. To find the new reactor composition, ΔN_i is varied until the corresponding Q is consistent with the defined equilibrium constant. This way of calculating the progress of a chemical reaction leaves the complexity of reaction kinetics aside and is only valid under the assumption that the thermodynamic equilibrium is achieved in the reaction step instantly.

The reaction step is followed by the permeation step. The molar flux j_i of a component i through a membrane is usually described by Equation 4-2 [19]:

$$j_i = \frac{P_i^G}{l} (\gamma_{io}^L x_{io}^L p_{io}^{sat} - y_i p^{perm}) \qquad \text{Equation 4-2}$$

where P_i^G is the membrane permeability, l is the thickness of the separating layer of the membrane thickness, γ_{io}^L is the activity coefficient of component i in the feed liquid, x_{io}^L is the mole fraction of component i in the feed liquid, p_{io}^{sat} is the pure component i feed vapor pressure, y_i is the mole fraction of component i in the permeate side, and p^{perm} is the pressure on the permeate side. Pure component feed vapor pressures p_{io}^{sat} are calculated with the corresponding Antoine equations [20]. Activity coefficients can be calculated by UNIQUAC equation for multicomponent systems [21]. Due to the lack of property data for ester and ketal compounds in reaction mixtures, using this equation with estimated data may lead to a significant deviation from the real value. Therefore, activity coefficients γ_{io}^L are assumed to be one for each component in this study. The normalized permeance P_i^G / l and the permeate pressure p^{perm} represent external variables, and are assumed to be constant during the entire reaction period. The molar fraction of component i in the feed side x_{io}^L is calculated as:

$$x_{i_0}^L = \frac{N_i}{\sum_i N_i} \qquad \text{Equation 4-3}$$

The molar fraction of component i in the permeate side y_i is calculated as:

$$y_i = \frac{j_i}{\sum_i j_i} \qquad \text{Equation 4-4}$$

By solving Equation 4-2 and Equation 4-4 simultaneously, the molar flux of each component in a permeation step can be found. The size of a permeation step depends on the fraction of the moles of a chosen component removed N_i^{perm} to its initial moles in the feed N_i^{feed}, termed *FM (Fractional Removal)*. The smaller the value to which *FM* is set, the more accurate the estimation but at the cost of more iteration steps. The component selected to be tracked is usually a by-product, whose removal intends to increase the overall conversion. The moles of chosen component removed, N_i^{perm}, can also be expressed as the product of molar flux, membrane area (A) and time (t) described in Equation 4-5:

$$N_i^{perm} = N_i^{feed} \cdot FM = j_i A t \qquad \text{Equation 4-5}$$

From Equation 4-5, the *At* value of the permeation step in an iteration can be obtained; and, using this *At* value, the moles of other components permeated in the permeation step can be calculated.

4.4 Materials and methods

4.4.1 Materials

For transesterification reactions, n-butanol (BuOH, 99%), methanol (MeOH, 99.9%, HPLC grade), methyl benzoate (MeBe, reagent grade), p-xylene (>=99%, certified), hexane (GC resolv grade) as internal standard for gas chromatography analysis, homogeneous catalyst *p*-toluenesulfonic acid (monohydrate, crystalline/certified), and sodium bicarbonate (99.7+%, reagent ACS, powder) were purchased from Fischer Scientific. Butyl Benzoate (BuBe, 98+%) and molecular sieves (4Å, 4-8 mesh) were purchased from Sigma-Aldrich. For acetalisation reactions, acetone (>=99.5%, certified ACS) was obtained from Fisher Scientific. Ammonium chloride (99.5%, reagent ACS), ethanol (EtOH, 99.5%, anhydrous, 200 proof) and p-xylene (>=99%, certified) as internal standard for GC analysis, were purchased from Acros Organics. 2,2-diethoxypropane (97%) for GC-calibration was obtained from Sigma-Aldrich. Sweep gas (nitrogen) for membrane reactors and compressed gases used for gas chromatography (hydrogen, air and helium) were of UHP/zero grade and were supplied by Linweld (Manhattan, KS).

The membranes, CMS-7-ePTFE®, used in this work were supplied by Compact Membrane Systems, Inc. (CMS). The membranes are made of perfluoro-2,2-dimethyl-1,1,3-dioxole copolymerized with tetrafluoroethylene with varying copolymer ratios (such as AF2400 and AF1600) and are commercially available from Dupont [22]. Gas permeation tests (constant pressure/variable volume apparatus) with nitrogen, oxygen and helium were performed on several disc membranes cut from a flat sheet. The measured average selectivities were 2.0 and 4.9 for oxygen/nitrogen and helium/nitrogen, respectively. Only disc membranes that had selectivities of above average values were employed for membrane reactor experiments.

4.4.2 Pervaporation assisted membrane reactor system

The pervaporation experimental setup is shown in Figure 4-2. This setup consisted of the reactor, circulation system, and vacuum system for pervaporation. The selected membrane was installed into a modified 47 mm stainless steel filter holder (EMD Millipore), which provided a filtration area of 13.8 cm^2. For transesterification reactions, a 500 mL three-neck round-bottom glass reactor with a condenser was used. The reactor temperature was controlled by a hemispherical mantle (Thermo Scientific). An inline filter in the reactor protected the suction tubing from any suspended solids. For acetalisation reactions, the pervaporation experiments were carried out in a 100 mL stainless steel Parr-reactor (Parr Instrument Company). A circulation pump (FMI lab pump Model QV, fluid metric Inc.) was used to circulate the reactant mixture through the membrane module. The temperature was measured at the inlet and outlet of the membrane cell. All components of the feed side circulation system were built using 1/8' stainless steel tubing and fittings (Swagelok, Inc.). On the permeate side, a liquid nitrogen cold trap was connected to condense the permeate, and a vacuum pump (RV5, BOC Edwards) created low pressure at the permeate side of the membrane cell (typically 0.0003-0.001 bar). The permeate pressure was measured using an absolute pressure transducer (type 122A, MKS instruments). To decrease the partial pressure of the by-product alcohol in the permeate during transesterification reactions, the permeate side of the membrane was purged with nitrogen.

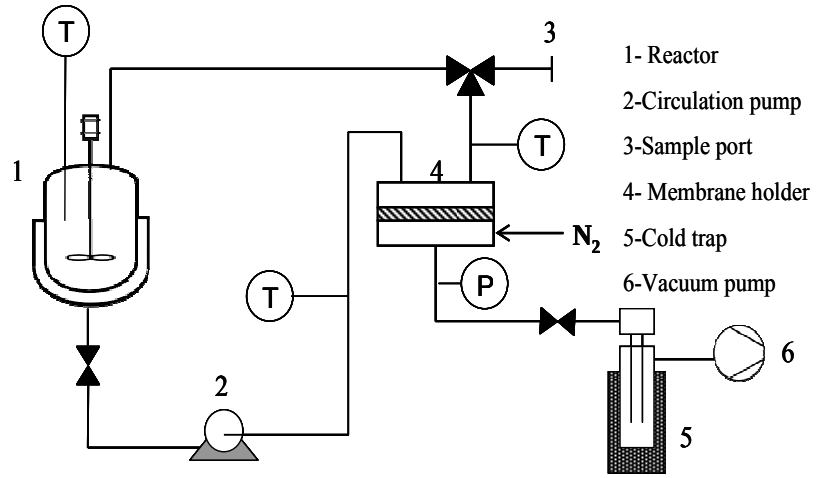

Figure 4-2 Schematic of the pervaporation assisted membrane reactor system.

4.4.3 Methods

In the transesterification study, methyl benzoate (40.0 mL, 0.32 mol), homogeneous catalyst *p*-toluenesulfonic acid (32.5 g, 0.17 mol), and organic solvent p-xylene (the molar ratio of p-xylene/methyl benzoate=4) were charged into the reactor. Reactor contents were stirred at 200 rpm. After the mixture was heated to 75°C, n-butanol (29.5 mL, 0.32 mol) was added. Aliquots (200 μL) were withdrawn periodically from the sample port. Then, 1 mL of hexane and 1 mL of oversaturated sodium bicarbonate solution was added to quench the reaction and neutralize the catalyst. Two phases were observed immediately. The supernatant was removed and injected into a Varian 3800 gas chromatograph equipped with a capillary column DB-WAX (30 m length, 0.25 mm i.d., J&W Scientific) and a flame ionization detector (FID). Permeate was collected in a cold trap over the entire duration of an individual transesterification experiment and was analyzed by GC at the end of each reaction. The mass of the collected permeate as well as its composition was determined.

To prepare the acetalisation reaction, 5g of NH_4Cl was dissolved in 100mL ethanol. 43.8 mL of this solution (containing 750 mmol ethanol) and 18.3mL acetone (250 mmol) were filled in the reactor and heated up to 25°C. When the reaction temperature was reached, the circulation flow over the membrane was started, and aliquots (200 μL) were sampled periodically from the sample port. 50 μL of p-xylene as internal standard was added to the sample solution, and 0.5 μL of this mixture was injected into a Hewlett-Packard 6890 gas chromatograph equipped with a Stabilwax capillary column (30m×0.25mm×0.25μm, Restek) and a thermal conductivity detector (TCD). The water content was determined by a Karl-Fischer titrator (Model 270, Denver Instruments).

All control experiments were carried out in the apparatus without the membrane and under the same conditions as the pervaporation experiments to determine the contribution of pervaporation to the completion of the reaction.

4.5 Experimental results

4.5.1 Pervaporation through the membrane

The membrane permeance is calculated from Equation 4-6, which is derived from Equation 4-2.

$$\frac{P_i^G}{l} = \frac{j_i}{\gamma_{i_0}^L x_{i_0}^L p_{i_0}^{sat} - y_i p^{perm}}$$ Equation 4-6

The membrane selectivity α is defined as the ratio of the permeabilities or permeances of components *i* and *j* through the membrane [19].

$$\alpha_{ij} = \frac{P_i^G}{P_j^G} = \frac{P_i^G / l}{P_j^G / l}$$ Equation 4-7

Note that the membrane separation factor ($\beta_{pervap_{ij}}$) is commonly reported as a measure of the performance of pervaporation membranes. The separation factor represents the ratio of the molar component concentrations on the permeate side of the membrane relative to that on the feed side. Hence:

$$\beta_{pervap_{ij}} = \frac{c_{i\ell} / c_{j\ell}}{c_{io} / c_{jo}}$$ Equation 4-8

where subscript *o* represents the fluid on the feed side of the membrane and ℓ represents the mixture on the permeate side. While beta represents the performance of the system for the enrichment of the component in the permeate stream, it is not strictly a function of the membrane employed. Rather, it represents the product of the enrichment due to the membrane and that due to the relative volatility of components *i* and *j*. In an attempt to differentiate the membrane enhancement from that of the thermodynamic vaporization process, Wijmans and Baker [23] analyzed the separation factor as

$$\beta_{pervap_{ij}} = \beta_{evap_{ij}} \times \beta_{mem_{ij}}$$ Equation 4-9

where $\beta_{evap_{ij}}$ represents the separation achieved by evaporation of a liquid mixture and $\beta_{mem_{ij}}$ represents the separation achieved by the membrane.

Table 4-1 shows the membrane selectivities for the transesterification reaction and the acetalisation reaction mixtures. It should be noted that, since the membrane selectivities were calculated from the reactor and the trap composition at the end of each experiment, the membrane selectivities listed here are average values during the entire reaction period.

Table 4-1 CMS-7-ePTFE® membrane binary selectivity measured in a multicomponent reaction mixture.

Reaction	Temperature (°C)	Selectivity (α_{ij})		
		H_2O/EtOH	***H_2O/Acetone***	***MeOH/BuOH***
Transesterification	75	-	-	3.2
Acetalisation	25	81	68	-

The measured selectivities for the separation of water from ethanol and acetone are quite large. In contrast, the separation of methanol from butanol is a more difficult for the membrane, and a selectivity of only 3.2 is achieved. No appreciable permeation of methyl benzoate, butyl benzoate, or 2,2-diethoxypropane was observed in any of the reactions performed.

Bhattacharyya and coworkers [22] have previously reported the performance of the CMS-3-ePTFE membrane for the separation of binary mixtures of ethanol and water. They showed that at 65°C the membranes exhibited high water permeance, which was independent of water content of the feed mixture and had a water/ethanol selectivity of approximately 21. Using the activation energies for permeation reported by Bhattacharyya, the separation selectivity at 25°C was calculated to be approximately 54. This compares reasonably well with the values reported here for a membrane made from the same polymers, but with a different ratio of the copolymer components. The CMS-7 membrane reported here is more selective than CMS-3, but the general trends within the two materials are similar.

4.5.2 Transesterification reaction results

Figure 4-3 compares the transesterification reaction conversions in a membrane reactor system to the one without a membrane. Compared to the batch reaction without pervaporation, a relatively fast reaction rate (nearly 30% conversion within the first hour) and a short reaction time prior to exceeding equilibrium were achieved in the membrane reactor system. Without the assistance of membrane pervaporation, the equilibrium yield is only 51.9%. With the assistance of pervaporation, the system rapidly reached conversions nearly 21% higher than the equilibrium

limit. This result indicates that the membrane reactor is capable of selectively removing methanol and increasing the reaction conversion.

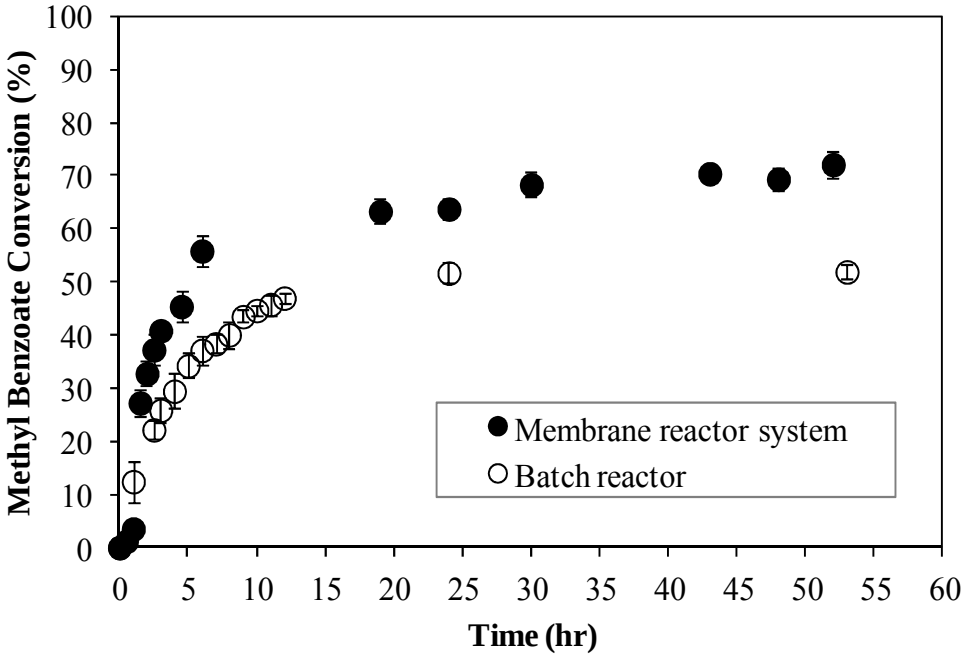

Figure 4-3 Transesterification reaction conversion vs. time. A membrane-assisted reactor equipped with a CMS7-ePTFE® membrane was employed. This run was made at 75°C and with a molar ratio of MeBe/BuOH =1.

4.5.3 Acetalisation reaction results

Figure 4-4 presents the yield of 2,2-DEP against the time for acetalisation reaction in the membrane reactor system and the conventional system. In the conventional system without a membrane, the product yield increases rapidly up to 2 % within a half hour and maintains this value. This indicates that the thermodynamic equilibrium is at 2%, consistent with the equilibrium conversion reported by Lorette, et al. [18]. In the membrane reactor system, a faster reaction rate (exceeding equilibrium within half hour) is observed, and the product yield is doubled with selective water removal. After reaching 4% yield, it seems to remain at this value over the remainder of the 36 hour test period. An explanation for this might be that the simultaneous removal of byproduct water as well as reactant acetone has reached a balance which leaves the equilibrium unaffected.

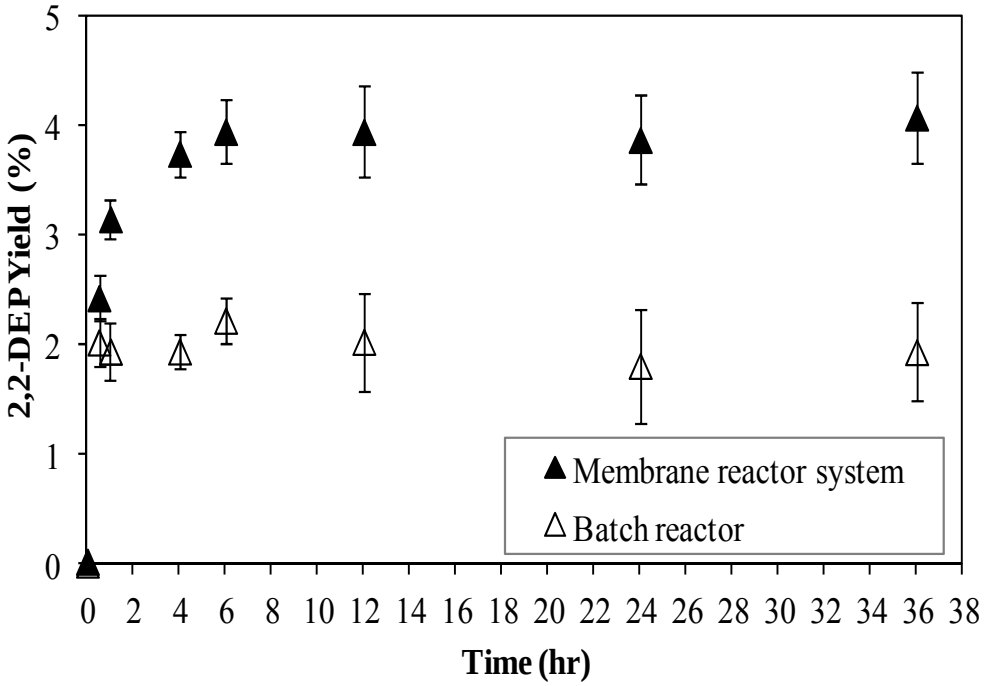

Figure 4-4 Acetalisation reaction yield vs. time. A membrane-assisted reactor equipped with a CMS7-ePTFE® membrane was employed. This run was made at 25°C and with a molar ratio of Acetone/EtOH =3.

4.6 Model validation

All plots presented in this section are plotted against the area-time product *At*. Since selective pervaporation of the water or alcohol by-product provides the mechanism through which the conversion can exceed the thermodynamic equilibrium, *At* represents the required pervaporation which should be provided to achieve a desired conversion. In membrane reactor applications, the reactor can be either operated with large membrane area (*A*) but short time (*t*) or operated with long time but small membrane area. Both operations can achieve the same conversion if *At* in both cases are equal. Therefore, plotting against area-time allows one to compare the membrane reactor performance at different conditions in comparable terms.

Since the prediction of the transient approach to the thermodynamic equilibrium conversion is not the focus of this model and we assumed that the thermodynamic equilibrium of the reaction mixture is reached instantaneously in each reaction step, the simulated results will jump to the thermodynamic equilibrium after one reaction step. Therefore, simulation curves in

all plots started at the thermodynamic equilibrium. The values of parameters used within the simulation in both cases are given in Table 4-2. For the experimental data, a membrane area of 13.8 cm^2 and the experimental sampling time were used to calculate *At*.

Table 4-2 Summary of values of parameters used for model simulation.

Parameters	Value
Transesterification	
N_{MeBe}	321 mmol
N_{BuOH}	321 mmol
$N_{p\text{-Xylene}}$	1278 mmol
K_{eq}	1.17
T	75°C
p^{perm}	2.80×10^{-3} bar
P^{G}_{MeBe}/l	9.23×10^{-2} mmol cm^{-2} h^{-1} bar^{-1}
P^{G}_{BuOH}/l	1.53 mmol cm^{-2} h^{-1} bar^{-1}
P^{G}_{BuBe}/l	0.23 mmol cm^{-2} h^{-1} bar^{-1}
P^{G}_{MeOH}/l	4.91 mmol cm^{-2} h^{-1} bar^{-1}
$P^{G}_{p\text{-Xylene}}/l$	9.68×10^{-4} mmol cm^{-2} h^{-1} bar^{-1}
Acetalisation	
$N_{Acetone}$	250 mmol
$N_{Ethanol}$	750 mmol
K_{eq}	1.85×10^{-4}
T	25°C
p^{perm}	6.67×10^{-4} bar
$P^{G}_{Acetone}/l$	2.66 mmol cm^{-2} h^{-1} bar^{-1}
$P^{G}_{Ethanol}/l$	2.25 mmol cm^{-2} h^{-1} bar^{-1}
P^{G}_{DEP}/l	0 mmol cm^{-2} h^{-1} bar^{-1}
P^{G}_{Water}/l	132 mmol cm^{-2} h^{-1} bar^{-1}

Figure 4-5 shows the comparison of experimental and simulated conversions of methyl benzoate reaction. As required by the calculation procedure, the simulated conversion reaches the batch equilibrium conversion instantly and increases with pervaporation. The simulated curve predicts MeBe conversions exceeding the thermodynamic equilibrium very well.

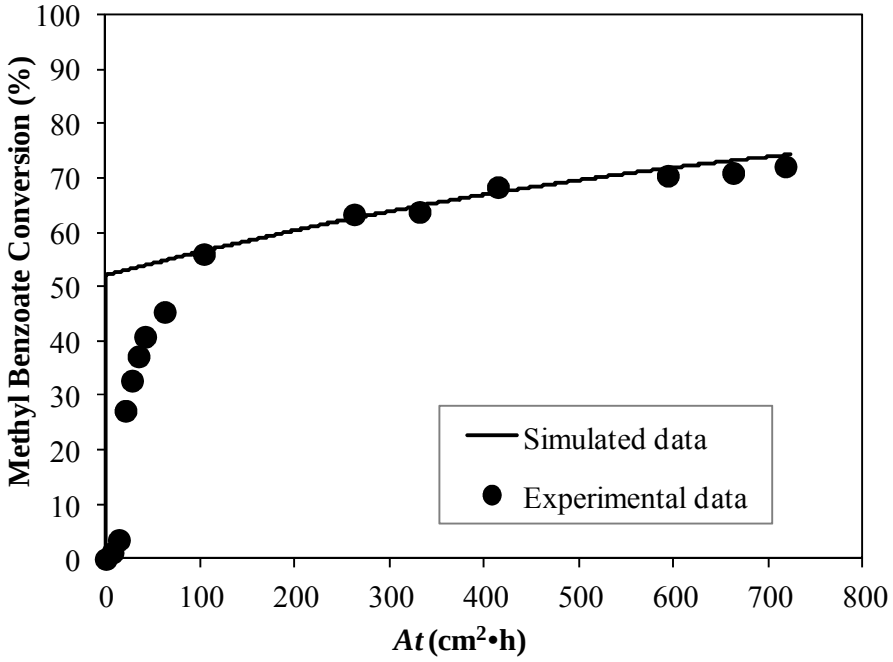

Figure 4-5 Comparison of model and transesterification experimental results of methyl benzoate conversion in a membrane reactor system.

Figure 4-6 shows the comparison of experimental and simulated yields of 2,2-DEP against *At*. Two simulations were completed. In each case, the experimentally measured permeance was employed in model predictions. The fundamental difference is the means by which the average flux was calculated. In case (a) the permeance was calculated by normalizing the mass of permeate collected by the total reaction time (36h). In case (b) the permeance was calculated using the measured permeate and the effective reaction time (6h). The effective reaction time was defined as the time over which chemical changes occur. Again, the simulated yield instantly achieves the batch equilibrium yield and increases slowly with progressing separation. For case (a) after At=400 cm^2h, the simulated curve shows reasonable agreement with the experimental yield. Comparing to the transesterification case, the agreement between the model and the experimental data did not start as soon as the experimental yield exceeding the

thermodynamic equilibrium. This is because that the goodness of fit between the model and the experimental data may be the result of several variables: (1) the actual rate of the reaction, (2) the validity of the other assumptions made in the model development; and (3) the applicability of the average permeance values measured over the entire reaction period to the instantaneous permeance occurring at each step in the process. In this reaction, the initial reaction rate was much faster than that in the transesterification reaction, and after reaching 4% yield at around 6 hour, the reaction yield increased very slowly and almost remained the same in the rest of the 30 hour reaction period. This means that the permeate composition did not change much after 6 hours and using the average permeance over 6 hours (case b) instead of 36 hours should provide a better fit between the experimental and model data for the first 6 hours. This is true as can be observed in Figure 6. Therefore, the more accurate permeance used in the model to its actual value in the process, the better prediction the model can get.

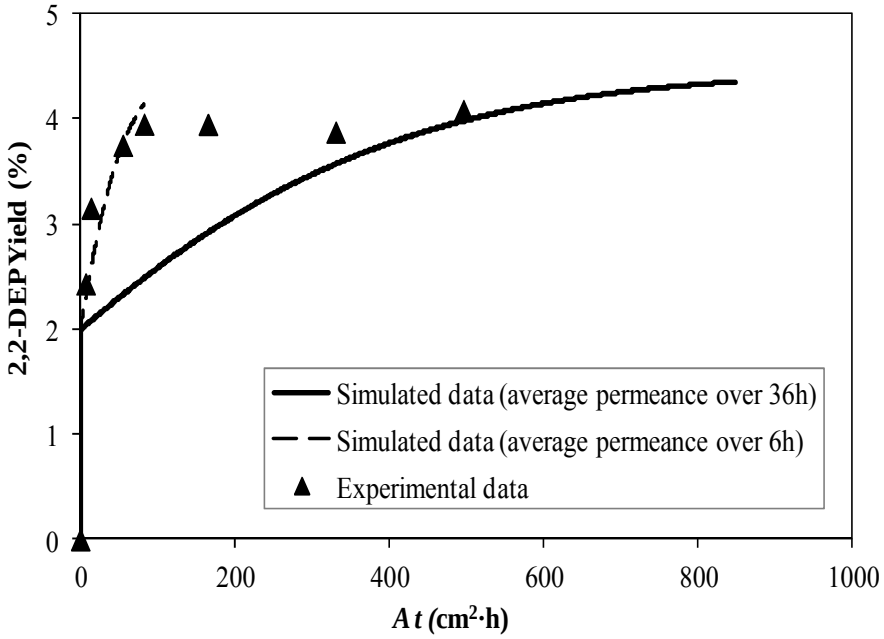

Figure 4-6 Comparison of model and acetalisation experimental results of 2,2-DEP yield in a membrane reactor system.

4.7 Predicted performance

4.7.1 Effect of membrane selectivity

Given the good agreement between the experimental performance and the system yields predicted by the models, it is possible to use the models to predict how the system will perform under new, previously untested conditions. Using the model, the performance of the membrane reactor system as a function of the selectivity of the membrane for the byproduct methanol over the reactant butanol (in the transesterification reaction) was predicted. Figure 4-7 shows the predicted effect of membrane MeOH/BuOH selectivity on transesterification conversions. Each simulation was halted when methanol removal reached 99%. From this plot, we can see that the reaction conversion increases as the membrane selectivity of MeOH/BuOH improves. The line marked α=1 represents the performance of a membrane with no intrinsic MeOH/BuOH membrane selectivity. The enhancement of the reaction conversion from the thermodynamic equilibrium value (52%) to 80% is entirely due to the preferential evaporation of MeOH from the reaction mixture. The membrane itself makes no contribution to the separation and promoted conversion. When the membrane MeOH/BuOH selectivity is larger than 1, the membrane preference for MeOH further enhances the volatility difference of MeOH and BuOH, resulting in an additional conversion enhancement. The MeOH/BuOH selectivity of CMS-7-ePTFE® membranes measured experimentally under reaction conditions was 3.2. Using this value, the conversion is promoted to 87%. While the natural tendency of membrane manufacturers and researchers might be driven to improve the MeOH/BuOH selectivity, in this system such an improvement has only a modest impact on the conversions achieved. As can be seen in Figure 4-7, even if this selectivity is improved by a factor of 1000, the final transesterification reaction conversion was only increased from 87% to 91%.

On the other hand, reducing the membrane selectivity below the experimentally measured 3.2 has a more pronounced impact on reaction conversion. When the membrane selectivity is less than 1, the membrane is BuOH selective. The membrane preference of BuOH adds a negative effect on the volatility difference of MeOH and BuOH, which will decrease the reaction conversion produced by simple evaporation (67% with $\alpha_{MeOH/BuOH}$=0.32) and may even promote the reverse reaction (50% with $\alpha_{MeOH/BuOH}$=0.1). The trends observed are consistent with those reported by Tanna [24].

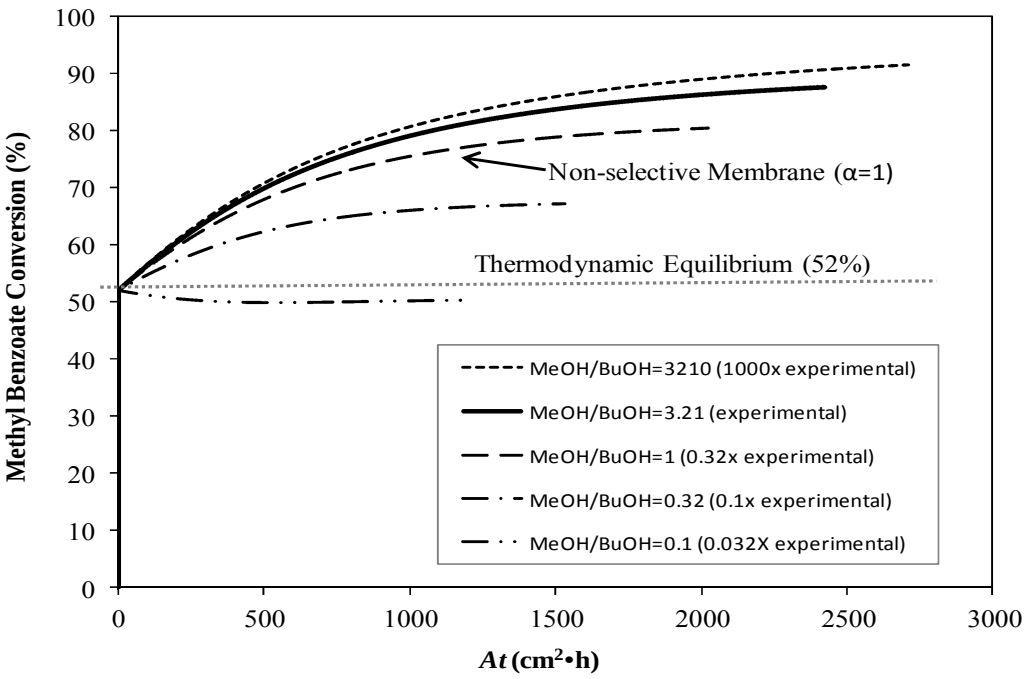

Figure 4-7 The effect of membrane selectivity of MeOH/BuOH on transesterification conversions in a membrane reactor (membrane selectivity: 3210, 3.21, 1, 0.32, and 0.1).

In Table 4-3, the properties of the system are reported in terms of both membrane selectivity and system separation factor. For this analysis, the selectivity of evaporation was estimated for a binary methanol/butanol equimolar mixture at the reaction conditions. While the composition of the feed mixture will change as the reaction proceeds, the experimentally evaluated permeate compositions were a cumulative average over the entire reaction period. Therefore, the evaporation selectivity was estimated based on an equimolar methanol/butanol mixture using UNIFAC vapor-liquid equilibrium model. This is the approximate composition that would be present once the equilibrium conversion was reached but before any permeation had begun. Because the precise feed-side composition was not measured as a function of reaction time, the evaporation selectivities reported are approximations only. The membrane separation factor was then calculated from Equation 4-9.

Table 4-3 The impact of membrane selectivity and pervaporation separation factor on the reaction conversion achieved in the transesterification of methyl benzoate with butanol at 75°C and equimolar reactant addition. Conversion results predicted from system model.

Membrane Selectivity ($\beta_{mem_{ij}}$)	Separation Factor ($\beta_{pervap_{ij}}$)	Final System Conversion (%)
0.1	0.85	50
0.12	1.0	52 (Equilibrium)
0.32	2.7	67
1	8.5	80
3.2 (experimental conditions)	27.5	87
3200	27,500	91

Analysis of Table 4-3 follows an expected trend, separation factors of less than 1 result in promotion of the reverse reaction. A separation factor of just above one results in a modest removal of methanol relative to butanol and a small enhancement of the reaction conversion. Further increases in separation factor result in additional enhancements to the reaction conversion. Therefore, an understanding of the impact of membrane selectivity on overall system performance allows for design of a membrane system with properties sufficient to achieve optimum performance without the need for excess selectivity which frequently impedes flux.

4.7.2 Effect of permeate pressure

Changing permeate pressure can have a dramatic impact on the performance of pervaporation-assisted membrane reactors, especially in the case of limited membrane selectivity studied here. In the present study of ketalization, acetone and ethanol react to form a ketal and water. As the driving force for the reactants (acetone and ethanol) are initially quite large as compared to that of the product water, the loss of reactants is a problem to be considered. In the simulations completed, the performance of the system was predicted until the water removal

reached 99%. Simulation results which examine the effect of permeate pressure on 2,2-DEP yield of acetalisation reactions are shown in Figure 4-8. The permeate pressure was varied from 1.33×10^{-4} bar to 1.33×10^{-2} bar. From the plot, we can observe that low permeate pressures increase product yields while high permeate pressures may decrease product yields. This effect can be explained by water and acetone flux changes with permeate pressure. A maximal yield of approximate 5%, even higher than that achieved experimentally, can be reached at 1.33×10^{-4} bar.

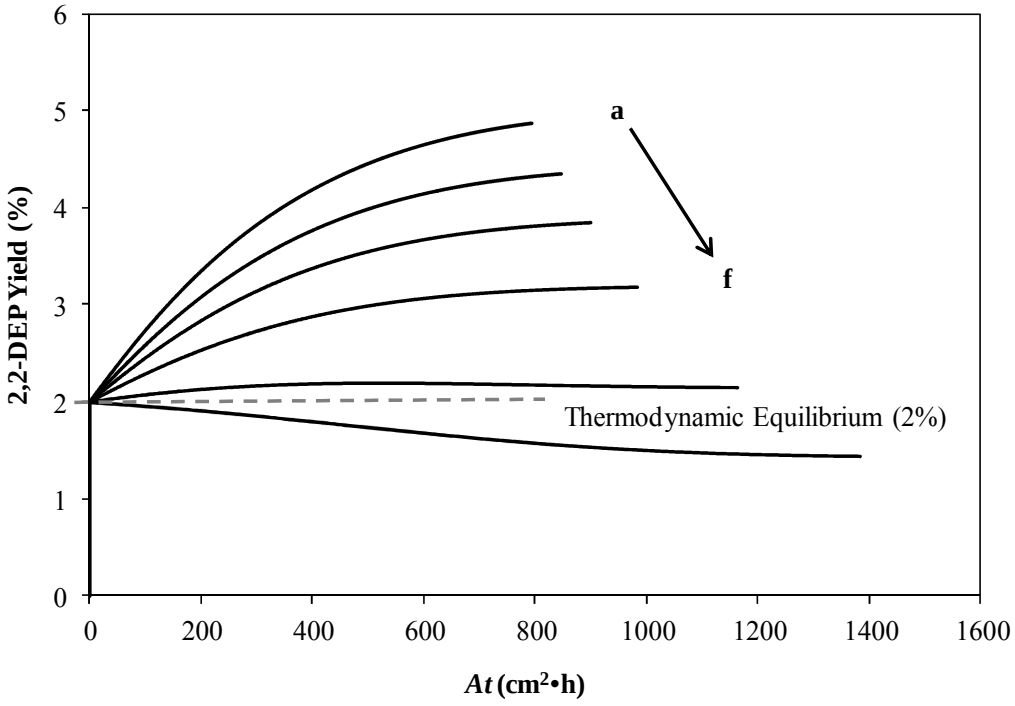

Figure 4-8 The effect of permeate pressure on 2,2-DEP yields. (p^{perm} for curve *a*: 1.33×10^{-4} bar, *b*: 6.67×10^{-4} bar (experimental), *c*: 1.33×10^{-3} bar, *d*: 2.67×10^{-3} bar, *e*: 6.67×10^{-3} bar, *f* : 1.33×10^{-2} bar).

Figure 4-9 and Figure 4-10 shows the corresponding water fluxes and acetone fluxes in the defined permeate pressure range. From these plots, we can observe that both water flux and acetone flux drops as permeate pressure increases (from curve *a* to curve *f*), but the water flux values drop much more rapidly than those for acetone. As the permeate pressure increases, both water and acetone fluxes decrease due to the drop of driving force. However, since the partial pressure of acetone on the feed side is many times higher than that of water, the change in the permeate pressure has less impact on the acetone flux than on the water. Therefore, a relatively

faster removal of reactant acetone than removal of byproduct water occurs and leads to a decreasing yield and in extreme cases to the promotion of the reverse reaction (observed when the permeate pressure was 1.33×10^{-2} bar).

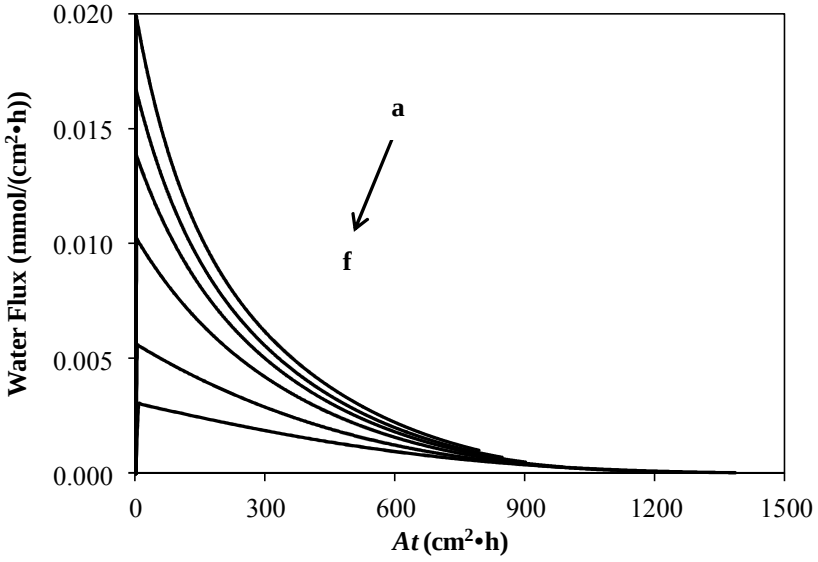

Figure 4-9 The effect of permeate pressure on water flux. (p^{perm} for curve *a*: 1.33×10^{-4} bar, *b*: 6.67×10^{-4} bar (experimental), *c*: 1.33×10^{-3}bar, *d*: 2.67×10^{-3} bar, *e*: 6.67×10^{-3} bar, *f* : 1.33×10^{-2} bar).

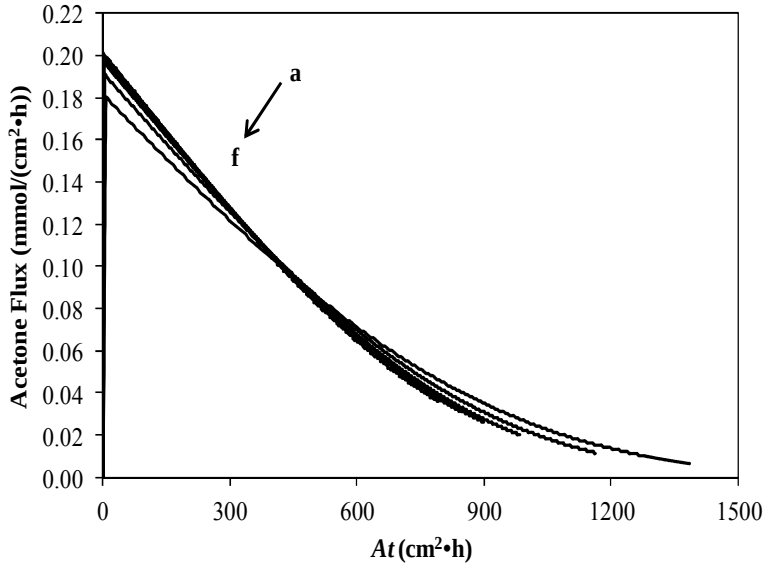

Figure 4-10 The effect of permeate pressure on acetone flux. (p^{perm} for curve *a*: 1.33×10^{-4} bar, *b*: 6.67×10^{-4} bar (experimental), *c*: 1.33×10^{-3}bar, *d*: 2.67×10^{-3} bar, *e*: 6.67×10^{-3} bar, *f* : 1.33×10^{-2} bar).

4.8 Conclusions

Transesterification of methyl benzoate with butanol and acetalisation of acetone with ethanol in a pervaporation membrane reactor system were studied as two model reactions for reversible organic reactions. By selective removal of a by-product (water or methanol), the reaction conversion was increased from 52% to 72% for transesterification reaction and 2 % to 4% for acetalisation reaction. Membrane reactors operating in pervaporation conditions significantly increased the conversion and reaction rate achieved in conventionally equilibrium-limited reactions. A model was developed to predict conversions exceeding thermodynamic equilibrium in a membrane reactor based on membrane permeation data and operating conditions (reactor temperature, permeate pressure and feed composition). The model was validated using available experimental data and a good agreement was found. The goodness of fit is affected by the accuracy of the permeance used in the model to the actual value in the process. Effects of membrane selectivities and permeate pressure on membrane reactor performance for two model reactions were investigated by the developed model. This model can also be used for the other reversible organic reactions with water or low molecular weight alcohol by-products liberated.

4.9 References

[1] R.W. Field, F. Lipnizki, P.K. Ten, Pervaporation-based hybrid process: a review of process design, applications and economics, Journal of Membrane Science, 153 (1999) 183-210.

[2] R.W. Baker, Membrane Technology and Applications, 2nd ed., John Wiley & Sons, Ltd., England, 2004.

[3] K. Bartling, J.U.S. Thompson, P.H. Pfromm, P. Czermak, M.E. Rezac, Lipase-catalyzed synthesis of geranyl acetate in n-hexane with membrane-mediated water removal, Biotechnol Bioeng, 75 (2001) 676-681.

[4] D. Barahona, P.H. Pfromm, M.E. Rezac, Effect of water activity on the lipase catalyzed esterification of geraniol in ionic liquid [bmim]PF6, Biotechnol Bioeng, 93 (2006) 318-324.

[5] I.J. Kang, M.E. Rezac, P.H. Pfromm, Membrane permeation based sensing for dissolved water in organic micro-aqueous media, Journal of Membrane Science, 239 (2004) 213-217.

[6] K. Okamoto, M. Yamamoto, S. Noda, T. Semoto, Y. Otoshi, K. Tanaka, H. Kita, Vapor-Permeation-Aided Esterification of Oleic-Acid, Ind. Eng. Chem. Res., 33 (1994) 849-853.

[7] K. Tanaka, R. Yoshikawa, C. Ying, H. Kita, K. Okamoto, Application of zeolite membranes to esterification reactions, Catalysis Today, 67 (2001) 121-125.

[8] J. Vital, L. Guerreiro, J.E. Castanheiro, I.M. Fonseca, R.M. Martin-Aranda, A.M. Ramos, Transesterification of soybean oil over sulfonic acid functionalised polymeric membranes, Catalysis Today, 118 (2006) 166-171.

[9] I. Agirre, M.B. Guemez, H.M. van Veen, A. Motelica, J.F. Vente, P.L. Arias, Acetalization reaction of ethanol with butyraldehyde coupled with pervaporation. Semi-batch pervaporation studies and resistance of HybSi (R) membranes to catalyst impacts, Journal of Membrane Science, 371 (2011) 179-188.

[10] X.H. Li, L.F. Wang, Kinetic model for an esterification process coupled by pervaporation, Journal of Membrane Science, 186 (2001) 19-24.

[11] M.E. Rezac, W.J. Koros, S.J. Miller, Membrane-assisted dehydrogenation of n-butane influence of membrane properties on system performance, Journal of Membrane Science, 93 (1994) 193-201.

[12] M.E. Rezac, W.J. Koros, S.J. Miller, Membrane-assisted dehydrogenation of normal-butane, Ind. Eng. Chem. Res., 34 (1995) 862-868.

[13] S.Y. Lim, B. Park, F. Hung, M. Sahimi, T.T. Tsotsis, Design issues of pervaporation membrane reactors for esterification, Chemical Engineering Science, 57 (2002) 4933-4946.

[14] J. Otera, Transesterification, Chemical Reviews, 93 (1993) 1449-1470.

[15] X. Rao, Z. Ding, H. Lou, J. Wu, Y. Fang, B. Deng, Method of preparing clarithromycin, US Patent US2010/0280230 A1, (2010).

[16] J.H. Teles, N. Rieber, K. Breuer, D. Demuth, H. Hibst, H. Etzrodt, U. Rheude, Method for producing enol ethers, US Patent US006211416 B1, (2001).

[17] C.H. Lin, R.H. Falk, C.R. Stocking, Rapid Chemical Dehydration of Plant material for light and electron-microscopy with 2,2-dimethoxypropane and 2,2-diethoxypropane, Am J Bot, 64 (1977) 602-605.

[18] N.B. Lorette, W.L. Howard, J.H. Brown, Preparation of ketone acetals from linear ketones and alcohols, J Org Chem, 24 (1959) 1731-1733.

[19] R.W. Baker, J.G. Wijmans, Y. Huang, Permeability, permeance and selectivity: A preferred way of reporting pervaporation performance data, Journal of Membrane Science, 348 (2010) 346-352.

[20] J.M.P. Bruce E. Poling, John P. O'Connell, The properties of gases and liquids, Fifth ed., McGraw-Hill Companies, Inc., 2001.

[21] J.M. Prausnitz, T.F. Anderson, E.A. Grens, C.A. Eckert, R. Hseih, Computer calculations for multicomponent vapor-liquid and liquid-liquid equilibria, Prentice Hall Professional Technical Reference, 1980.

[22] V. Smuleac, J. Wu, S. Nemser, S. Majumdar, D. Bhattacharyya, Novel perfluorinated polymer-based pervaporation membranes for the separation of solvent/water mixtures, Journal of Membrane Science, 352 (2010) 41-49.

[23] J.G. Wijmans, R.W. Baker, A simple predictive treatment of the permeation process in pervaporation, Journal of Membrane Science, 79 (1993) 101-113.

[24] N.P. Tanna, S. Mayadevi, Analysis of a membrane reactor: Influence of membrane characteristics and operating conditions, Int J Chem React Eng, 5 (2007).

Chapter 5 - Scale-up of a Pervaporation Membrane Assisted Transesterification Reactor for Butyl Acetoacetate Production

5.1 Abstract

Pervaporation membrane reactors are promising systems for reversible reactions since they can selectively remove the by-product water or low molecular weight alcohols to shift reactions toward higher conversions than those achieved in batch reactors. In the past, the coupling of esterification with pervaporation has been intensively studied using flat sheet membranes. In this study, a series of membrane reactor systems with various scale and complexity was developed for the transesterification of methyl acetoacetate with *n*-butanol to *n*-butyl acetoacetate and methanol catalyzed by immobilized lipase Novozym® 435. The membrane modules investigated include a bench-scale flat sheet membrane, a bench-scale hollow fiber membrane module, and a pilot-scale hollow fiber membrane module. Our results indicate that all membrane modules have a high permselectivity of methanol over butanol that is greater than 350. The enhanced membrane reactor can selectively remove the by-product methanol and achieve 100% conversion, nearly 55% in excess of that achieved in the conventional system. Our results also show that the reaction time to achieve a given conversion continuously decreases with increasing the methanol removal capacity of the reactor system within our experimental range. However, this is a highly nonlinear relationship.

5.2 Introduction

Pervaporation membrane reactors are promising systems that can be used to increase reaction conversions and reaction rates of reversible reactions since membranes inside these reactors can selectively remove the by-product water or low molecular weight alcohols from reaction mixtures [1-3]. Pervaporation membrane reactor systems have been widely investigated in assisting esterification reactions [4-15]. While pervaporation-aided esterification reactions have been intensively studied, pervaporation-aided transesterification reactions have rarely been investigated [16-19]. Compared to the esterification reaction coupling with pervaporation, which requires a membrane to selectively remove water from esters and reactant alcohols (water/organic separation), the pervaporation-aided transesterification reaction is more

challenging because the separation to be achieved in this case is between the by-product and reactant alcohols (organic/organic separation), Currently, the by-product removal from transesterification reactions is being done by reactive distillation at high cost. The lack of economical pervaporation membrane modules that have sufficient selectivity for organic/organic separations and good solvent resistance has restricted the integration of pervaporation process into transesterification reactions. According, membranes for pervaporation organic/organic separations and solvent-resistant modules are ranked 1 and 7 respectively out of 38 research needs in the membrane separation industry [20].

Some studies have also been done on the scale-up of pervaporation membrane assisted esterification reactions [21-25]. The effect of membrane area to reaction volume ratio (S/V) on reaction time was discussed in these papers. However, experimental data obtained from these studies were limited to a relatively small range of S/V (0 ~ 250 m^{-1}) since almost all of these studies employed flat sheet membranes with limited membrane area. From an industrial scale perspective, it will be useful to investigate a broader range of S/V ratio while employing different scales of membrane modules.

In this work, the transesterification of methyl acetoacetate with b-butanol catalyzed by the immobilized lipase Novozym® 435 (Scheme 5-1) has been investigated as a model reaction in membrane reactor systems. The membrane modules employed includes both flat sheet membranes for bench-scale systems and hollow fiber membrane modules for pilot-scale systems. The product butyl acetoacetate is a β-keto ester, which is an important intermediate in organic synthesis for the production of natural products and biologically active heterocyclic molecules [26-29]. Yadav et al. reported this reversible reaction only achieved 46% conversion with equimolar reactants at 30°C without pervaporation [30]. Therefore, this reaction is well-suited for the use of a membrane reactor system in that if the methanol could be selectively removed from the reaction mixture, complete conversion is theoretically possible without adding a large excess of one of the reactants.

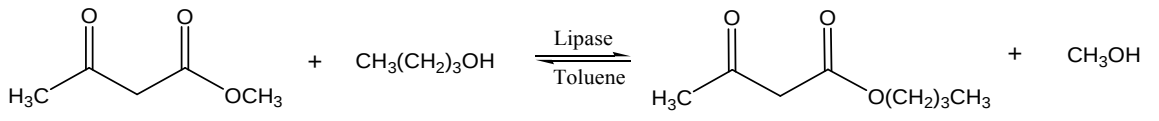

Scheme 5-1 Transesterification of methyl acetoacetate and butanol to butyl acetoacetate and methanol.

5.3 Materials and methods

5.3.1 Membranes and membrane reactor system

The CMS-3 flat sheet membranes and hollow fiber membrane modules used in this study were supplied by Compact Membrane Systems, Inc. (CMS), and these modules are shown in Figure 5-1. The selective layer of membranes are made of perfluoro-2,2-dimethyl-1,1,3-dioxole copolymerized with tetrafluoroethylene with varying copolymer ratios (such as AF2400 and AF1600) [31, 32]. Gas permeation tests with nitrogen and oxygen were performed on membrane modules before and after they were used for pervaporation experiments.

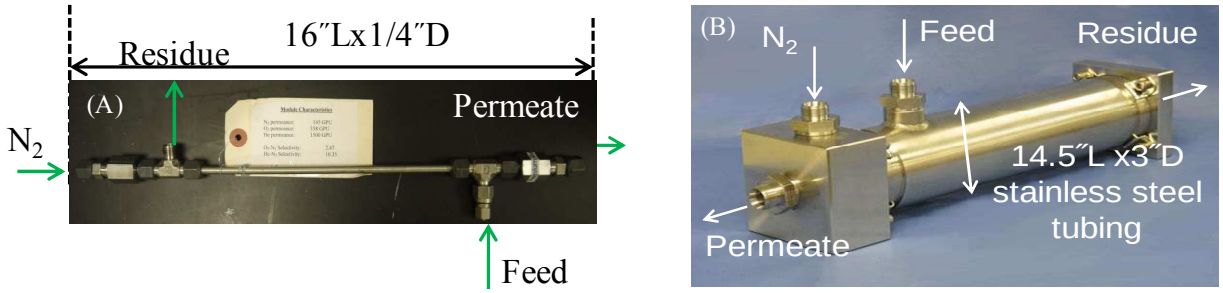

Figure 5-1 Hollow fiber membrane modules used in this research: (A) a bench-scale hollow fiber membrane module (B) a pilot-scale hollow fiber membrane module.

The set-up of a bench-scale pervaporation membrane reactor system has been described in our previous work [18]. A schematic and a photo of the pilot-scale pervaporation membrane reactor system is presented in Figure 5-2 and Figure 5-3, respectively. The capacity of the reactor was 2 gallons. The outlet port of the feed tank was filled with glass wool (fiber diameter: 8μm) and an inline filter (140μm pore size) was installed to maintain the catalyst inside the reactor. All components in the reactor system were built using 1/2' stainless steel tubing and fittings (Swagelok, Inc.). On the permeate side, either trap I or trap II, along with the safety trap were connected to condense the permeate. The switch between trap I and trap II allowed for the continuity of the permeate collection process and minimized the loss of permeate. A vacuum pump created low pressure at the permeate side of the membrane module (typically 0.02-0.04 bar). The permeate side of the membrane was swept with nitrogen (UHP/zero grade) to assist the by-product removal.

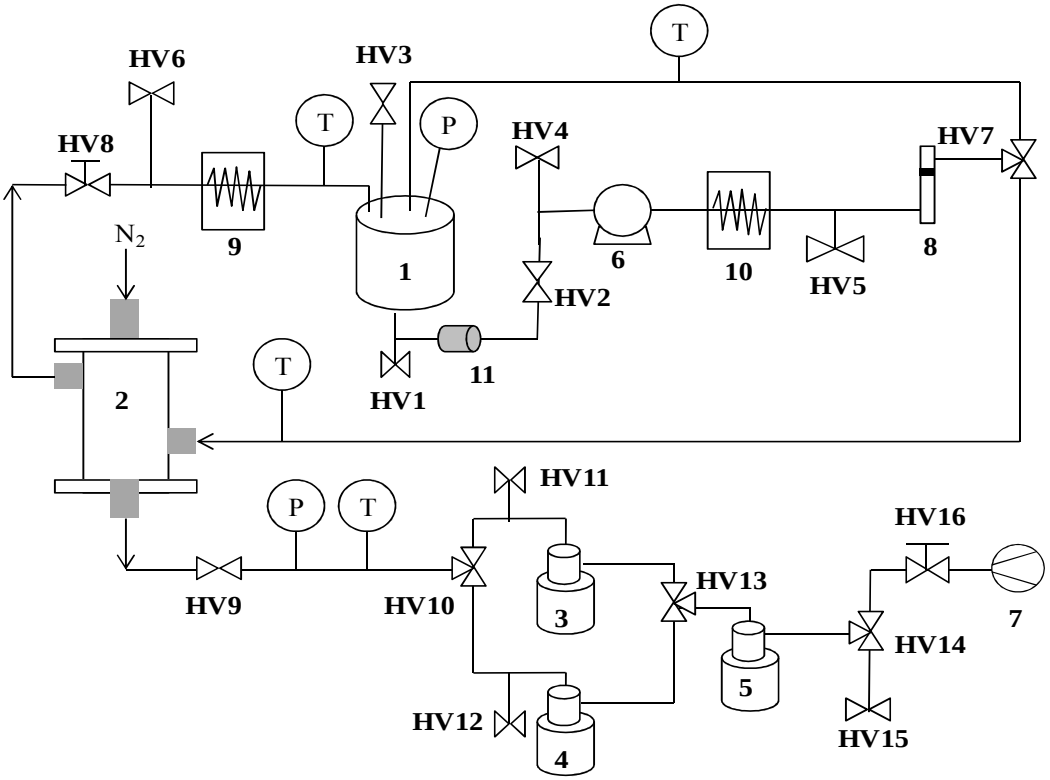

Figure 5-2 Schematic of the pilot-scale pervaporation membrane reactor system. 1–reaction vessel; 2–membrane module; 3,4,5–liquid nitrogen cold trap I, trap II and safety trap; 6–circulation pump; 7–vacuum pump; 8-flow meter; 9,10–heat exchanger; 11–inline filter; HV1–feed evacuation port; HV2–feed valve; HV3–relief valve; HV4–N_2 purge; HV5–feed sample port; HV6–residule sample port; HV7–feed/bypass switch; HV8–back pressure needle valve; HV9–permeate valve; HV10,HV13–trap I/trap II switch; HV11–trap I vent; HV12–trap II vent; HV14–vacuum/ N_2 purge switch; HV15–N_2 purge; HV16–vacuum control needle valve.

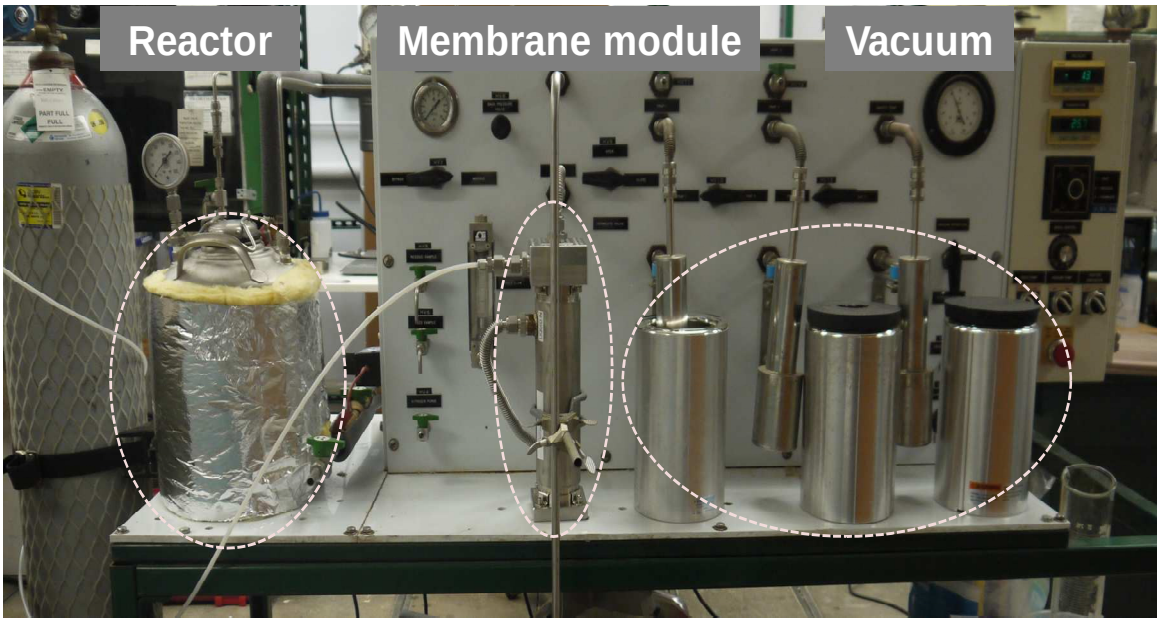

Figure 5-3 The pilot-scale pervaporation membrane reactor system.

5.3.2 Transesterification experiments

Methyl acetoacetate (MeAe, ≥99%), *n*-butanol (BuOH, ≥99.8%) and toluene (HPLC grade, 99.8%) were obtained from Acros Organics. The catalyst Novozym® 435 (lipase from *Candida antarctica*, immobilized on macroporous polyacrylate resin (bead size 0.3-0.9 mm, activity 11075 U/g) was purchased from Sigma-Aldrich. A typical reaction mixture consisted of equimolar methyl acetoacetate and *n*-butanol diluted with solvent toluene (1.0 mol reactants /L toluene). The reactor was preheated to 30°C and then was charged sequentially with toluene, MeAe and BuOH. In the bench-scale reactor, the reaction mixture was agitated at 30°C for 20 min at a speed of 350 rpm. In the pilot-scale reactor, the agitation was achieved by reaction mixture recirculation in the reactor system. After the reaction mixture temperature was stable at 30°C, 3 wt% (catalyst/total reactants) of catalyst was then added to initiate the reaction. Liquid samples were withdrawn periodically from the sample port. Then, *p*-xylene (an internal standard for gas chromatography analysis) was added into the sample (0.1 mL p-xylene/mL sample) and mixed by a vortex mixer. 0.2 μL Analyte was injected into a HP 6890 series gas chromatograph equipped with a flame ionization detector and a capillary column (OV-1, 30 m length, 0.25 mm i.d., film thickness 0.25 μm) for analysis. During pervaporation experiments, permeate was collected in cold traps and was analyzed by GC. The batch reactor runs were carried out inside a

round bottom flask and under the same conditions as pervaporation experiments to determine the contribution of pervaporation to the completion of the reaction.

5.4 Results and discussion

5.4.1 Transesterification reaction without pervaporation

Kinetic curves of methyl acetoacetate conversion for both forward reaction and reverse reaction carried out in a bench-scale batch reactor are shown in Figure 5-4. The forward reaction kinetic curve and the reverse reaction kinetic curve are almost symmetric. After 6 hours, the reaction conversion reached 46% and remained constant for the rest of the test period, which indicated that the thermodynamic equilibrium is 46% conversion when operated with an equimolar reactant ratio at 30°C. The equilibrium constant K_{eq} is calculated to be 0.767 based on the experimental data. This result also indicates that there is no side reaction in the reaction system.

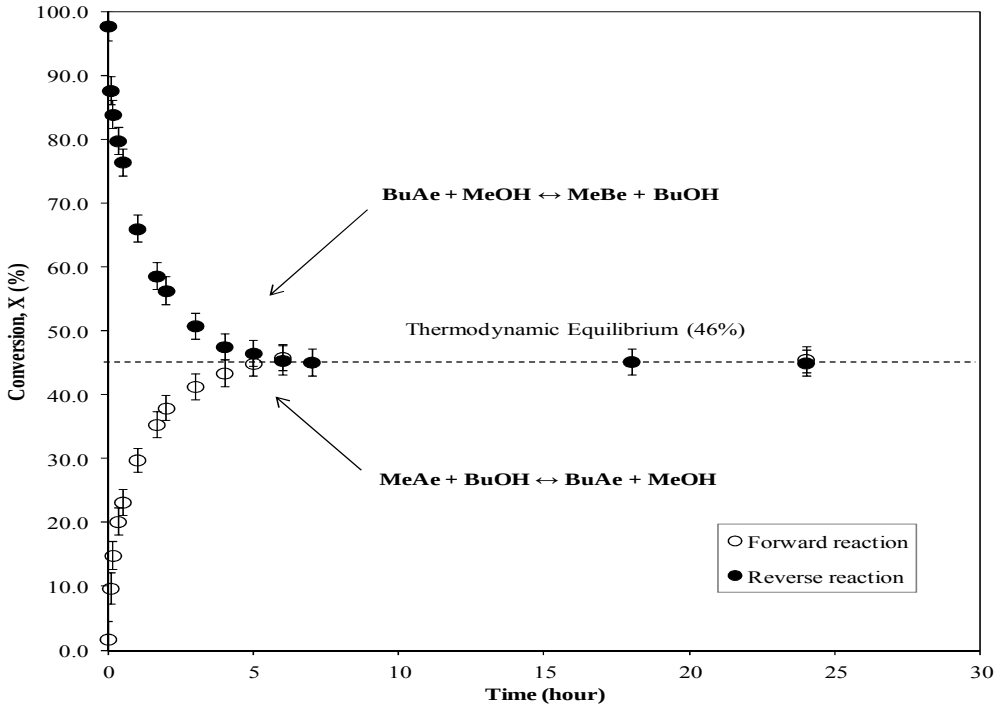

Figure 5-4 Transesterification forward and reverse reaction conversion versus time in a batch reactor without pervaporation. Reactions were carried out at 30°C and started with equimolar reactants, 1.0 L toluene/mol reactants and 3 wt% catalyst.

5.4.2 Methanol removal capacity of a pervaporation membrane reactor

In this research, flat sheet membranes and hollow fiber membrane modules are employed in different scales of membrane reactors. Membrane area (S), reaction mixture volume (V), as well as methanol permeance (P_{MeOH}/l) may be different from module to module and each parameter can be varied independently to influence the pervaporation process. It is desirable to combine the influence s of each variable into a single parameter which can express the capacity of removing methanol from the reaction system. Thus, we introduce the methanol removal capacity parameter and define it as $P_{MeOH}/l \cdot S/V$. In this work, we replace P_{MeOH}/l with P_{N_2}/l and use $P_{N_2}/l \cdot S/V$ (GPU$\cdot$m^{-1}) as an indication of the methanol removal capacity. This is because that it is much easier to measure nitrogen permeance than methanol permeance in a reaction mixture under various operation conditions. We have measured P_{N_2}/l for all of our membrane modules. Moreover, a linear relationship between P_{N_2}/l and P_{MeOH}/l can be assumed for our membrane modules due to the limited solute solubility in these perfluorinated membranes [33].

5.4.3 Transesterification reaction in pervaporation membrane reactor systems

The kinetic curves of transesterification reaction conversions in membrane reactor systems with different methanol removal capacities are shown in Figure 5-5. The conversion is calculated as mol butyl acetoacetate in the reactor/(mol methyl acetoacetate in the reactor + mol butyl acetoacetate in the reactor)×100%. In the flat sheet membrane reactor system, the conversion achieved at 48 hours was approximately equal to the thermodynamic equilibrium conversion. This might be because the methanol production rate in the reactor system was much faster than its removal rate of the flat sheet membrane. With a relatively small $P_{N_2}/l \cdot S/V$ value, the methanol removal was slow. When increasing the $P_{N_2}/l \cdot S/V$ value, the membrane modules would have a faster methanol removal rate which could lead to a lesser accumulation of methanol in the reactor, hence a higher conversion within a shorter reaction time. As can be observed in Figure 5-5, the hollow fiber membrane reactor systems rapidly overcame the thermodynamic equilibrium limitation. In the bench-scale hollow fiber membrane reactor with $P_{N_2}/l \cdot S/V$=3383 GPU$\cdot$m^{-1}, at 48 hours, a conversion of 71% was achieved. In the bench-scale hollow fiber membrane reactor with $P_{N_2}/l \cdot S/V$=5043 GPU$\cdot$m^{-1}, a conversion of 87% was achieved at 48 hours and 100% conversion was finally obtained at 245 hour. At a $P_{N_2}/l \cdot S/V$ value

of 25700 GPU·m^{-1}, complete conversion was obtained at 42 hours. Since complete conversion was achieved, it also can be concluded that membrane modules have high operational selectivity of methanol over butanol.

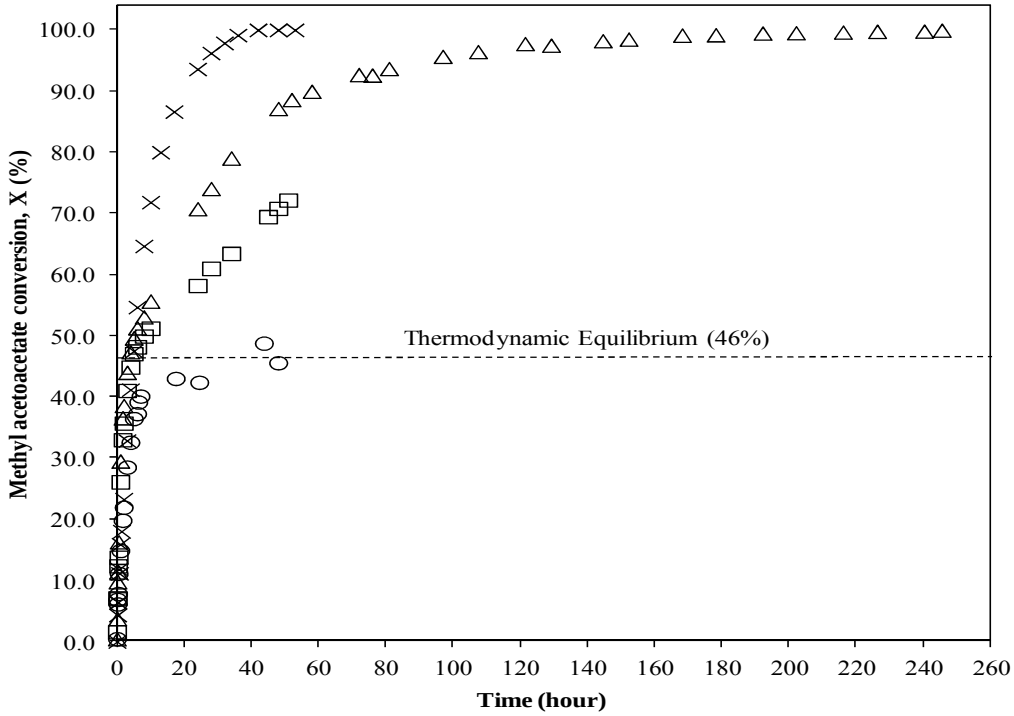

Figure 5-5 Comparison of transesterification reaction conversions in membrane reactor systems with different methanol removal capacities (Initial molar ratio of MeAe/BuOH=1, 1.0 L toluene/mol reactants, T=30°C, 3 wt% catalyst). ○: Flat sheet membrane with P_{N_2}/l·S/V=282 GPU·m^{-1}; □: Bench-scale hollow fiber membrane module with P_{N_2}/l·S/V=3383 GPU·m^{-1}; Δ: Bench-scale hollow fiber membrane module with P_{N_2}/l·S/V=5043 GPU·m^{-1}; ×: Pilot-scale hollow fiber membrane module with P_{N_2}/l·S/V =25700 GPU·m^{-1}. Error bars on individual data points are omitted to improve clarity. Error bars are approximately equivalent to the symbol size.

To better understand the performance of different scale membrane reactors, the methanol molar concentration and the butyl acetoacetate molar concentration (mol/L) in the reactor during transesterification reactions were analyzed and presented in Figure 5-6 and Figure 5-7, respectively. In Figure 5-6, an initial increase in methanol molar concentration was observed for all runs. This initial increase was due to the fact that at the beginning of the reaction, the methanol production rate was faster than the methanol removal rate (zero in a batch reactor),

which caused an accumulation of methanol in the reactor. In the batch reactor, the methanol molar concentration reached a plateau after the thermodynamic equilibrium conversion was achieved. While in the membrane reactor systems, this initial increase was followed by a decrease. As the pervaporation assisted reaction went on, the reaction rate slowed down, and the methanol removal rate began to dominate. Therefore, a decrease in the molar concentration of methanol occurred after the initial increase. In the flat sheet membrane reactor system, the methanol removal capacity was small, and the methanol removal rate was slow. Thus, the decrease in the methanol concentration was not as fast as that in hollow fiber membrane reactor systems. As increasing the methanol removal capacity, the decrease started at a lower methanol concentration. Eventually, this initial increase can be eliminated and the methanol concentration can be held constant [34].

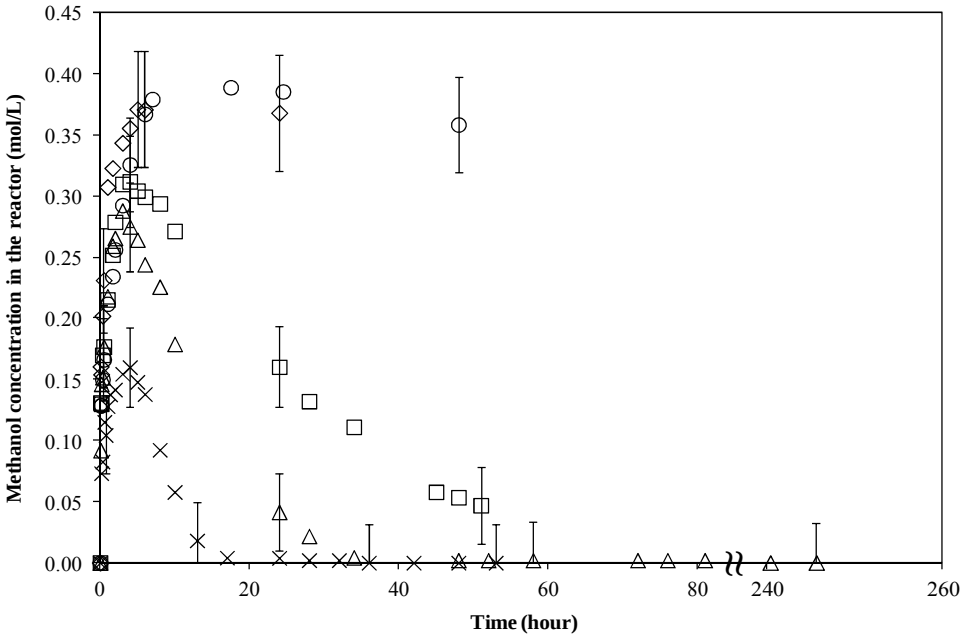

Figure 5-6 Comparison of methanol concentration (mol/L) in the reactor during transesterification reactions. All runs started with initial MeAe/BuOH ratio of 1 and solvent toluene (1.0 L toluene/mol reactants). ◊: Batch reactor; ○: Flat sheet membrane with P_{N2}/l·S/V=282 GPU·m^{-1}; □: Bench-scale hollow fiber membrane module with P_{N2}/l·S/V=3383 GPU·m^{-1}; Δ: Bench-scale hollow fiber membrane module with P_{N2}/l·S/V=5043 GPU·m^{-1}; X: Pilot-scale hollow fiber membrane module with P_{N2}/l·S/V=25700 GPU·m^{-1}. To decrease the optical density of the plot, error bars are displayed every five data points.

In Figure 5-7, the molar concentration of the product butyl acetoacetate in the reactor was compared for all runs. When Figure 5-6 and Figure 5-7 are combined, it is obvious that the equilibrium was shifted toward the formation of butyl acetoacetate by methanol removal. It can be seen in Figure 5-7 that, without the methanol removal by pervaporation in membrane reactors, the molar concentration of butyl acetoacetate in a batch reactor increased first and then flattened out after reaching thermodynamic equilibrium conversion. In the flat sheet membrane reactor system, the butyl acetoacetate molar concentration at 48 hours was approximately the same as that in the batch reactor and increased slowly due to the limited methanol removal. In all hollow fiber membrane reactor runs, the butyl acetoacetate molar concentration increased fast as a consequence of the relatively fast methanol removal rate.

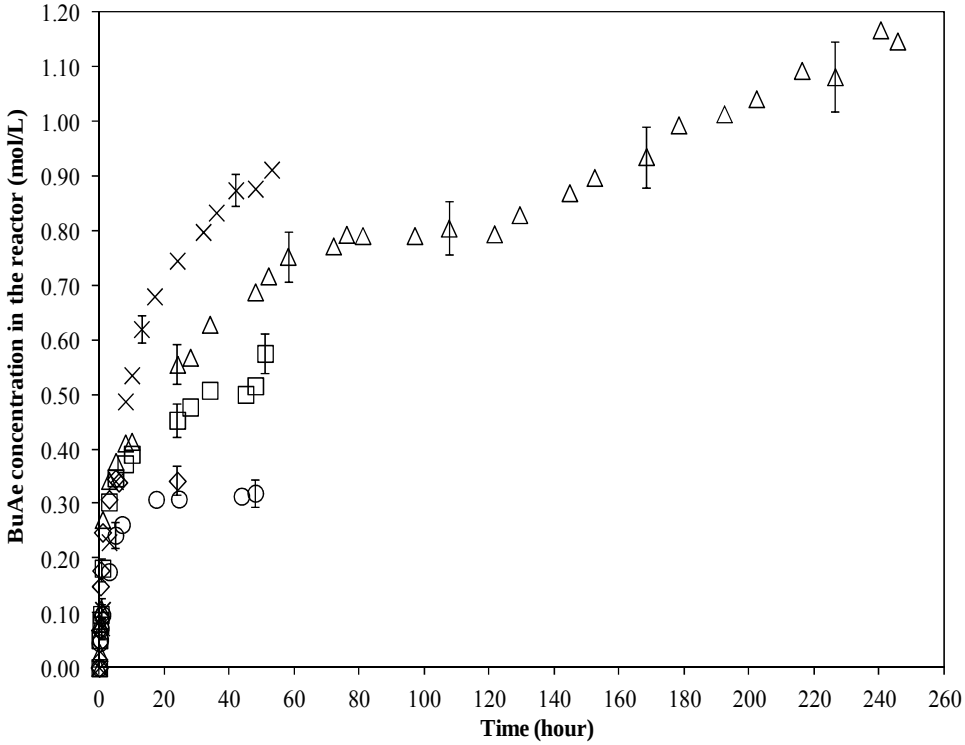

Figure 5-7 Comparison of butyl acetoacetate concentration (mol/L) in the reactor during the transesterification reactions (Initial molar ratio of MeAe/BuOH=1, 1.0 L toluene/mol reactants, T=30°C, 3 wt% catalyst). ◊: Batch reactor; ○: Flat sheet membrane with P_{N_2}/l·S/V=282 GPU·m^{-1}; □: Bench-scale hollow fiber membrane module with P_{N_2}/l·S/V=3383 GPU·m^{-1}; ∆: Bench-scale hollow fiber membrane module with P_{N_2}/l·S/V=5043 GPU·m^{-1}; ×: Pilot-scale hollow fiber membrane module with P_{N_2}/l·S/V =25700 GPU·m^{-1}. To decrease the optical density of the plot, error bars are displayed every five data points.

Table 5-1 listed reaction conversion, methanol concentration and butyl acetoacetate concentration at 30 hours from different membrane reactor runs. It is obvious from the data that for equal reaction time, with higher methanol removal capacity, the methanol concentration is lower while the product butyl acetoacetate concentration and the reaction conversion are higher at the same reaction time. Therefore, we can conclude that the increase in the conversion is due to the selective methanol removal from the reaction mixture.

Table 5-1 Comparison of methanol concentration, butyl acetoacetate concentration and conversion in the reactor from different membrane reactor systems at 30 hours reaction time (Initial molar ratio of MeAe/BuOH=1, 1.0 mol reactant /L toluene, T=30°C, 3 wt% catalyst).

$P_N2/l \cdot S/V$ (GPU·m^{-1})	Reaction Time (hour)	Reaction Conversion (%)	MeOH Conc. (mol/L)	BuAe Conc. (mol/L)
0 (batch reactor)	30	46±2	0.36±0.05	0.34±0.03
282	30	47±2	0.35±0.04	0.32±0.03
3383	30	60±2	0.13±0.03	0.49±0.03
5043	30	76±2	0.016±0.03	0.59±0.04
25700	30	97±2	0.002±0.03	0.78±0.03

5.4.4 Permeate composition analysis results

Figure 5-8A-D compares the toluene-free based permeate composition in membrane reactor systems with different methanol removal capacity. By analyzing permeate of all pervaporation assisted transesterification reaction runs, we have found that all permeate was primarily methanol and nearly no esters (less than 0.005 mol in all cases). Membrane modules had high methanol over butanol selectivity which is greater than 350. In Table 5-2, we compared the measured percentage of methanol captured in cold traps and the calculated percentage of methanol needed to be removed to achieve the measured conversion. For all runs, these two values match reasonably well.

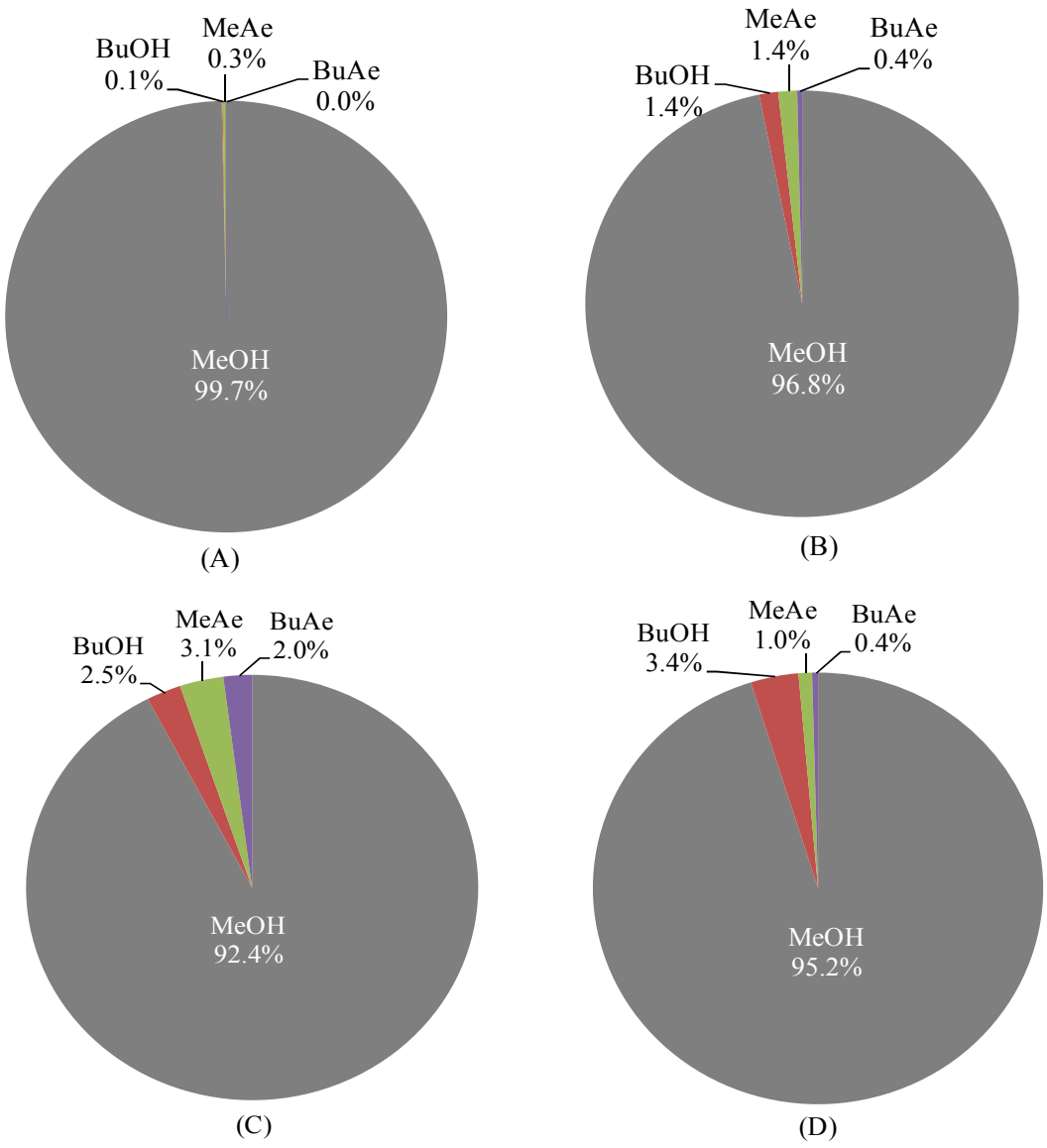

Figure 5-8 Comparison of permeate composition obtained in membrane reactor systems with different methanol removal capacity. (A) MBR with a flat sheet membrane (P_{N_2}/l·S/V=282 GPU·m^{-1}) (B) MBR with a bench-scale hollow fiber membrane module (P_{N_2}/l·S/V=3383 GPU·m^{-1}) (C) MBR with a bench-scale hollow fiber membrane module (P_{N_2}/l·S/V=5043 GPU·m^{-1})) (D) MBR with a pilot-scale hollow fiber membrane module (P_{N_2}/l·S/V=25700 GPU·m^{-1}). All runs were made at 30°C and started with initial MeAe/BuOH molar ratio of 1, 1.0 L toluene/mol reactants and 3 wt% catalyst.

Table 5-2 Comparison of methanol captured in permeate and required methanol removal for transesterification reactions in membrane reactor system. Permeate was analyzed at the end of each run and data were toluene-free basis.

$P_{N_2}/l \cdot S/V$ ($GPU \cdot m^{-1}$)	Reaction Time (hour)	Reaction Conversion (%)	Reactants Fed (mol)	Permeate (mol)	MeOH Capture[a] (%)	MeOH Removal[b] (%)
282	48	47	0.4	0.08	9	2
3383	51	73	0.4	0.14	94	89
5043	145.6	100	0.27	0.15	100	100
25700	42	100	2.4	1.3	100	100

a. MeOH Capture (%)=measured mmol of MeOH in trap/(mmol MeAe fed ×reaction conversion) ×100%

b. MeOH Removal (%)=calculated mmol of MeOH needed to be removed to achieve reaction conversion/(mmol MeBe fed ×reaction conversion) ×100%

The toluene in permeate corresponding to all cases in Figure 5-8 were: (A) 1 mmol after 48 hours (B) 62mol after 51hours, (C) 500 mmol after 246 hours and (D) 3060 mmol after 53 hours. It is noticed that the molar concentration of toluene in the permeate increases as the reaction time increases. To further understand the influence of reaction time on toluene concentration in permeate, we analyzed the compositions of permeate collected at different reaction time during the pilot-scale membrane reactor run. The results were plotted in Figure 5-9. The relative change of methanol and toluene concentration in permeate can be divided into three stages. At the beginning of the reaction (less than 1 hour), the collected permeate contained more than 90 mol % of toluene and almost no methanol. This is because that at the beginning of the reaction, the concentration of toluene was much higher than that of produced methanol. As the reaction went on, there was a relatively large amount of methanol produced in the reactor; and, since the membrane was more selective to methanol than toluene, the concentration of methanol in permeate started increasing while the toluene concentration began to decrease. When the reaction reached the stage that it was almost completed (X=95% at 30 hours), the reaction rate was not as fast as the beginning, and the amount of methanol that can be produced in the reactor for the rest of the reaction time was very limited compared to that at the beginning of the

reaction. Besides, with a large methanol removal capacity, the membrane module was capable of removing all available methanol in the reactor at a fast rate. This means that there was no accumulation of methanol in the reactor at this stage. Meanwhile, there was still a large amount of toluene in the reactor. Therefore, for the rest of the reaction time, toluene was the major species continually permeating through the membrane module and the concentration of toluene in permeate increased as the reaction time increased. For other compounds in the reaction mixure (BuAe, MeAe and BuOH), their concentrations in permeate did not change much as increasing reaction time, which was due to the membrane module not being selective for permeating these compounds.

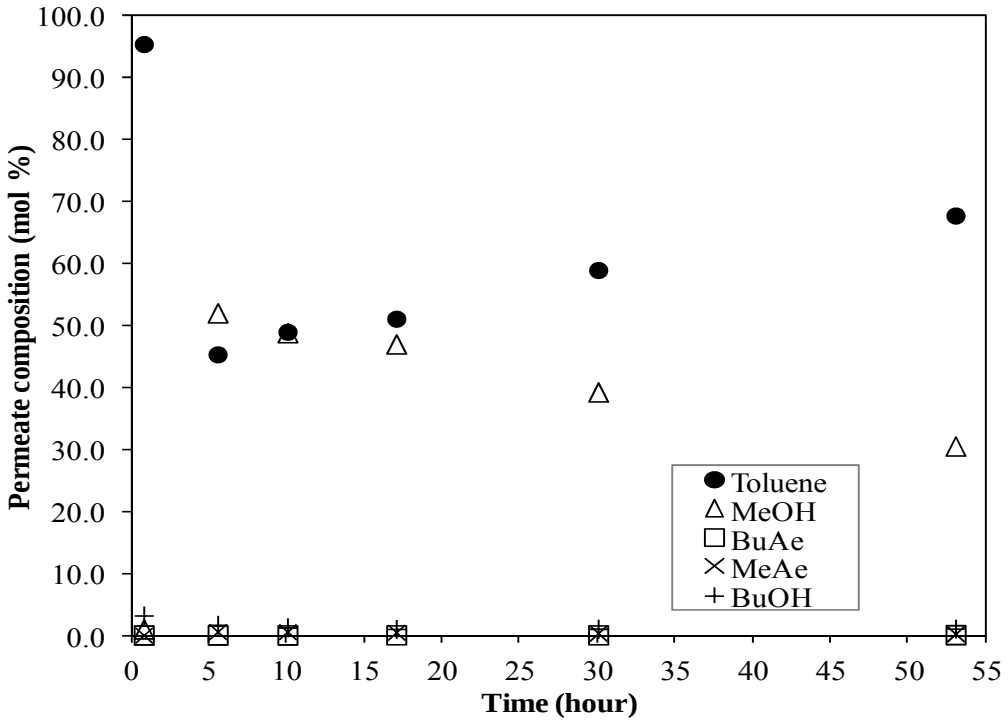

Figure 5-9 Permeate composition versus reaction time obtained in the membrane reactor system with a pilot-scale hollow fiber membrane module (P_{N_2}/l·S/V=25700 GPU·m^{-1}). This run was made at 30°C and started with initial MeAe/BuOH molar ratio of 1, 1.0 L toluene/mol reactants and 3 wt% catalyst.

Figure 5-10 shows toluene concentration profiles in different reactors versus reaction time. A conclusion drawn from these curves is consistent with that from the analysis of permeate toluene concentration. In a batch reactor, there was no permeation of any compounds. Therefore, the toluene concentration in the reactor remained constant. In all membrane rector systems, the

toluene concentration has an initial increase which was caused by the fast methanol production rate and large flux of methanol. For the two runs that obtained 100% conversion (P_{N_2}/l·S/V=5043 GPU·m^{-1} and P_{N_2}/l·S/V=25700 GPU·m^{-1}), we observed a decrease of toluene concentration in the reactor after the initial increase. For both runs, the highest toluene concentration was achieved at the time when the reaction conversion was approximately 95%. It was easy to understand that after achieving 95% conversion, the amount of methanol that could be produced was small, and the amount of methanol permeating through the membrane module was limited while the amount of toluene available in the reactor was large. Thus, toluene was the primary permeating species for the last several hours of operation.

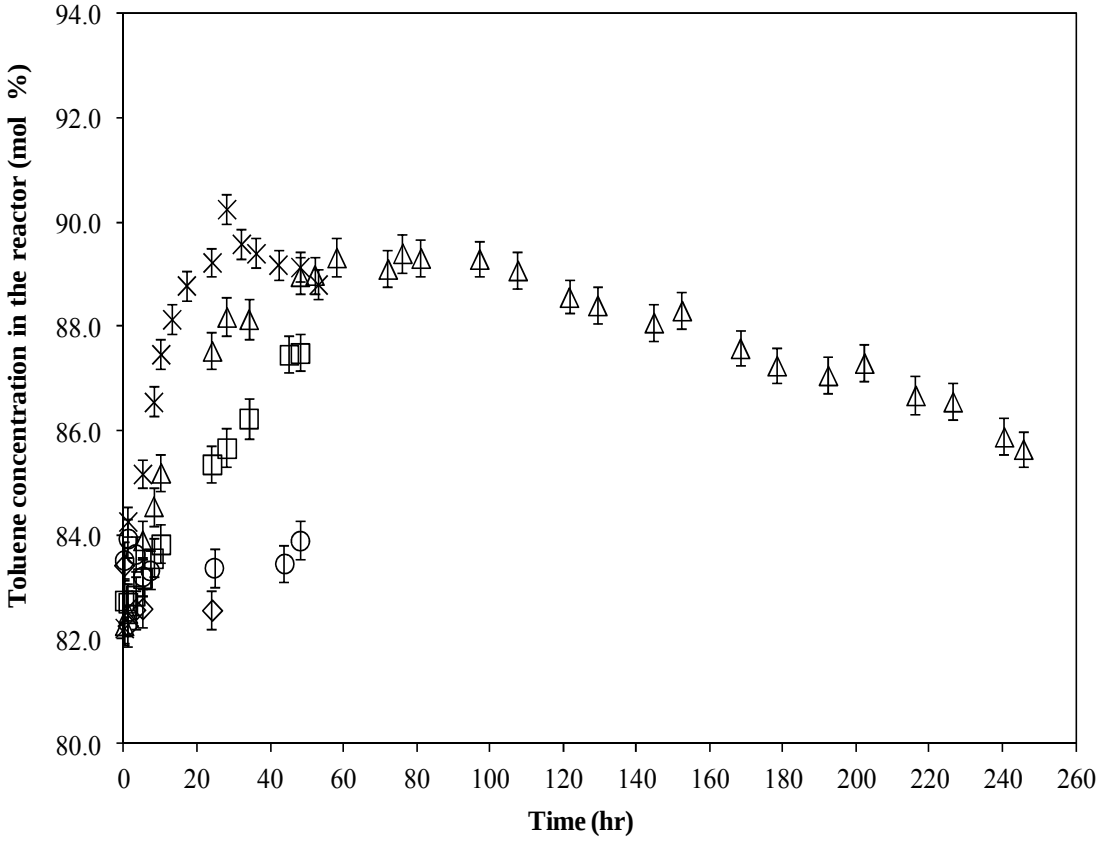

Figure 5-10 Toluene concentration (mol %) in different reactors versus reaction time. All runs were made at 30°C with an initial MeAe/BuOH molar ratio of 1, 1.0 L toluene/mol reactants and 3 wt% catalyst. ◊: Batch reactor; ○: Flat sheet membrane with P_{N_2}/l·S/V=282 GPU·m^{-1}; □: Bench-scale hollow fiber membrane module with P_{N_2}/l·S/V=3383 GPU·m^{-1}; ∆: Bench-scale hollow fiber membrane module with P_{N_2}/l·S/V=5043 GPU·m^{-1}; ×: Pilot-scale hollow fiber membrane module with P_{N_2}/l·S/V =25700 GPU·m^{-1}.

5.4.5 Pervaporation membrane module performance

A series of pervaporation experiments was carried out in a membrane reactor system with different CMS-3 membrane modules. The flat sheet membrane module was under reaction condition for over 96 hours. The bench-scale hollow fiber membrane module was under reaction condition for 297 hours, and the pilot-scale hollow fiber membrane module was under reaction condition for 106 hours. The chemicals and solvents that contacted with these membrane modules include methanol, butanol, methyl acetoacetate, butyl acetoacetate and toluene. The measured gas selectivities for this CMS-3 membrane modules employed in all pervaporation experiments are listed in Table 5-3. From the data, we can observe that there is no significant decrease in membrane selectivities and permeance after it was used for pervaporation-assisted transesterification reactions. Therefore, we can conclude that CMS-3 membrane modules have excellent long-term stability as well as chemical resistance when they are used in the presence of organic solvents involved this transesterification reaction.

Table 5-3 CMS-3 membrane module gas permeance and selectivity

Membrane module	Permeance (GPU*)				Selectivity	
	Before		After		Before	After
	N_2	O_2	N_2	O_2	O_2/N_2	O_2/N_2
Flat sheet	54	138	49	125	2.6	2.5
Bench-scale hollow fiber membrane module	131	324	123	310	2.5	2.5
Pilot-scale hollow fiber membrane module	53	141	N/A	N/A	2.7	N/A

* 1 GPU = 1×10^{-6} cm^3 (STP)/cm^2 ·s · cmHg

5.4.6 Influence of the methanol removal capacity of the reactor system

In the literature on membrane reactor scale-up, two typical types of graphical shapes can be found when describing the influence of S/V ratio on reaction time. The first type is a “U” shape. For this shape, the reaction time will decrease as the S/V ratio increases. After reaching a minimum value, the reaction time will start increasing as the S/V ratio increases. This is because

these membrane modules have a low by-product over reactants selectivity; and, when S/V is too high, a significant amount of reactant alcohol will be removed, which leads to a decrease in forward reaction rate [21]. The second type is a "L" shape. These membrane modules have a higher by-product/reactants selectivity than that of membrane modules displaying a "U" shape. Therefore, the reaction time will continuously decrease with increasing S/V ratio [24]. In this work, since different scales of membrane modules were employed for pervaporation-assisted transesterification reactions, we investigated the influence of methanol removal capacity (P_{N_2}/l·S/V) on reaction time and the equivalent S/V range is 0~500 m^{-1}, which is two times broader compared to literature data.

In Figure 5-11 the reaction time required to achieve 70% conversion (t_{70}) is plotted versus the methanol removal capacity of the membrane reactor system. The time for membrane reactors with high P_{N_2}/l·S/V values (3383, 5043 and 25700 GPU·m^{-1}) were taken from experimental data. The time for membrane reactor with P_{N_2}/l·S/V=282 GPU·m^{-1} was predicted from the model developed in our previous research [12]. The permeance used in the model was the average flux calculated by normalizing the mass of permeate collected by the total reaction time (48 hours). The values of parameters required for the model are initial feed of MeAe=200 mmol, initial feed of BuOH=200 mmol, initial feed of Toluene=200 mL, permeance of MeAe=0.46 mmol/(cm^2·h·bar), permeance of BuOH=8.3×10^{-3} mmol/(cm^2·h·bar), permeance of BuAe=7.5×10^{-5} mmol/(cm^2·h·bar), permeance of MeOH=2.82 mmol/(cm^2·h·bar), permeance of toluene=3.8×10^{-2} mmol/(cm^2·h·bar), permeate pressure=0.004 bar and K_{eq}=0.767. As can be seen from Figure 5-11, the reaction time to achieve 70% conversion is strongly dependent on the methanol removal capacity. At low P_{N_2}/l·S/V value, the methanol removal rate is too slow, resulting in a very long reaction time to achieve 70% conversion. The increase in the P_{N_2}/l·S/V value, which is the factor that directly influences the pervaporation kinetics, enables a fast removal of the methanol and leads to a faster conversion. In contrast with the literature, the response of reaction time to the change of methanol removal capacity in this study is an "L" shape, which means t_{70} continuously decreases with increasing P_{N_2}/l·S/V due to the high methanol over butanol selectivity. However, this is a highly nonlinear relationship between t_{70} and P_{N_2}/l·S/V. There is a dramatic improvement of reaction time when increasing the methanol removal capacity from P_{N_2}/l·S/V=282 GPU·m^{-1} to about 4200 GPU·m^{-1}. Further increase in the

methanol removal capacity can only mildly decrease the reaction time. Therefore, there exists a methanol removal capacity inflection point.

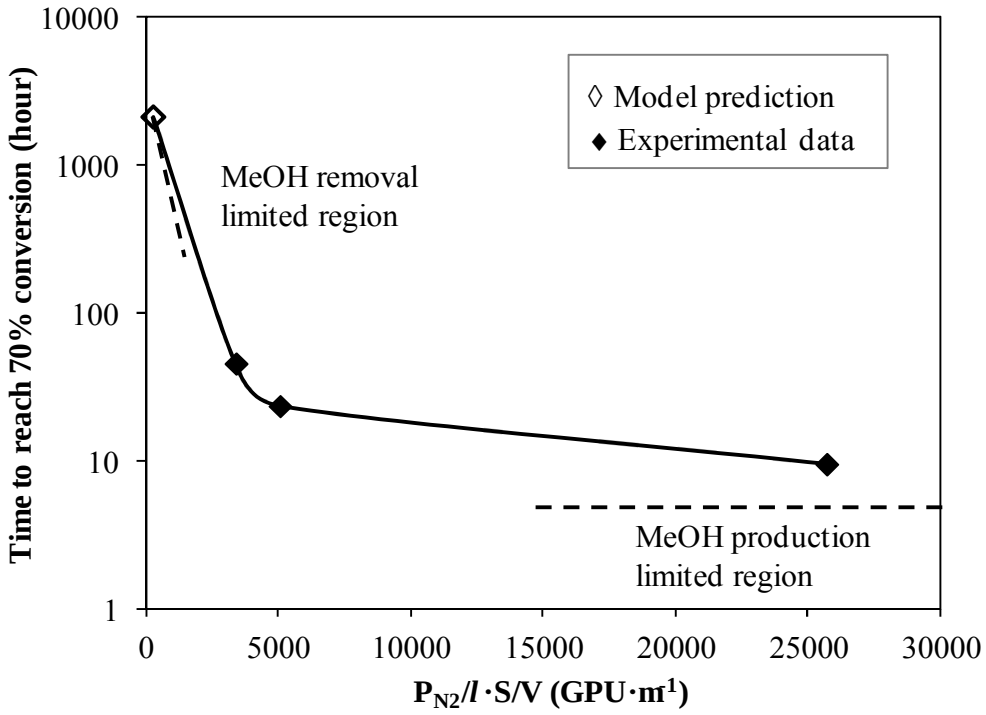

Figure 5-11 Influence of methanol removal capacity on reaction time required to achieve 70% conversion for transesterification reaction in a membrane reactor (Initial molar ratio of MeAe/BuOH=1, 1.0 L toluene/mol reactants, T=30°C, 3 wt% catalyst). At very low P_{N2}/l·S/V region, system performance is limited by the methanol removal rate. At very high P_{N2}/l·S/V region, system performance is limited by the methanol production rate.

The existence of this inflection point is due to the balance between reaction rate and methanol removal capacity, which can be distinguished into three regions and are illustrated in Figure 5-11. When the system has very low methanol removal capacity (e.g. P_{N2}/l·S/V<2000 GPU·m^{-1}), the performance of the membrane reactor system is mainly determined by the methanol removal rate. When the system has very high methanol removal capacity (e.g. P_{N2}/l·S/V>15000 GPU·m^{-1}), the performance of the membrane reactor system is mainly determined by the methanol production rate. This curve should eventually reach a plateau at high methanol removal rate region because when the methanol removal rate is very high, the produced methanol can be removed instantly and further increase in the removal capacity will not make any difference in the methanol removal rate. The inflection point will fall in the

intermediate region between these two extreme cases, in which both the methanol production rate and removal rate affect the membrane reactor performance.

To predict the behavior of an industrial-scale membrane reactor system for the transesterification production of butyl acetoacetate, operation at or above this methanol removal capacity inflection point is recommended to be done in advance.

5.5 Conclusions

In this study, a continuous pervaporation-assisted membrane reactor system with CMS-3 flat sheet membranes was developed for the transesterification production of butyl acetoacetate. The membrane reactor system was then scaled up to pilot-scale with CMS-3 hollow fiber membrane modules. In the flat sheet membrane reactor system, the methanol removal capacity was limited and the enhancement in reaction conversion than that achieved in a batch reactor was not obvious within test period. Increasing of methanol removal capacity value increased the methanol removal rate which led to a faster reaction rate and markedly higher conversion than that obtained in a batch reactor. By fast and highly selective removal of methanol, in the pilot-scale hollow fiber membrane reactor system, a 100% conversion, nearly 55% higher than that in a batch reactor, was achieved after 48 hours. In all cases, CMS-3 membrane modules have high selectivity of methanol over butanol and esters. The loss of esters and reactant alcohols into permeate during reactions carried out in membrane reactor systems can be neglected under experiment conditions in this work. The loss of solvent toluene into permeate increases as reaction time increases. Excellent long-term stability and chemical resistance of these membranes have been proved by no significant loss of gas permeance and selectivity after all pervaporation experiments. Increasing the methanol removal capacity can decrease the reaction time. However, the improvement of the reaction time slowed down after the inflection point. From an industrial application perspective, operation at or above methanol removal capacity inflection point is recommended to be carried out before scaling up the membrane reactor to full-scale.

5.6 Reference

[1] R.W. Baker, Membrane Technology and Applications, 2nd ed., John Wiley & Sons, Ltd., England, 2004.

[2] M. Mulder, Basic Principles of Membrane Technology, Springer, 1996.

[3] R.W. Field, F. Lipnizki, P.K. Ten, Pervaporation-based hybrid process: a review of process design, applications and economics, Journal of Membrane Science, 153 (1999) 183-210.

[4] Q.L. Liu, Z.B. Zhang, H.F. Chen, Study on the coupling of esterification with pervaporation, Journal of Membrane Science, 182 (2001) 173-181.

[5] K. Bartling, J.U.S. Thompson, P.H. Pfromm, P. Czermak, M.E. Rezac, Lipase-catalyzed synthesis of geranyl acetate in n-hexane with membrane-mediated water removal, Biotechnol Bioeng, 75 (2001) 676-681.

[6] K. Tanaka, R. Yoshikawa, C. Ying, H. Kita, K. Okamoto, Application of zeolite membranes to esterification reactions, Catalysis Today, 67 (2001) 121-125.

[7] D. Barahona, P.H. Pfromm, M.E. Rezac, Effect of water activity on the lipase catalyzed esterification of geraniol in ionic liquid [bmim]PF6, Biotechnol Bioeng, 93 (2006) 318-324.

[8] S. Korkmaz, Y. Salt, A. Hasanoglu, S. Ozkan, I. Salt, S. Dincer, Pervaporation membrane reactor study for the esterification of acetic acid and isobutanol using polydimethylsiloxane membrane, Appl Catal a-Gen, 366 (2009) 102-107.

[9] J. Ma, M.H. Zhang, L.Y. Lu, X. Yin, J. Chen, Z.Y. Jiang, Intensifying esterification reaction between lactic acid and ethanol by pervaporation dehydration using chitosan-TEOS hybrid membranes, Chem Eng J, 155 (2009) 800-809.

[10] S.G. Adoor, L.S. Manjeshwar, S.D. Bhat, T.M. Aminabhavi, Aluminum-rich zeolite beta incorporated sodium alginate mixed matrix membranes for pervaporation dehydration and esterification of ethanol and acetic acid, J Membrane Sci, 318 (2008) 233-246.

[11] P. Delgado, M.T. Sanz, S. Beltran, L.A. Nunez, Ethyl lactate production via esterification of lactic acid with ethanol combined with pervaporation, Chem Eng J, 165 (2010) 693-700.

[12] F. Zhang, V. Bliem, M.E. Rezac, P. Kosaraju, S. Nemser, Pervaporation membrane reactors for reversible organic reactions: modeling of the membrane-reactor performance to system design and operating conditions, accepted by the Journal of Membrane Science, 2011.

[13] A. Hasanoglu, Y. Salt, S. Keleser, S. Dincer, The esterification of acetic acid with ethanol in a pervaporation membrane reactor, Desalination, 245 (2009) 662-669.

[14] S.Y. Lim, B. Park, F. Hung, M. Sahimi, T.T. Tsotsis, Design issues of pervaporation membrane reactors for esterification, Chemical Engineering Science, 57 (2002) 4933-4946.

[15] K.C.D. Figueiredo, V.M.M. Salim, C.P. Borges, Synthesis and characterization of a catalytic membrane for pervaporation-assisted esterification reactors, Catal Today, 133 (2008) 809-814.

[16] A.Y. Tremblay, P.G. Cao, M.A. Dube, Biodiesel production using ultralow catalyst concentrations, Energy & Fuels, 22 (2008) 2748-2755.

[17] A.P. de los Rios, F.J. Hernandez-Fernandez, M. Rubio, D. Gomez, G. Villora, Highly selective transport of transesterification reaction compounds through supported liquid membranes containing ionic liquids based on the tetrafluoroborate anion, Desalination, 250 (2010) 101-104.

[18] F. Zhang, M.E. Rezac, S. Majumdar, P. Kosaraju, S. Nemser, Improving chemical production processes by selective by-product removal in a pervaporation membrane reactor, manuscript submitted to the Journal of Membrane Science, 2012.

[19] J.M. Fraile, R. Mallada, J.A. Mayoral, M. Menendez, L. Roldan, Shift of multiple incompatible equilibriums by a combination of heterogeneous catalysis and membranes, Chem-Eur J, 16 (2010) 3296-3299.

[20] R.W. Baker, Research needs in the membrane separation industry: Looking back, looking forward, Journal of Membrane Science, 362 (2010) 134-136.

[21] J.T.F. Keurentjes, G.H.R. Janssen, J.J. Gorissen, The esterification of tartaric acid with ethanol - kinetics and shifting the equilibrium by means of pervaporation, Chemical Engineering Science, 49 (1994) 4681-4689.

[22] S. Korkmaz, Y. Salt, S. Dincer, Esterification of acetic acid and isobutanol in a pervaporation membrane reactor using different membranes, Ind. Eng. Chem. Res., 50 (2011) 11657-11666.

[23] K. Okamoto, M. Yamamoto, Y. Otoshi, T. Semoto, M. Yano, K. Tanaka, H. Kita, Pervaporation-aided esterification of oleic-acid, Journal of Chemical Engineering of Japan, 26 (1993) 475-481.

[24] T. Roth, S. Lauterbach, A. Hoffmann, P. Kreis, Scale-up and detailed process analysis of a membrane assisted esterification reaction, Chem-Ing-Tech, 83 (2011) 456-464.

[25] M.O. David, T.Q. Nguyen, J. Neel, Pervaporation-esterification coupling .2. modeling of the influence of different operating parameters, Chemical Engineering Research & Design, 69 (1991) 341-346.

[26] S. Benetti, R. Romagnoli, C. Derisi, G. Spalluto, V. Zanirato, Mastering beta-keto-esters, Chemical Reviews, 95 (1995) 1065-1114.

[27] T. Parvin, Methyl Acetoacetate: A useful reagent in multicomponent reactions, Synlett, (2009) 2713-2714.

[28] I.M. Lagoja, P. Herdewijn, A potential prebiotic route to adenine from hypoxanthine, Chem Biodivers, 2 (2005) 923-927.

[29] M.D. Hill, M. Movassaghi, New strategies for the synthesis of pyrimidine derivatives, Chem-Eur J, 14 (2008) 6836-6844.

[30] G.D. Yadav, P.S. Lathi, Lipase catalyzed transesterification of methyl acetoacetate with n-butanol, J Mol Catal B-Enzym, 32 (2005) 107-113.

[31] A.Y. Alentiev, Y.P. Yampolskii, V.P. Shantarovich, S.M. Nemser, N.A. Plate, High transport parameters and free volume of perfluorodioxole copolymers, Journal of Membrane Science, 126 (1997) 123-132.

[32] S.M. Nemser, I.C. Roman, Perfluorodioxole Membranes, US Patent 5051114, (1991).

[33] V. Smuleac, J. Wu, S. Nemser, S. Majumdar, D. Bhattacharyya, Novel perfluorinated polymer-based pervaporation membranes for the separation of solvent/water mixtures, Journal of Membrane Science, 352 (2010) 41-49.

[34] I.J. Kang, P.H. Pfromm, M.E. Rezac, Real time measurement and control of thermodynamic water activities for enzymatic catalysis in hexane, J Biotechnol, 119 (2005) 147-154.

Chapter 6 - Conclusions and recommendations

6.1 Summary

This project created a general protocol that can guide one to carry out experiments and collect necessary data for transferring membrane reactor design concepts to the construction of industrial-scale pervaporation membrane reactors for organic synthesis. Demonstration of this protocol was achieved by (1) experimental evaluation of membrane reactor performance, (2) modeling, and (3) scale-up.

First, experiments were carried out in bench-scale membrane reactor systems equipped with perfluorinated composite membranes to investigate the selective by-product removal capability of membranes during model reversible reactions. Three types of reversible reactions were investigated: esterification (oleic acid with ethanol), acetalisation (acetone with ethanol) and transesterification (methyl benzoate with n-butanol). The first two reactions were studied as model reactions for the water/organic separation. Water was the target compound to be removed to shift the equilibrium in these cases. The transesterification reaction was selected to investigate the organic/organic separation. Methanol was to be separated from esters and butanol reactant to overcome the thermodynamic limitation. Our results indicated that enhanced membrane reactors selectively removed the by-product water or methanol from reaction mixtures and achieved high conversions for all investigated reactions. The membranes employed in these pervaporation membrane reactors have high selectivity of by-product over other compounds in reaction mixtures, as well as good stability and chemical resistance to aggressive solvents.

Second, modeling and simulation of pervaporation membrane reactor performance for reversible reactions were carried out. A computational model was developed to predict membrane reactor conversions based on membrane permeation data and operating conditions (reactor temperature, permeate pressure and feed composition). The simulated performance agrees well with experimental data. Using the developed model, the effects of permeate pressure and membrane selectivity on membrane reactor yield were examined. For the transesterification of methyl benzoate with butanol, the reaction conversion increased as the membrane selectivity of methanol/butanol improved. However, after the selectivity increased above current experimental selectivity, such an improvement had only a modest impact on the conversions achieved. For the acetalisation of acetone with ethanol, the model prediction revealed that low

permeate pressures promoted product yields while high permeate pressure might decrease product yields.

At last, a series of membrane reactor systems with various scale and complexity was developed for the transesterification of methyl acetoacetate with n-butanol. The membrane modules investigated included a bench-scale flat sheet membrane, a bench-scale hollow fiber membrane module, and a pilot-scale hollow fiber membrane module. Complete conversion was obtained with selective methanol removal. All membrane modules have high methanol/butanol selectivity (greater than 350) and good long-term stability. With high methanol selectivity membrane modules, the reaction time to achieve a given conversion continuously decreases with increasing the methanol removal capacity of the reactor system. However, this is a highly nonlinear relationship.

6.2 Conclusions

The major conclusions from this research follow.

For a membrane reactor for reversible reaction applications, where the design is to selectively remove low molecular weight by-products,

(1) Given a membrane with sufficient selectivity for the removal of by-products and good stability in reaction environment, the conversion attainable in this membrane reactor can be markedly higher than that achieved in a conventional reactor. In cases where membranes prohibit the loss of reactants, complete conversions are achievable.

(2) Increasing the byproduct selectivity can improve the system performance up to a certain level. Beyond that level, there is only a neglectable performance enhancement by further increases in selectivity.

(3) The permeate pressure and the product yield attainable are inversely related for cases with the loss of reactant(s) into the permeate.

(4) Reaction time to reach a given conversion is strongly dependent on the by-product removal capacity. For cases like ours where membranes have high selectivities of byproducts over other species in reaction mixtures, an increase in the by-product removal capacity value leads to a shorter reaction time. After increasing the capacity value above the inflection point, the time decrease slows down and will flatten out eventually.

Based on all the work that have been done during this research, the general protocol for transferring membrane reactor design concepts to the construction of industrial-scale membrane reactors for organic synthesis can be described by the flowchart in Figure 6-1.

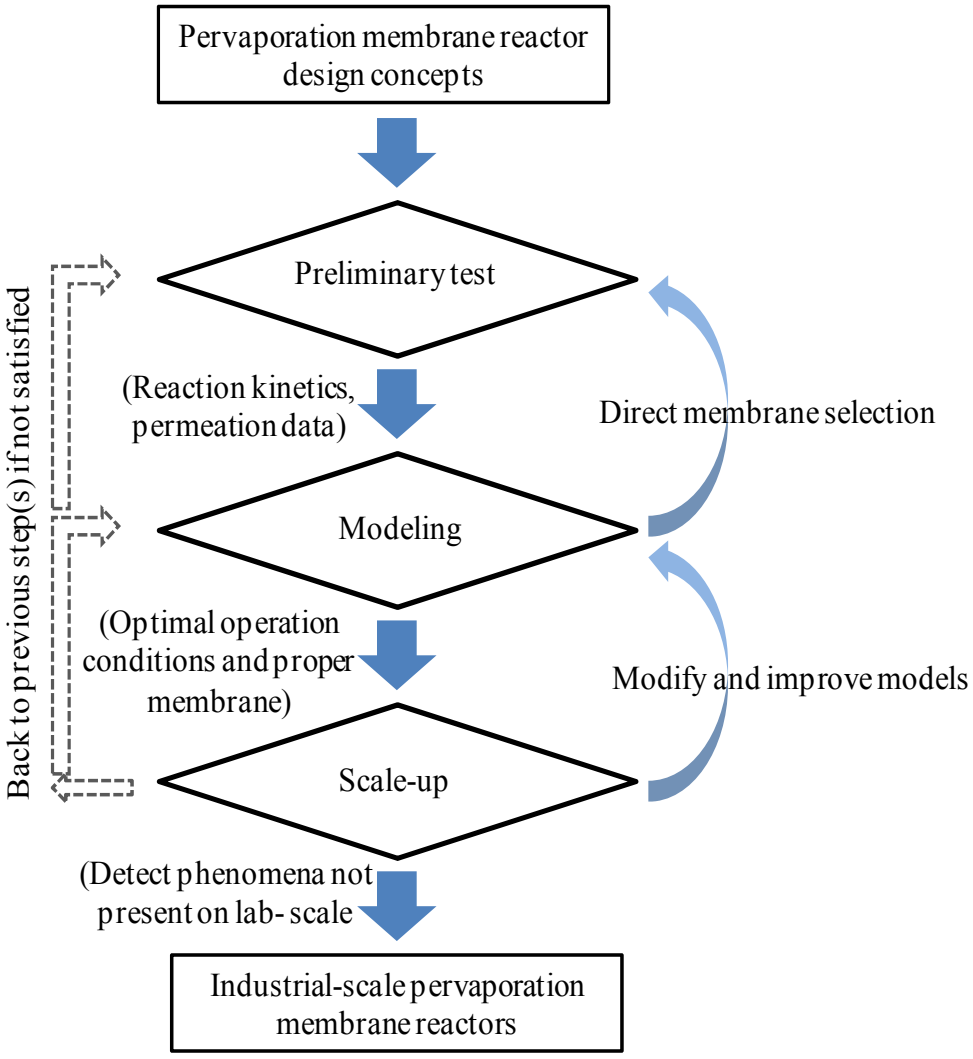

Figure 6-1 Schematic overview of the protocol developed in this research

The preliminary test will be first carried out to test the feasibility of a new design concept. This step can provide information such as reversible reaction kinetics and permeation data of the selected membrane. Using the data, a predictive model can be developed to provide optimal operation conditions and system design, as well as to predict the best case scenario based on current experiment configurations. The model will also allow the desired membrane properties for interested membrane reactor applications to be identified. Hence, this can direct

the selection of suitable membrane materials in the first step. After completing the second step, a scale-up can be done based on the information obtained from the model and preliminary test. This step is not intended only to prove that an existing laboratory system yields the same results on a larger scale. Its main purpose is to test the apparatuses and conditions that will be used on an industrial scale, which may not be the same as employed in the laboratory-scale, in order to find out any phenomena not present on the laboratory-scale. If there is any, the model in the second step can be improved by taking into consideration of these phenomena. One can always go back to previous step(s) if the current step cannot yield desirable results. Finally, a full-scale system can be designed and built up after acquiring a complete understanding of the process from former steps.

6.3 Recommendations

- Acquiring reaction kinetics information. The model developed in this research assumes that the thermodynamic equilibrium of the reaction mixture is reached instantaneously during each iteration step. This model successfully predicted conversions exceeding thermodynamic equilibrium in a membrane reactor but not the precise transient behavior. Knowing the final product composition achievable from a membrane with given flux and selectivity properties is important in terms of the membrane selection. Knowing reaction kinetics information is always helpful. In Chapter 5, the transesterification of methyl acetoacetate with *n*-butanol catalyzed by the lipase Novozym® 435 in membrane reactors was investigated. It is found that there is an inflection point in the curve that correlates reaction time with methanol removal capacity. A ping-pong bi-bi reaction mechanism has been proposed for this reaction in a batch reactor by Yadav [1]. Acquiring the reaction rate from this mechanism, along with the methanol removal rate information available, the exact location of this inflection point can be predicted. How the methanol production rate and the methanol removal rate play their roles in determining the location of the inflection point can be better understood.

- Carrying out economic evaluation. Economics is a significant part of any process. The membrane reactor system developed in this research can overcome the inhibition of the chemical equilibrium of a reversible reaction and therefore obtains an increased productivity at a reduced reaction time. This does save operational costs. However, the pervaporation-based hybrid

processes often offer significant savings on operating costs but not necessarily on investment costs [2]. An economic evaluation is still needed on this system before it can be implemented widely in industry. Details about how to carry out an economic evaluation on these hybrid processes can be found in literature [3-5].

- Additional applications of this system. The pervaporation membrane reactor system developed may also be applied to step-wise reactions that have water or a low molecular alcohol as the by-product to shift the equilibrium towards the formation of final products (i.e. $A \underset{-D}{\overset{+B}{\rightleftharpoons}} C \underset{-D}{\overset{+B}{\rightleftharpoons}} E$, removing D to promote the formation of E).

6.4 References

[1] G.D. Yadav, P.S. Lathi, Synergism between microwave and enzyme catalysis in intensification of reactions and selectivities: transesterification of methyl acetoacetate with alcohols, J Mol Catal a-Chem, 223 (2004) 51-56.

[2] F. Lipnizki, R.W. Field, P.K. Ten, Pervaporation-based hybrid process: a review of process design, applications and economics, Journal of Membrane Science, 153 (1999) 183-210.

[3] S. Sommer, T. Melin, Design and optimization of hybrid separation processes for the dehydration of 2-propanol and other organics, Ind. Eng. Chem. Res., 43 (2004) 5248-5259.

[4] R. Rautenbach, R. Albrecht, The separation potential of pervaporation .2. process design and economics, Journal of Membrane Science, 25 (1985) 25-54.

[5] M. Schembra, J. Schulze, Estimation of investment costs in process-development, Chem-Ing-Tech, 65 (1993) 41-47.